IDENTIFICATION AND CHARACTERIZATION OF TWO POTENTIAL NOVEL REGULATORS OF APOPTOSIS, MAGE-D2 AND SUMI-1

Hilary VanTassell Clegg

A dissertation submitted to the faculty of the University of North Carolina at Chapel Hill in partial fulfillment of the requirements for the degree of Doctor of Philosophy in Genetics and Molecular Biology in the Curriculum of Genetics and Molecular Biology.

Chapel Hill
2011

Approved by

Yanping Zhang, Ph.D.

Adrienne Cox, Ph.D.

Mohanish Deshmukh, Ph.D.

Norman Sharpless, M.D.

ABSTRACT

HILARY CLEGG: Identification and Characterization of Two Potential Novel Regulators of Apoptosis, MAGE-D2 and SUMI-1
(Under the direction of Yanping Zhang, Ph.D.)

Apoptosis is a genetically-programmed form of cell death that is critical for proper development, tissue homeostasis, and immune function in vertebrate organisms. Disrupted regulation of this process contributes to diverse diseases such as cancer, neurodegenerative disorders, and autoimmune dysfunction. Our knowledge of apoptosis is incomplete, especially the mechanisms governing MOMP (mitochondrial outer membrane permeabilization)—a critical control point during which cytochrome *c* and other mitochondrial intermembrane space proteins are released, triggering the execution of apoptosis. Our understanding of this process can be enhanced by identifying proteins involved in its regulation. In this work, two proteins—MAGE-D2 (melanoma antigen family D2) and SUMI-1 (survival-promoting mitochondrial protein 1, also known as CHCHD2 for coiled-coil-helix-coiled-coil-helix-domain containing 2)—are identified as novel potential regulators of apoptosis. Initially, these proteins were identified in a screen for novel interacting partners of the pro-apoptotic protein p32/C1QBP (complement component 1, q subcomponent binding protein). This screen was undertaken in an effort to better understand the mechanisms by which p32 regulates apoptosis; however, in this work, the functions of MAGE-D2 and SUMI-1 are characterized

separately from p32. Here, we show that MAGE-D2 is localized to the nucleolus, nucleus, and possibly the mitochondria, and preliminary data suggest potential roles for MAGE-D2 in apoptosis and cell cycle control. SUMI-1 is characterized more extensively in this work, and the data presented here establish SUMI-1 as a novel mitochondria-localized regulator of mitochondrial fission-fusion dynamics and BAX-mediated apoptosis. The data shown here support a model in which SUMI-1 resides at the mitochondrial outer membrane, where it regulates mitochondrial fusion and protects cells from apoptosis. Upon treatment with apoptosis-inducing stimuli, SUMI-1 translocates from the mitochondria, inhibiting mitochondrial fusion while fission continues unperturbed. This imbalance results in mitochondrial fragmentation, promoting BAX oligomerization on the mitochondrial outer membrane and ultimately leading to MOMP, cytochrome *c* release, and apoptosis. This body of work provides a subcellular localization and functional data for two previously uncharacterized proteins and contributes to our understanding of the signaling pathways regulating apoptosis. These data, as well as discussion of the results and future directions, are described herein.

This work is dedicated to my daughters, Natalie and Katherine.

ACKNOWLEDGMENTS

I owe many thanks to the people who have supported me throughout my graduate career. First, I thank my mentor, Yanping Zhang, for treating me as a colleague, for respecting my opinions and allowing me to pursue my ideas, for always having an open door, for his flexibility and patience regarding family issues, and for his positive and encouraging attitude when discussing my project and my data. I feel fortunate to have been a part of the Zhang lab—while it has evolved throughout my years in graduate school, it has always been filled with people who are supportive, intelligent, friendly, and willing to help. I thank our lab manager, Aiwen Jin, for her quick assistance whenever anything is needed, for keeping the lab such an organized environment to work in, and for her motherly advice and discussions. I thank Yoko Itahana, Koji Itahana, and Michael Lindström for patiently answering my questions, for helping me with experiments, and for making me feel at home when I first joined the lab. I thank Chad Deisenroth for encouraging me, through his example, to be a better and more independent graduate student. I thank Everardo Macias for his sense of humor and for answering many questions about assays and techniques. I thank Laura Tollini for frequent and helpful discussions of my data, for taking the time to give great feedback to improve my writing and talks, for her organizational tips, her support and friendliness, her incredible cakes and other baked treats, and for

being a ray of sunshine in the lab. I thank Yizhou He for his extensive help resolving computer issues and for always being willing to discuss data and ideas. I thank Paula Miliani de Marval, who has gone above and beyond as a mentor to me, for taking the time to review my talks and papers and give extensive feedback, for extensive assistance with techniques and assays, for many helpful discussions about my project, and for being a tremendous source of support. I thank Brittany Daughtry, Yidi Turman, Kim Gooding, and Aaron Dinerman for their hard work and helpful attitudes, and all the other technicians and undergraduates who have provided help along the way. I thank Yong Liu, Jiehui Di, Laura Tollini, Yizhou He, Aiwen Jin, and Paula Miliani de Marval for stepping up and working so hard and so quickly when asked to help with the SUMI-1 project in the last few months. I thank my dissertation committee members—Adrienne Cox, Mohanish Deshmukh, Ned Sharpless, and Yi Zhang—for taking the time to be a part of my committee and for their helpful feedback on my project. I thank Adrienne Cox for being like a second mentor to me. She is a great advocate for students, critical in a positive way, and is always willing to help and to answer my questions. I thank Mohanish Deshmukh for generously taking the time to discuss my project and apoptosis outside of committee meetings, and for providing feedback in such a constructive and positive manner. I thank Sharon Milgram for running a model interdisciplinary biomedical sciences program (IBMS), for nominating me for a university merit fellowship, and for her support in my first year of graduate school. I thank the IBMS class of 2004 for being such a wonderful, friendly, and supportive group of people. I am grateful to

my IBMS friends for making graduate school fun and for being an amazing source of support, especially during my difficult first year. I thank Pat Phelps and Patrick Brandt for establishing and carrying out the TIBBS training program—I have gained so much from the career workshops and other resources that TIBBS provides. I thank my parents, Janet and Linden Davis, for all their years of support and encouragement, for the knowledge, wisdom, and values that they have imparted on me, and for shaping the person who I am today. I thank my brother, Trevor Davis, for making my transition to North Carolina so much easier, and I thank my sister, Laura Davis, for being a great support and listening ear on the phone whenever I have struggled. Finally, I thank my husband, Neal Clegg, for being my best friend and an incredible father, for moving to N.C. with me for graduate school and for all the other sacrifices he has made, for balancing our two careers and fatherhood so well, for taking care of household and childcare obligations, especially during my dissertation writing, for being so patient with my evenings and weekends in the lab or library, and for being such an invaluable source of support and encouragement throughout my years of graduate school. I will be forever grateful to each of these people for their help, encouragement, and support.

TABLE OF CONTENTS

LIST OF TABLES

TABLE

LIST OF FIGURES

FIGURE

LIST OF ABBREVIATIONS AND SYMBOLS

BAK:	BCL-2-antagonist/killer 1
BAX:	BCL-2-associated X protein
BCL-2:	B-cell lymphoma 2
BCL-xL:	BCL-2-like 1
BHD:	BCL-2 homology domain
CHCH:	Coiled-coil-helix-coiled-coil-helix
CHCHD2:	Coiled-coil-helix-coiled-coil-helix domain containing 2
C1QBP:	Complement component 1, q subcomponent binding protein
EM:	Electron microscopy
HMW:	High molecular weight
IP:	Immunoprecipitation
LUV:	Large unilamellar vesicle
MAGE:	Melanoma antigen family
MAGE-D2:	Melanoma antigen family D2
MFN1:	Mitofusin 1
MFN2:	Mitofusin 2
MOMP:	Mitochondrial outer membrane permeabilization
NEM:	N-ethylmaleimide
PARP:	Poly (ADP-ribose) polymerase
REDOX:	Reduction-Oxidation
SUMI-1:	Survival-promoting mitochondrial protein 1
TNF:	Tumor necrosis factor

CHAPTER I

INTRODUCTION

An Overview of Apoptosis

Apoptosis is a tightly-regulated form of programmed cell death that is critical for proper embryonic development, tissue homeostasis, and immune response, and aberrant regulation of apoptosis contributes to diseases such as autoimmune disorders, neurodegenerative disease, and cancer. Unlike necrosis, or “accidental” cell death, which is usually triggered by acute cellular injury, apoptosis is genetically programmed and is characterized by distinct morphological changes such as membrane blebbing, chromatin condensation, DNA fragmentation, and cell shrinkage (Kerr et al., 1972). In vertebrates, apoptosis usually occurs through one of two major pathways: extrinsic, or receptor-mediated apoptosis, and intrinsic, or mitochondria-mediated apoptosis. Both pathways result in the activation of executioner cysteine proteases (Caspases), which cleave downstream targets to carry out the execution phase of apoptosis.

Apoptotic cell death was first described in 1842 by German scientist Carl Vogt (Vogt, 1842), but the process was not described in detail until 1972 when Kerr, Wyllie and Currie published a paper describing the phenomenon and assigning the term “apoptosis” based on a suggestion from a professor of Greek language, James Cormack. Apoptosis (Greek: *apo* – from/off/without, *ptosis* –

falling) translates to the "dropping off" of petals or leaves from plants or trees (Kerr et al., 1972). The pronunciation of this word is still debated; Kerr et al. suggested that the second “p” be silent to reflect the word’s Greek roots, while others have pointed out that, while the “p” is often silent in Greek-derived words that begin with a “pt” combination, a “pt” found in the middle of a word is typically pronounced, as in “helicopter” and “cryptic.”

For many multicellular organisms, apoptosis is essential during embryonic development. In vertebrates, many tissue and organ systems produce an overabundance of cells, and those cells that are not utilized must be destroyed in a way that does not induce an inflammatory response and is not otherwise detrimental to the organism. In this manner, apoptosis eliminates neurons that fail to establish connections (Nijhawan et al., 2000) and immune cells that fail to produce antigen specificity (Opferman and Korsmeyer, 2003). In adult organisms, apoptosis is essential for maintaining tissue homeostasis. It is estimated that 50-70 billion cells are produced in the human body die each day to replace those that are eliminated by apoptosis (Chen and Lai, 2009). During wound healing, apoptosis removes inflammatory cells that might otherwise lead to scarring or fibrosis (Greenhalgh, 1998). Apoptosis is also critical for proper immune response, targeting cells infected with viruses or other pathogens to prevent their proliferation (Roulston et al., 1999).

Apoptosis in Disease

Defective regulation of apoptosis contributes to a number of human diseases including cancer, neurodegenerative disorders, and autoimmune

disorders. More than ten years ago, evasion of apoptosis was introduced as one of the six hallmarks of cancer that enable or promote tumor growth (Evan and Littlewood, 1998; Hanahan and Weinberg, 2000). The human body uses apoptosis as a defense against extensive DNA damage that may otherwise promote carcinogenesis; in other words, if a cell's genetic material is sufficiently damaged, apoptosis is triggered in order to prevent the cell from progressing into a tumor (Kerr et al., 1994). Cells that escape this defense mechanism can potentially undergo additional changes and become transformed. Cancer cells employ a variety of strategies to disable induction of apoptosis. Most notable is inactivation of the tumor suppressor p53, which normally responds to DNA damage, abnormal proliferative signals, and other cellular stresses by triggering apoptosis, primarily through transactivation of apoptosis-promoting targets such as PUMA and BAX (Levine, 1997). Many chemotherapeutic agents, such as cisplatin, doxorubicin, and paclitaxel, fight tumors through induction of apoptosis, and identification of novel apoptosis-inducers and apoptosis-sensitizing agents is an area of ongoing investigation in cancer biology.

Defective apoptosis or impaired clearance of apoptotic cells can also contribute to immune dysfunction and development of autoimmune disorders such as systemic lupus erythematosus (SLE) (Stuart and Hughes, 2002). During T-cell development, T-cells with self-recognizing antigens are normally destroyed by apoptosis. If these T-cells evade apoptosis and continue to proliferate, autoimmune disorders can result. Type I (juvenile-onset) diabetes mellitus is thought to arise from T-cells that recognize and attack insulin-producing beta-

cells in the pancreas. Similarly, inappropriate T-cell targeting of joints is presumed to occur in rheumatoid arthritis (Hayashi and Faustman, 2003), and the impaired apoptosis of these T-cells may result from induction of apoptosis-inhibiting BCL-2 and MCL-1 proteins (Liu and Pope, 2003). In systemic lupus erythematosus, reduced apoptosis leads to lymphoproliferation and general autoimmunity (Hayashi and Faustman, 2003).

On the other hand, an excess of apoptosis can contribute to development of neurodegenerative disorders, the most prevalent of which is Alzheimer's Disease, affecting more than 25 million people worldwide and predicted to affect one out of every 85 individuals by the year 2050 (Brookmeyer et al., 2007). Alzheimer's Disease causes progressive neurological decline involving extensive neuronal loss through mechanisms that are not entirely clear but are known to involve accumulation of neurofibrillary tangles and β-Amyloid plaques in the extracellular space between neurons (Masters et al., 1985; Selkoe, 2001; Yankner, 1996). β-Amyloid aggregates have been shown to induce neuronal cell death *in vivo* and in cell culture (Estus et al., 1997; Hartman et al., 2005; Pike et al., 1991) and are thought to induce aberrant apoptosis in part through generation of oxidative stress and by inducing expression of Fas ligand (Ethell and Buhler, 2003). In addition, the pro-apoptotic BH3-only protein BIM is elevated in Alzheimer's disease, and it was shown that BIM is required for β-Amyloid-induced neuronal cell death. β-Amyloid was shown to elevate BIM levels by regulating cyclin-dependent kinase 4 (CDK4) and its downstream effector B-Myb in neuronal cell culture (Biswas et al., 2007). However, the exact

mechanisms that induce neuronal apoptosis in Alzheimer's Disease are still unclear.

Parkinson's Disease is another progressive cognitive disorder involving neuronal death and is the second most common neurodegenerative disease, affecting six million people worldwide (Dauer and Przedborski, 2003). In this disorder, neuronal death occurs in dopamine-producing cells in the substantia nigra located in the midbrain (Levy et al., 2009). Apoptosis has been postulated as a mechanism for the neuronal death in Parkinson's Disease, but controversy surrounds the issue because one marker of apoptosis—nuclear DNA cleavage—is not robustly present in brains of Parkinson's Disease patients. However, a number of apoptotic signaling pathways have been implicated in the disorder, including involvement of BCL-2 family proteins, mitochondrial dysfunction, JNK (Jun Kinase) signaling, and activation of p53; furthermore, an apoptotic pathway involving BAX activation, cytochrome *c* release, and activation of Caspase-9 and Caspase-3 has been implicated in the development of the disease (Levy et al., 2009; Tatton et al., 2003). Understanding whether apoptosis regulates Parkinson's Disease, and through what specific mechanisms and signaling pathways, will be essential for developing targeted therapies for this disorder.

Signaling Pathways and Regulatory Mechanisms in Apoptosis

Both the intrinsic (mitochondria-mediated) and extrinsic (receptor-mediated) pathways converge upon a common execution pathway initiated by activation of executioner Caspases—Caspases-3, -7, and -9—which cleave

downstream targets to induce the biochemical, biophysical, and morphological changes that constitute apoptosis (Slee et al., 2001). Caspase-3 activates the endonuclease CAD by cleaving its inhibitor, ICAD, leading to chromatin condensation and degradation of chromosomal DNA (Sakahira et al., 1998). The DNA repair enzyme poly (ADP-ribose) polymerase (PARP) is cleaved and inactivated in order to prevent ATP depletion (Simbulan-Rosenthal et al., 1998). The actin-binding protein Gelsolin is cleaved, and the resulting fragments subsequently cleave actin polymers, disrupting the cytoskeleton (Kothakota et al., 1997). The cell disintegrates into smaller, membrane-enclosed fragments called apoptotic bodies. *In vivo*, the final step of apoptosis occurs when phagocytic cells uptake these apoptotic bodies and recycle their contents. Cells undergoing apoptosis are recognized by phagocytes when phospholipids of the plasma membrane change orientation. Phosphatidylserine, for example, flips from the inner to the outer leaflet, providing a signal for disposal by noninflammatory phagocytes (Fadok et al., 2001; Ferraro-Peyret et al., 2002).

Extrinsic apoptosis is initiated when extracellular pro-apoptotic ligands activate transmembrane death receptors embedded in the cell surface. For example, the Fas Ligand (FasL) activates the Fas Receptor (FasR), while Tumor Necrosis Factor (TNF-α) activates the Tumor Necrosis Factor Receptor 1 (TNFR1). These death receptors are part of the TNF superfamily of receptors, and they contain a cysteine-rich domain exposed outside the cell and a death domain facing inward (Ashkenazi and Dixit, 1998; Locksley et al., 2001). Upon binding of ligands to receptors, the death domains of the receptors interact with

and activate adaptor proteins inside the cell (Grimm et al., 1996; Hsu et al., 1995), forming the death-inducing signaling complex (DISC). This complex induces auto-catalytic cleavage of pro-Caspase-8, leading to activation of Caspase-8 followed by subsequent cleavage and activation of executioner Caspases (Kischkel et al., 1995).

This research presented here will focus on the role of proteins that mediate the intrinsic apoptotic pathway (Figure 1-1), which can be activated by diverse stimuli such as UV radiation, ionizing radiation, and other forms of DNA damage as well as hypoxia, cytotoxic drugs, viral infections, and oxidative stress. During intrinsic apoptosis, cellular stressors such as DNA damage lead to mitochondrial outer membrane permeabilization (MOMP), releasing cytochrome *c* and other factors from the mitochondrial intermembrane space. Upon its release into the cytosol, cytochrome *c* interacts with APAF-1 and Caspase-9 to form the apoptosome, leading to auto-activation and cleavage of Caspase-9 and subsequent activation of Caspase-3, Caspase-7, and downstream targets. This process can also be regulated by other proteins released from the mitochondria during MOMP, such as XIAP, DIABLO/SMAC, and HtrA2/OMI (Du et al., 2000; Duckett et al., 1996; Faccio et al., 2000; Tait and Green, 2010; Verhagen et al., 2000).

Mitochondrial outer membrane permeabilization (MOMP) is regulated primarily by the BCL-2 family of proteins—a large group of both pro-apoptosis and pro-survival proteins, the balance of which determines a cell's fate (reviewed recently by (Chipuk et al., 2010) and (Youle and Strasser, 2008)). The anti-

apoptotic protein BCL-2 (B-cell lymphoma 2) was the first family member to be identified, after expression of the *BCL-2* gene was discovered to be altered in B-cell follicular lymphomas following a chromosomal translocation between chromosomes 14 and 18. This translocation places the gene behind an immunoglobulin heavy chain promoter and enhancer, leading to excessive transcription of BCL-2, thereby allowing the cell to evade apoptosis (Bakhshi et al., 1985; Cleary et al., 1986; Tsujimoto et al., 1985; Vaux et al., 1988). The finding that BCL-2's anti-apoptotic function promotes carcinogenesis established a paradigm for apoptosis as a tumor suppressor mechanism, and evasion of apoptosis is now widely accepted as a hallmark of cancer (Hanahan and Weinberg, 2000). The BCL-2 family now contains at least twenty identified members, all of which share one or more of four BCL-2 homology domains (BH1-4) (Youle and Strasser, 2008). The anti-apoptotic BCL-2 family members include BCL-2, BCL-XL, BCL-W, A1A, and MCL-1 and contain anywhere from two to four BH domains. Pro-apoptotic BCL-2 proteins include BAX and BAK, each of which contains BH1, BH2, and BH3 domains, and which permeabilize the mitochondrial outer membrane (MOM) during apoptosis. Another set of pro-apoptotic BCL-2 family members known as the "BH3-only" proteins activate apoptosis by antagonizing the function of anti-apoptotic members and/or by directly activating pro-apoptotic BAX or BAK; these include BAD, BIK, BID, HRK, BIM, BMF, NOXA, and PUMA, all of which share a BH3 domain but have little sequence or structural similarity to the other BCL-2 family members aside from this domain.

The BCL-2 family members' functions and domains are summarized in Figure 1-2.

The mitochondrial outer membrane is permeabilized directly by effector proteins BAX and/or BAK (Figure 1-3). BAX continually cycles between the mitochondria and cytosol, while BAK is constitutively localized to the mitochondria. In healthy cells, BAX is retro-translocated from the mitochondria to the cytoplasm by BCL-XL, but during apoptosis, the interaction between BCL-XL and BAX is disrupted, and BAX accumulates at the mitochondria (Edlich et al., 2011). Upon induction of apoptosis, both BAX and BAK undergo conformational changes to become "activated" and oligomerize on the mitochondrial outer membrane (Wei et al., 2001), leading to membrane permeabilization through a mechanism that is not yet clear but that may occur through formation of a proteinaceous or lipid pore (Chipuk and Green, 2008). Rather than being evenly distributed around the mitochondria, active BAX accumulates in massive clusters at the ends of mitochondria or co-localized with mitochondrial fission and fusion sites (Karbowski et al., 2002), leading to the proposal that BAX may either hijack the fission/fusion machinery and/or take advantage of the altered mitochondrial membrane structure at these sites in order to permeabilize the membrane. The exact biochemical mechanism by which BAX and BAK permeabilize the membrane is currently an area of intense investigation and has been described as one of the "holy grails" of apoptosis research (Youle and Strasser, 2008).

BAX and BAK become activated during apoptosis by pro-apoptotic BH3-only BCL-2 family proteins such as BIM, BID, and PUMA (Chipuk et al., 2005;

Gavathiotis et al., 2010; Kim et al., 2006; Kim et al., 2009; Kuwana et al., 2005; Letai et al., 2002; Lovell et al., 2008; O'Connor et al., 1998; Ren et al., 2010; Wei et al., 2000). Conversely, the pro-apoptotic function of BAX and BAK can be inhibited by pro-survival BCL-2 family proteins such as BCL-xL, MCL-1, and BCL-2 itself (Boise et al., 1993; Chipuk et al., 2010; Kozopas et al., 1993; Oltvai et al., 1993). The precise mechanisms by which BCL-2 family members interact to mediate apoptosis are still under debate, and several models have been proposed that are not necessarily mutually exclusive (Chipuk et al., 2010) (Figure 1-4).

The direct activation model proposes that pro-apoptotic BH3-only proteins bind directly to BAX or BAK to induce their activation, and that the role of anti-apoptotic proteins in healthy cells is to bind and sequester BH3-only proteins to prevent them from activating BAX and BAK. Several BH3-only proteins are capable of directly activating BAX and/or BAK in isolated mitochondria or large unilamellar vesicles (LUVs) meant to mimic the mitochondrial outer membrane. It is difficult to detect an interaction between in BAX or BAK and BH3-only proteins *in vivo*, likely because the interaction is thought to be transient. However, a recent study utilizing a mouse model in which the genes encoding BIM, BID, and PUMA were simultaneously deleted demonstrated that at least one of these “direct activator” proteins is necessary for activation of BAX and BAK *in vivo* (Ren et al., 2010).

Other BH3-only proteins, such as BAD, BIK, HRK, and NOXA, cannot directly activate BAX or BAK and are thought to function by binding with, and

thereby deactivating, anti-apoptotic proteins such as BCL-2 and BCL-xL (Chen et al., 2005; Chipuk et al., 2008; Kuwana et al., 2005; Letai et al., 2002). These BH3-only proteins may act as either sensitizers or de-repressors for the effector proteins. The sensitization model purports that the interaction between BH3-only proteins and anti-apoptotic BCL-xL or BCL-2 would not induce apoptosis, but would sensitize cells to apoptotic stimuli. In this scenario, BAX or BAK would still require direct activation by BIM, BID, or PUMA, but the “sensitizer” BH3-only proteins would deactivate the anti-apoptotics (e.g. BCL-2), preventing inhibition of the direct activators. In this way, the sensitizer BH3-only proteins would lower the threshold for BAX and BAK activation (Chipuk et al., 2010).

According to the derepression model, direct activator proteins (e.g. BIM or BID) are bound and sequestered by anti-apoptotic proteins (e.g. BCL-xL or BCL-2). During apoptosis, a derepressor BH3-only protein such as BAD competes with the direct activator for binding with the anti-apoptotic protein, releasing the direct activator. The direct activator is then free to interact with and activate BAX or BAK (Chipuk et al., 2010). This model is supported by *in vitro* FRET (fluorescence resonance energy transfer) studies using LUVs; in the presence of these membranes, anti-apoptotic BCL-xL was bound with the direct-activator BID. Introduction of the derepressor BAD disrupted the BCL-xL-BID complex, freeing BID to directly interact with and activate BAX, leading to permeabilization of the LUV (Lovell et al., 2008). Furthermore, when a pharmacological derepressor BH3 mimetic was used to treat chronic lymphocytic leukemia (CLL),

mitochondrial outer membrane permeabilization was induced (Certo et al., 2006; Del Gaizo Moore et al., 2007).

Finally, a neutralization model has been proposed in which the effector proteins BAX and BAK are always active but are sequestered by anti-apoptotic proteins such as BCL-2 or BCL-xL. For apoptosis to occur, BH3-only proteins compete for binding with the anti-apoptotic proteins, releasing the already-active BAX or BAK. According to this model, direct activator BH3-only proteins are not required for apoptosis; release of the effector proteins from their inhibitors is sufficient to activate apoptosis.

One difficulty in reconciling these contradictory models is that many of the studies examining the interactions between BCL-2 family members are based on *in vitro* experiments such as those involving isolated mitochondria or artificial LUVs, and many have utilized extensive ectopic expression of tagged proteins. These types of studies do not always recapitulate what occurs in a live cell *in vivo*; other proteins and lipids present in a live cell are likely to be important, as are stoichiometric ratios among BCL-2 family members. Two recent studies have partially resolved this issue by providing evidence that a direct activator protein is required for BAX and BAK to induce MOMP *in vivo*. In one study, mice were generated in which the BH3 domain of BIM was replaced by BAD, NOXA, or PUMA (Merino et al., 2009). In another, BIM, BID, and PUMA were knocked out simultaneously (Ren et al., 2010). Both of these genetic approaches demonstrated that direct activator proteins are necessary for BAX and BAK activation, BAX oligomerization, MOMP, and apoptosis *in vivo*. It is likely that in

intact cells, apoptosis is regulated by a combination of these models; sensitization and direct activation probably both contribute. As induction of MOMP is often a life-or-death decision for a cell, it is logical for it to be regulated by a complex mechanism. For example, one subset of BH3-only proteins may be required for direct activation of BAX and BAK, while another subset of sensitizing or derepressing BH3-only proteins must interact with anti-apoptotic proteins such as BCL-2 and BCL-xL to release their inhibition of the effector proteins.

Aside from BCL-2 family members, a handful of unrelated proteins have been found to regulate MOMP. Some of these proteins, while not considered BCL-2 family members, do contain a putative BH3 domain. These include MAP-1 and RAD9 (a DNA repair protein), which can directly activate BAX and BAK (Chipuk et al., 2010). Other proteins that do not have any known homology to the BCL-2 family are also reported to regulate apoptosis either through direct activation of BAX or BAK, or by interaction with anti-apoptotic BCL-2 family members. The transcription factor Nur77 is reported to convert BCL-2 from an anti-apoptotic to a pro-apoptotic protein (Thompson and Winoto, 2008). The tumor suppressor p53, which transcriptionally upregulates pro-apoptotic proteins following DNA damage, also interacts directly with BAX to induce its activation. Furthermore, p53 is reported to be sequestered by anti-apoptotic BCL-2 proteins and may also have a derepressor role (Chipuk et al., 2004; Leu et al., 2004; Marchenko et al., 2000; Mihara et al., 2003). Other non-BCL-2 inducers of MOMP include nucleophosmin, ASC, and ATG5 (reviewed by (Chipuk et al., 2010)). However, data from a triple knockout mouse model lacking BIM, BID, and

PUMA, in which activation of BAX and BAK did not occur, suggests that these non-BCL-2 proteins may not always be sufficient *in vivo* to induce BAX- or BAK-mediated apoptosis (Ren et al., 2010). VDAC2 can regulate MOMP by binding to BAK, restraining it in an inactive monomer conformation. The following non-BCL-2 proteins are also reported to regulate MOMP through mechanisms that are unclear: Histone H1.2, 14-3-3θ , Ku70, and BRCC2 (reviewed by (Chipuk et al., 2010)).

Mitochondria themselves are not passive bystanders in their permeabilization during apoptosis. Components of the membrane are known to be important, as BAX and t-BID fail to interact in the absence of natural or artificial membranes (Lovell et al., 2008). Recently, mitochondrial dynamics have emerged as another means by which MOMP may be regulated (Martinou and Youle, 2011). In healthy cells, individual mitochondria continually fuse and divide. Fusion is regulated primarily by Mitofusin proteins 1 and 2 (MFN1, MFN2). Mitofusins located on adjacent mitochondria dimerize, anchoring mitochondria together to initiate the fusion process (Chen et al., 2003; Santel and Fuller, 2001). Fission is mediated largely by dynamin-related protein 1 (DRP1), (Karbowski et al., 2002; Labrousse et al., 1999; Otsuga et al., 1998; Smirnova et al., 2001). Fission and fusion occur continuously, and if the balance between these two processes is altered, aberrant mitochondrial structure results. With an excess of fusion, mitochondria become elongated and form networks, while overabundant fission causes mitochondria to fragment into smaller, yet intact, organelles.

Mitochondrial fragmentation occurs during apoptosis prior to cytochrome *c* release (Brooks et al., 2007; Lee et al., 2004), and evidence has accumulated to support the idea that fragmentation plays an active role in MOMP. Inhibition of fusion-promoting proteins MFN1 or MFN2 causes mitochondria to become fragmented and sensitizes cells to MOMP and apoptosis (Sugioka et al., 2004), while overexpression of MFN1 or MFN2 reduces fragmentation and protects cells from apoptosis (Brooks et al., 2011). Additionally, a chemical inhibitor of fission, Mdivi-1, as well as fusion-inducing cysteine alkylators and N-ethyl-maleimide (NEM), partially inhibit fragmentation, MOMP, and apoptosis (Bowes and Gupta, 2005; Cassidy-Stone et al., 2008). Likewise, inhibition of fission-mediating DRP1 by RNAi or by introducing dominant-negative mutations in the GTPase domain partially inhibits mitochondrial fragmentation while delaying MOMP and apoptosis (Brooks et al., 2011; Frank et al., 2001). Furthermore, a recent study showed compelling evidence that DRP1 modulates apoptosis by altering mitochondrial dynamics, stimulating BAX oligomerization (Montessuit et al., 2010).

Unknowns in Field of Apoptosis Research

While much has been learned about mechanisms and signaling pathways regulating apoptosis, especially the roles of pro- and anti-apoptotic BCL-2 family proteins, our understanding is incomplete in several areas. Many of the non-BCL-2 proteins' specific biochemical mechanisms in regulating apoptosis are unknown, and additional proteins that regulate apoptosis remain to be identified. Currently, much research is focused on the mechanisms regulating MOMP, as

this process is often the point of no return for deciding a cell's fate. More specifically, controversy still exists regarding the competing models (direct activation, sensitization, derepression, and neutralization) for interactions among BCL-2 family members in regulating MOMP. There is also a high level of interest in elucidating the precise biochemical mechanisms by which BAX and BAK permeabilize the mitochondrial outer membrane (i.e. through formation of a protein or lipid pore, or an alternate mechanism). Gaining a better understanding of these processes will contribute to our knowledge of organismal development and homeostasis and may aid in the design of targeted therapeutic drugs to treat diseases affected by aberrant regulation of apoptosis, such as autoimmune disorders, neurodegenerative disease, and cancer.

p32/C1QBP: a Multifunctional Protein Recently Identified as a Regulator of Apoptosis

Previous work in our laboratory ((Itahana and Zhang, 2008) and unpublished data) uncovered a critical role for the mitochondria-localized non-BCL-2 protein p32 in regulating apoptosis. This multifunctional protein (also known as GC1QR for receptor for C1q; HABP1 for hyaluronic acid binding protein 1; C1QBP for globular head component factor C1q binding protein) is thought to be localized primarily in the mitochondrial matrix (Dedio et al., 1998; Muta et al., 1997). p32 is reported to interact with complement component C1q (Ghebrehiwet et al., 1994), may play roles in RNA splicing (Petersen-Mahrt et al., 1999) and oxidative phosphorylation (Muta et al., 1997), and was recently

reported to mediate apoptotic response (Chowdhury et al., 2008; Kamal and Datta, 2006).

Our laboratory discovered a novel role for p32 in regulating ARF-mediated apoptosis through regulation of mitochondrial membrane potential prior to MOMP (Itahana and Zhang, 2008), and a second role for p32 downstream of MOMP following release of mature, cleaved p32 from the mitochondria (Itahana and Zhang, unpublished data). However, a precise biochemical mechanism for the function of p32 in these two roles was lacking. In order to learn more about the mechanism of p32 in regulating apoptosis, we sought to identify novel binding partners for p32. Thus, a large-scale co-immunoprecipitation was carried out for p32, and potential p32-interacting partners were identified by mass spectrometry. Of these, we selected two uncharacterized proteins for further study: MAGE-D2 (melanoma antigen family D2) and SUMI-1 (survival-promoting mitochondrial protein 1, also known as CHCHD2 for coiled-coil-helix coiled-coil-helix domain-containing 2). While the initial rationale for identifying novel p32-interacting proteins was to provide a means to better understand the mechanism of p32's apoptotic functions, we opted instead to study MAGE-D2 and SUMI-1 individually prior to pursuing studies regarding their interaction with p32. In this body of work, the research performed to characterize these two proteins' localization and functions will be presented. In Chapter VI, future experiments are proposed for examining the function of these proteins' interactions with p32.

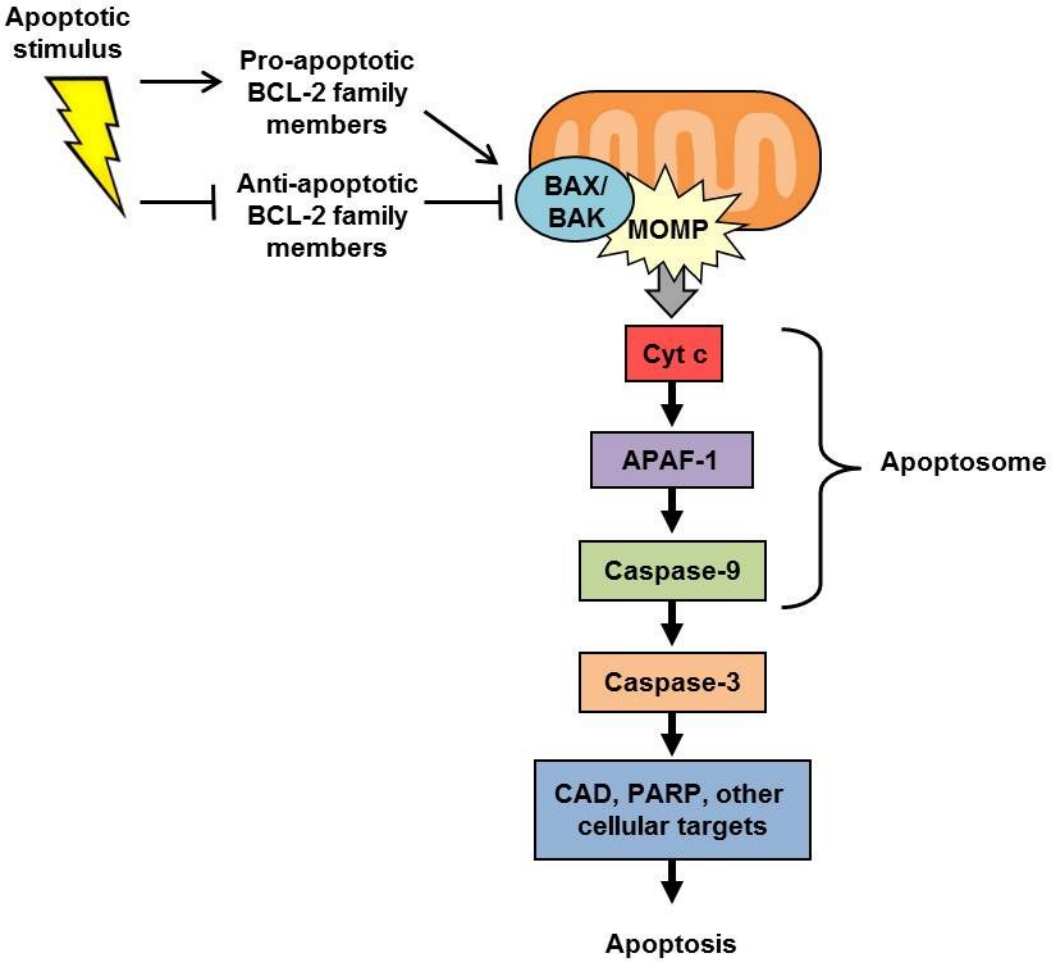

Figure 1-1. Key signaling molecules in the intrinsic apoptosis pathway.
This illustration depicts a simplified version of key signaling events in the intrinsic (mitochondria-mediated) apoptosis pathway. During apoptosis, an important regulatory event is mitochondrial outer membrane permeabilization (MOMP). MOMP is regulated primarily by pro- and anti-apoptotic BCL-2 family proteins. Upon treatment with apoptotic stimuli such as UV radiation, pro-apoptotic proteins are induced, leading to activation and oligomerization of pro-apoptotic effector proteins BAX and/or BAK. Oligomerization of these effectors induces MOMP, causing release of mitochondrial intermembrane space proteins such as cytochrome *c* into the cytosol. Cytochrome *c* then interacts with APAF-1 and Caspase-9 to form the apoptosome, leading to Caspase-9 auto-cleavage and activation. Active Caspase-9 then cleaves and activates Caspase-3, leading to cleavage of CAD, PARP, and other downstream targets to induce apoptosis.

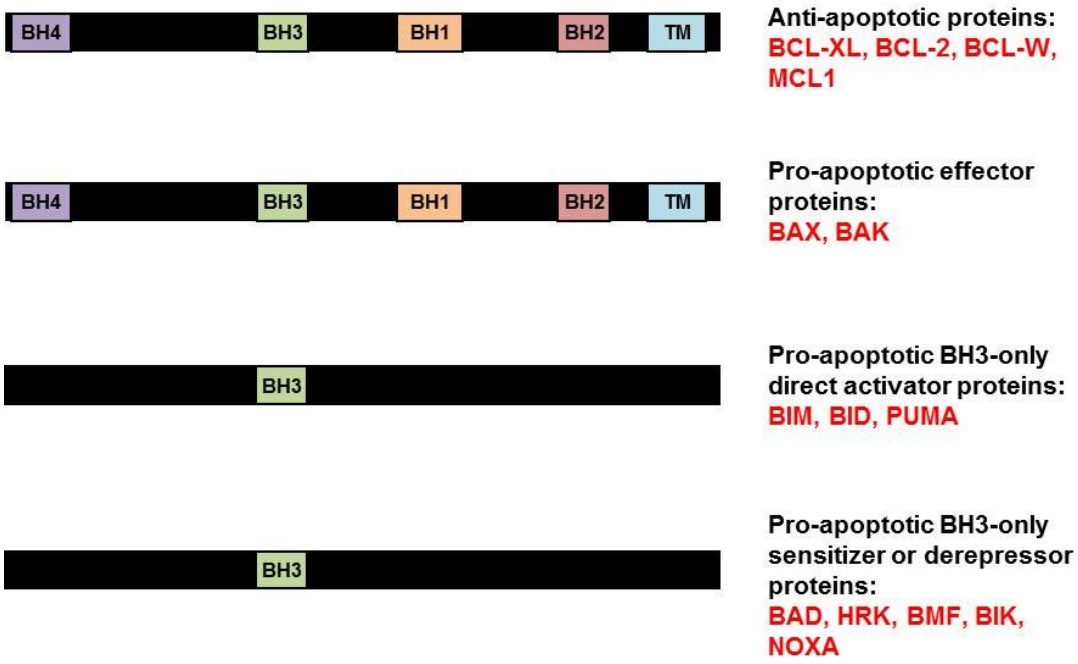

Figure 1-2. Functional organization and general domain structure of BCL-2 family proteins.
BCL-2 family members can be divided into four categories according to function, as shown. BH (BCL-2 homology) domains and TM (transmembrane) domains that are present among most members of each category are indicated. Illustrations are not to scale.

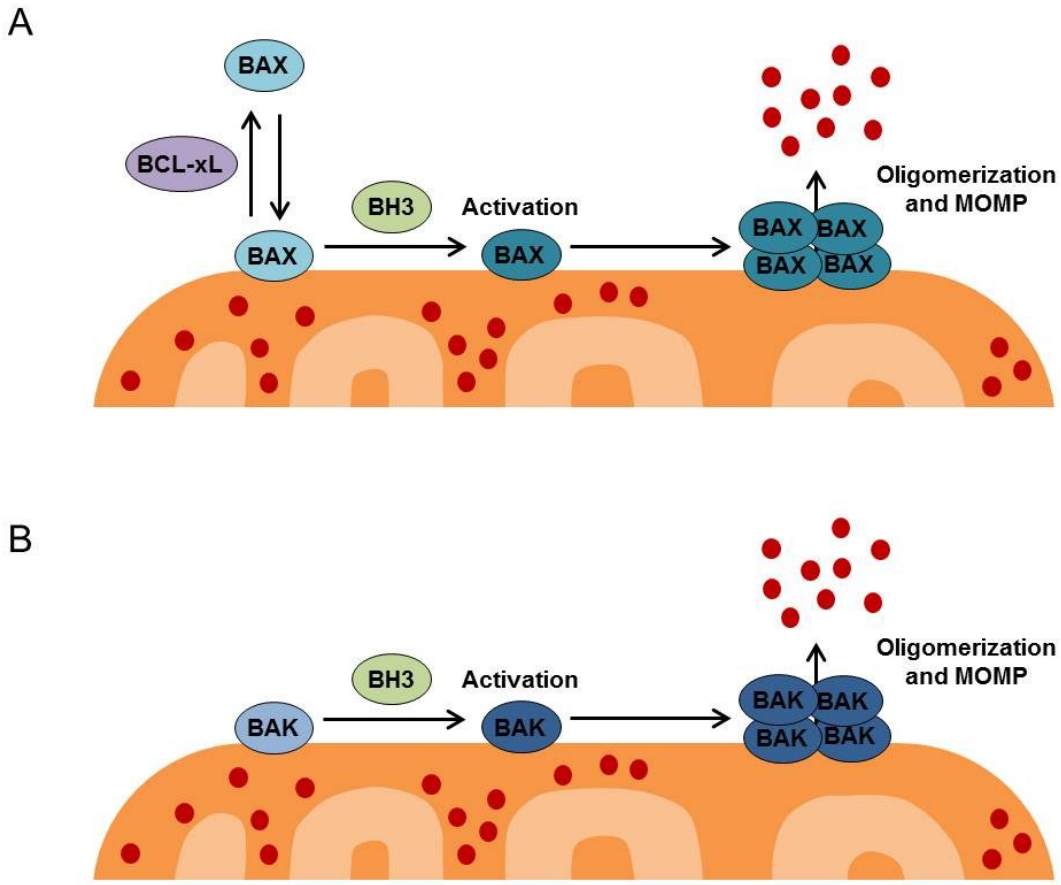

Figure 1-3. Regulation of mitochondrial outer membrane permeabilization (MOMP) by BAX and BAK.
A) In healthy cells, BAX continually cycles between the cytosol and mitochondria, with the majority of BAX existing in a soluble, cytosolic form. BCL-xL promotes retro-translocation of BAX to the cytosol. During apoptosis, BCL-xL is inhibited, allowing BAX to accumulate at the mitochondria. Upon activation by BH3-only proteins, BAX undergoes a conformational change and subsequently oligomerizes, inducing MOMP and cytochrome *c* release.
B) BAK is constitutively localized to the mitochondria. During apoptosis, BAK is activated by BH3-only proteins, leading to BAK oligomer formation and MOMP.

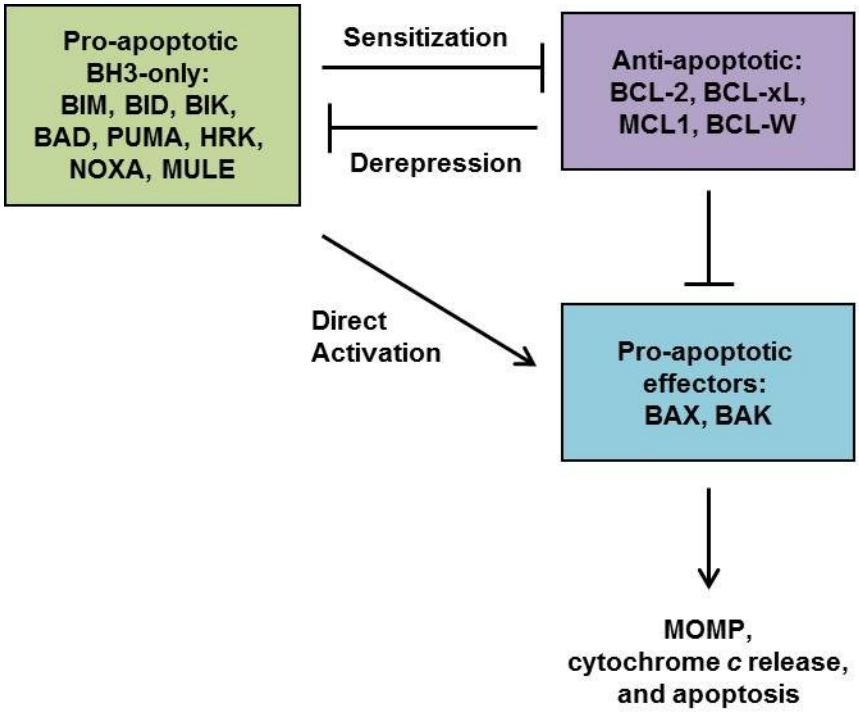

Figure 1-4. Competing models of apoptosis regulation by BCL-2 family proteins.
The direct activation model proposes that specific BH3-only proteins can directly interact with and activate the effector proteins BAX and BAK. The sensitization model says that certain BH3-only proteins can bind to and inactivate anti-apoptotic proteins, releasing their inhibition of BAX and BAK, thereby sensitizing cells to apoptosis. According to the derepressor model, anti-apoptotic proteins bind and sequester direct-activator BH3-only proteins, preventing their activation of BAX and BAK. When activated, the effector proteins BAX and BAK induce MOMP and cytochrome *c* release, leading to apoptotic cell death.

CHAPTER II

IDENTIFICATION OF MAGE-D2 AND SUMI-1 AS NOVEL INTERACTING PARTNERS FOR THE PRO-APOPTOTIC PROTEIN P32/C1QBP

Introduction

Recently, our lab uncovered novel roles for the multifunctional protein p32/C1QBP in regulating apoptosis by two distinct mechanisms. First, p32 was found to be required for apoptosis induced by the tumor suppressor ARF (Itahana and Zhang, 2008). Later, p32 was found to be a critical mediator for apoptosis induced by a broad range of stimuli (unpublished data). Thus, p32 regulates apoptosis by two mechanisms: 1) It recruits ARF to the mitochondria, where ARF induces a change in mitochondrial membrane potential ($\Delta\Psi_m$), sensitizing cells to apoptosis (Itahana and Zhang, 2008), and 2) Once released into the cytoplasm, mature (cleaved) p32 activates Caspase-9 and Caspase-3 to induce apoptosis (unpublished data). However, the exact mechanisms by which p32 induces apoptosis have been elusive. One means by which a protein's functional mechanisms can be elucidated is through identification of novel interacting proteins. Thus, in order to learn more about this novel critical regulator of apoptosis, we performed a screen to search for previously unknown p32 binding partners.

Screen for Novel p32-Interacting Proteins

In order to identify potential novel interacting partners for p32, a large-scale co-immunoprecipitation was carried out for Flag-tagged p32. First, cell lines were generated to express p32-Flag in a stable manner. U2OS (human osteosarcoma) cells were transfected with a pcDNA3-p32-Flag plasmid, and clones expressing the plasmid were selected for with the antibiotic G418. Clones stably-expressing p32-Flag were obtained, and expression of p32-Flag was confirmed by western blotting (Figure 2-1). Correct mitochondrial localization of p32-Flag was confirmed by immunofluorescence imaging, as indicated by co-localization with the mitochondria-labeling dye MitoTracker™ Red (Figure 2-2).

A large-scale co-immunoprecipitation (co-IP) was then carried out with the p32-Flag stable cell lines, using mock-transfected U2OS cells as a negative control. Fifteen 100-mm plates of each cell type were lysed with 0.1% NP-40 lysis buffer, and a co-IP was performed using gel beads pre-conjugated with Flag antibody in order to pull down protein complexes containing p32-Flag. These complexes were resolved by SDS-PAGE, and the resulting gel was stained with Coomassie Brilliant Blue to visualize bands representing potential p32 binding partners (Figure 2-3). Each band was subjected to mass spectrometry to identify the proteins likely to be present in the band. A list of bands identified, representing potential p32 interacting partners, is shown in Table 2-1.

Selection of MAGE-D2 and SUMI-1 for Further Study

After careful examination of the eight putative p32-interacting proteins identified, two were selected for further study: MAGE-D2, an uncharacterized melanoma antigen family protein, and SUMI-1, an uncharacterized protein predicted to localize to the mitochondria.

MAGE-D2 was selected primarily because its close homolog, NRAGE/MAGE-D1 is known to regulate apoptosis (Barker and Salehi, 2002; Chomez et al., 2001). The MAGED genes, including MAGE-D1 and MAGE-D2, are clustered on chromosome Xp11, and the gene encoding MAGE-D2 is located at Xp11.2, a hot spot for X-linked mental retardation. Unlike the initially-discovered MAGE family members, whose expression is detected only during embryonic development and in tumor cells, MAGE-D2 is ubiquitously expressed in adult tissues (Langnaese et al., 2001). No studies have been published regarding the function of MAGE-D2, but its expression has been linked to cancer initiation and/or progression. MAGE-D2 overexpression is associated with small-intestinal carcinoid neoplasia (Kidd et al., 2006a) and with progression of gastric neoplasia, and the level of MAGE-D2 differentiates Type III/IV gastric neoplasias from Type I/II (Kidd et al., 2006b). MAGE-D2 upregulation is also linked to liver metastasis of colon cancer (Li et al., 2004). A close homolog of MAGE-D2—NRAGE/MAGE-D1—was reported to interact with the p75 neurotrophin receptor to promote nerve growth factor-dependent apoptosis (Salehi et al., 2000). NRAGE can also interact with the apoptosis inhibitory factor XIAP (X-linked

inhibitor of apoptosis) and appears to accelerate degradation and inactivation of XIAP during apoptosis (Jordan et al., 2001).

SUMI-1 is a small, CHCH domain-containing protein, and no studies regarding its functions were published when we began our research on this protein. SUMI-1 was selected for further study primarily because another protein reported to be a mouse ortholog of SUMI-1 (NDG1; Nur77 downstream gene 1) was shown to regulate apoptosis after induction by the nuclear steroid orphan receptor Nur77 (Rajpal et al., 2003). However, upon further investigation, this protein was found not to be a direct ortholog of SUMI-1 as reported. In addition, unlike the majority of putative p32-interacting proteins identified, SUMI-1 was predicted to localize to the mitochondrion (Claros and Vincens, 1996), an organelle with strong ties to apoptotic cell death.

Confirmation of Binding Between p32-SUMI-1 and p32-MAGE-D2

To determine whether MAGE-D2 and SUMI-1 represent genuine binding partners for p32, additional co-immunoprecipitation experiments were carried out. U2OS cells were transfected with p32-Flag, Myc-SUMI-1, and/or Myc-MAGE-D2 and immunoprecipitated for Flag to pull down p32-Flag-containing complexes. Samples were resolved by SDS-PAGE and blotted for Myc or Flag, where indicated. Binding was confirmed between p32-Flag and SUMI-1-Myc, with no signal detected in cells not transfected with p32-Flag, indicating that SUMI-1-Myc did not interact nonspecifically with the Flag antibody. A strong interaction was also confirmed between p32-Flag and MAGE-D2-Myc. A small amount of signal

was detected in the negative control lane, which likely represents spillover from another lane and/or incomplete washing of beads; however, a dramatically higher signal was detected in cells transfected with p32-Flag, despite lower expression of MAGE-D2-Myc (see loading panel), indicating that MAGE-D2-Myc does interact nonspecifically with the Flag antibody (Figure 2-4). Thus, we detected binding of ectopically expressed p32 with both SUMI-1 and MAGE-D2

Interaction of endogenous proteins was also examined. Untreated U2OS cell lysates were immunoprecipitated for SUMI-1 or MAGE-D2, using two different antibodies for each protein. Samples were resolved by SDS-PAGE and blotted for SUMI-1, MAGE-D2, and p32. One SUMI-1 antibody successfully immunoprecipitated SUMI-1, and p32 was also detected in this lane, demonstrating endogenous SUMI-1-p32 binding. Both MAGE-D2 antibodies were capable of pulling down MAGE-D2 and also immunoprecipitated p32, albeit with lower affinity than that of the SUMI-1-p32 interaction (Figure 2-5). Thus, the p32-SUMI-1 and p32-MAGE-D2 interactions were both confirmed in three ways: 1) Immunoprecipitation of ectopic p32 and detection of endogenous SUMI-1 and MAGE-D2 by mass spectrometry, 2) IP of ectopically-expressed proteins and detection with Flag and Myc antibodies, and 3) IP of endogenous proteins in untransfected cells and detection with antibodies toward endogenous proteins.

Materials and Methods

Cell culture, transfections, and generation of stable cell lines. U2OS cells were obtained from ATCC and cultured in a 37°C incubator with 5% CO_2 in

DMEM supplemented with 10% FBS, 100 U/ml penicillin, and 100 g/ml streptomycin. DNA transfections were carried out with Effectene® (Qiagen) according to the manufacturer's instructions. Cells were transfected with pcDNA3-p32-Flag or pcDNA3 vector and subject to selection with G418. Individual clones were isolated and cultured, and expression of p32-Flag was examined by immunofluorescence staining and/or western blotting.

Co-immunoprecipitation, SDS-PAGE, and western blotting. For co-immuno-precipitations (co-IP), cells were lysed in 0.1% NP-40 lysis buffer, pre-cleared for 30 minutes with CL-4 beads, and incubated in primary antibody for 4 hours to overnight followed by incubation in Protein A beads for 1 hour. Beads were washed 3x and protein complexes were eluted using 1x SDS-PAGE sample buffer. For the large-scale co-IP, cells were treated as above but incubated in beads pre-conjugated with Flag antibody (ANTI-FLAG® M2 Affinity Gel, Sigma). Where indicated, a portion of lysate was reserved prior to IP and used as a loading control. Beads were washed 3x, and 1x-SDS sample buffer was added to remove protein complexes from beads. IP samples and loading controls were resolved by SDS-PAGE with a 12.5% or 15% polyacrylamide gel and transferred onto a 0.2 μM nitrocellulose membrane. Membranes were blocked for a minimum of 30 minutes in phosphate-buffered saline buffer with 0.1% Tween-20 (PBST) and 5% nonfat dried milk. Membranes were incubated for 2h to overnight in primary antibody, incubated for 1-2 hours in secondary HRP-conjugated antibody, and exposed with Supersignal West Pico (Pierce).

DNA Plasmids. C-terminally Flag-tagged p32, N-terminally Myc-tagged SUMI-1, and N-terminally Myc tagged MAGE-D2 were cloned into a pcDNA3.1 vector (Invitrogen) and confirmed by restriction digest and DNA sequencing.

Antibodies. Monoclonal mouse ANTI-FLAG® M2 antibody was purchased from Sigma. Rabbit anti-Myc antibody was purchased from Abcam. Rabbit anti-SUMI-1 (94, 124) and rabbit anti-MAGE-D2 (180, 262) antibodies were used for endogenous co-IP.

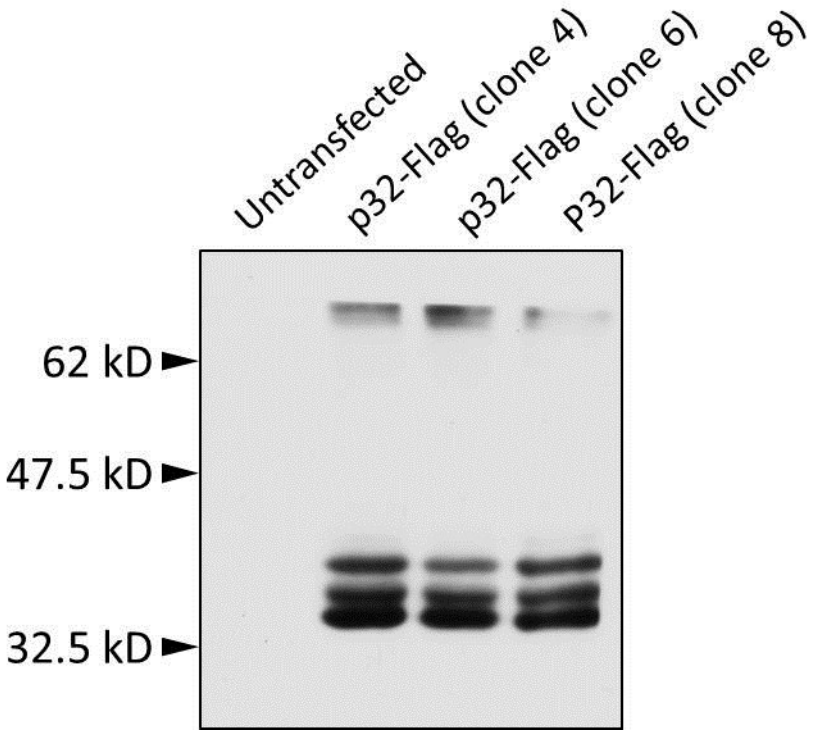

Figure 2-1. Clones stably expressing p32-Flag.
Western blot showing expression of p32-Flag fusion protein, detected with Flag antibody, in whole cell extracts of three U2OS clones stably transfected with p32-Flag plasmid. Untransfected U2OS cell lysate was used as a negative control.

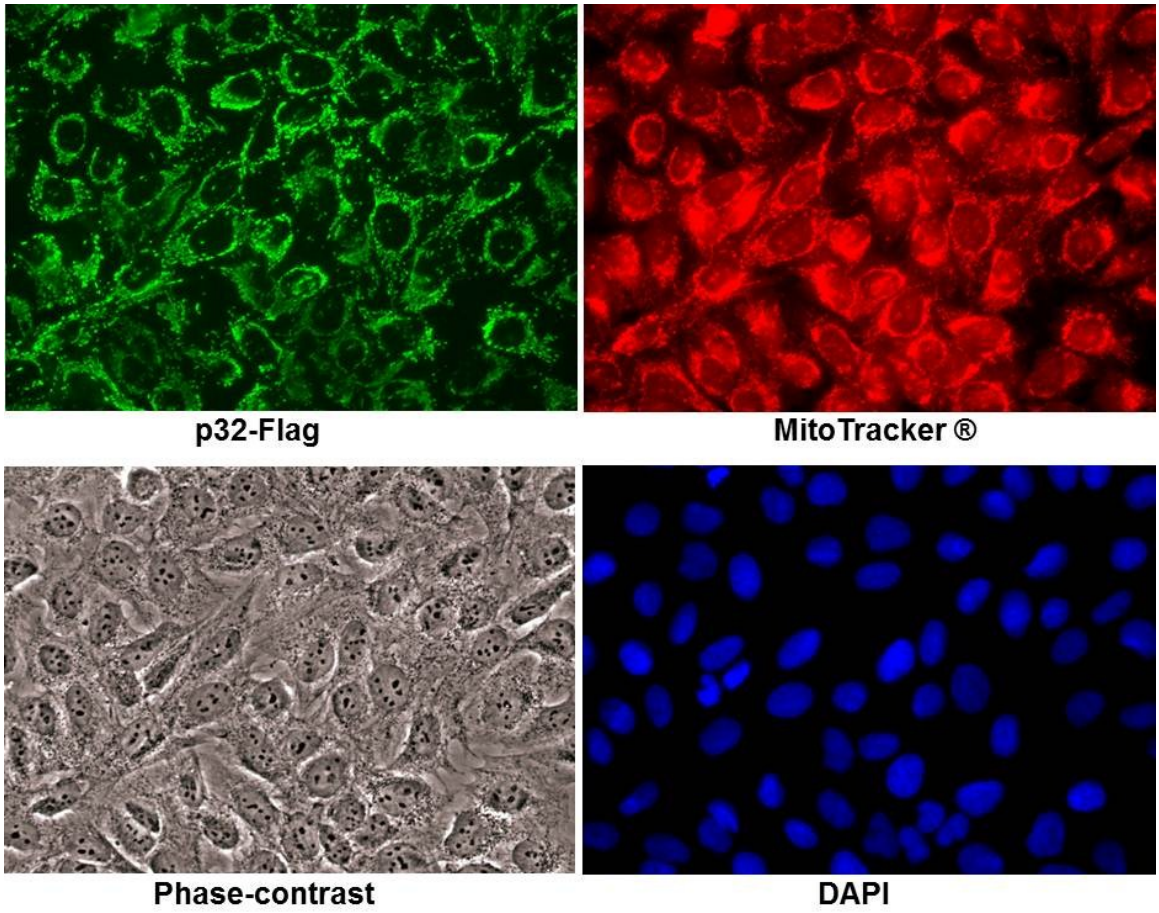

Figure 2-2. U2OS cells stably expressing p32-Flag.
Immunofluorescence imaging shows that p32-Flag in stably-transfected U2OS cells is correctly localized to the mitochondria, as indicated by staining with MitoTracker® Red.

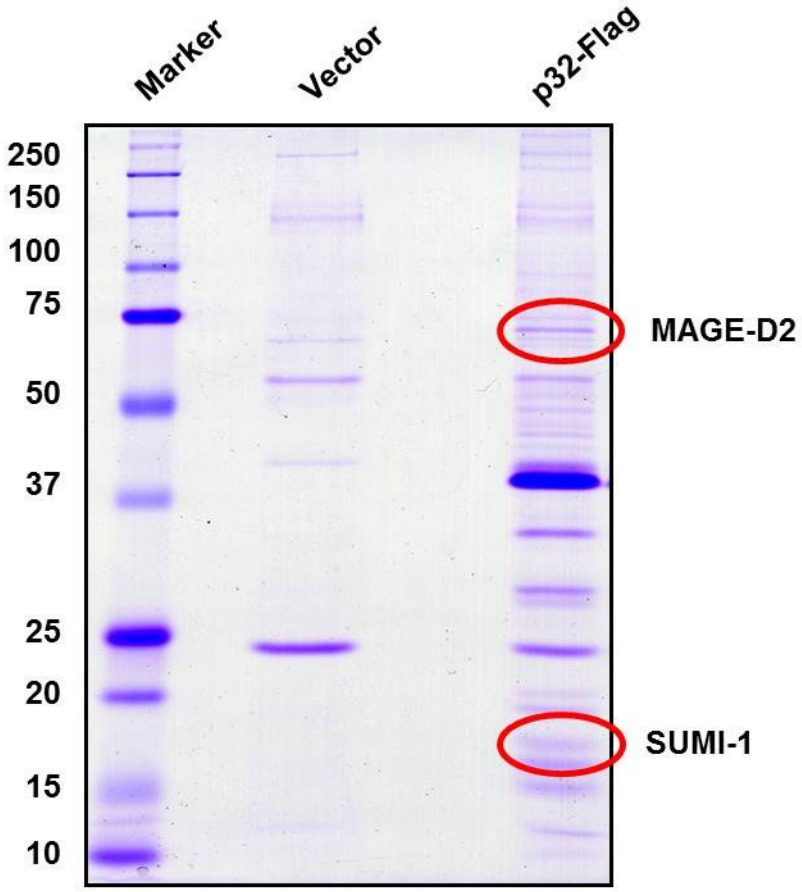

Figure 2-3. Large-scale co-immunoprecipitation of p32.
U2OS (human osteosarcoma) cells stably transfected with empty plasmid (Vector) or p32-Flag were lysed with 0.1% NP-40 lysis buffer and incubated with Flag-conjugated beads. Immunoprecipitated complexes were resolved by SDS-PAGE and visualized with Coomassie Blue staining. Bands that are present in p32-Flag IP but not the vector-only control represent putative p32-interacting proteins and were analyzed by mass spectrometry. Bands representing MageD2 and SUMI-1 are indicated. Other identified bands are shown in Table 2-1.

Protein	Function
ZFP91 (zinc finger protein 91 homologue)	Putative transcription factor; upregulated in acute myeloid leukemia (Unoki et al., 2003)
NO66 (nucleolar protein 66)	Ribosomal biogenesis, chromatin remodeling (Eilbracht et al., 2004)
MAGE-D2 (melanoma antigen family D2)	Uncharacterized; homolog MAGE-D1 regulates apoptosis (Chomez et al., 2001)
YB1 (Y-box binding protein 1)	Transcription factor; regulates cell cycle (Jurchott et al., 2003)
ALY-THOC4 (THO complex subunit 4)	Transcriptional co-activator; couples transcription to mRNA export (Bruhn et al., 1997; Luo et al., 2001)
Ribosomal protein S7	Translation of proteins (Annilo et al., 1995)
SUMI-1/CHCHD2	Uncharacterized
Ribosomal protein S17	Translation of proteins (Chen and Roufa, 1988)

Table 2-1. Potential p32-interacting proteins.
Bands identified by mass spectrometry following a large-scale co-immunoprecipitation of p32-Flag in stably-transfected U2OS cells.

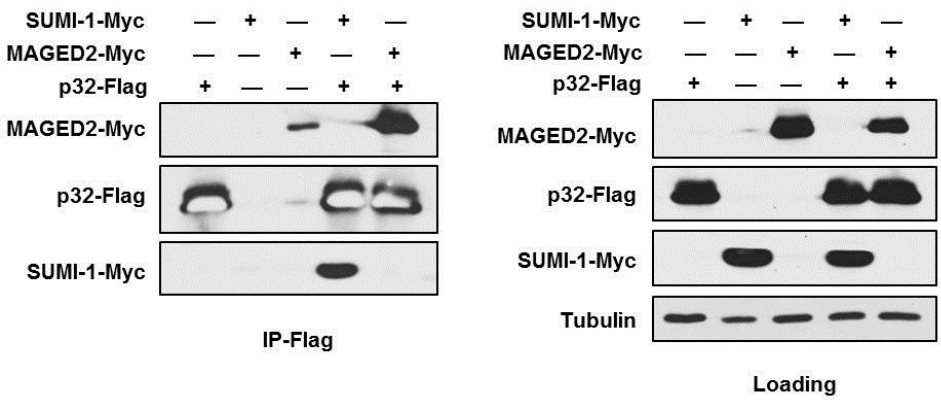

Figure 2-4. Confirmation of p32-MAGE-D2 and p32-SUMI-1 binding.
Western blots showing interaction between ectopically-expressed proteins. U2OS cells were transfected with p32-Flag and either SUMI-1-Myc or MAGED2-Myc where indicated. Lysates were immunoprecipitated with Flag antibody and resolved by SDS-PAGE. IP is shown in panel on left, and loading is shown on right.

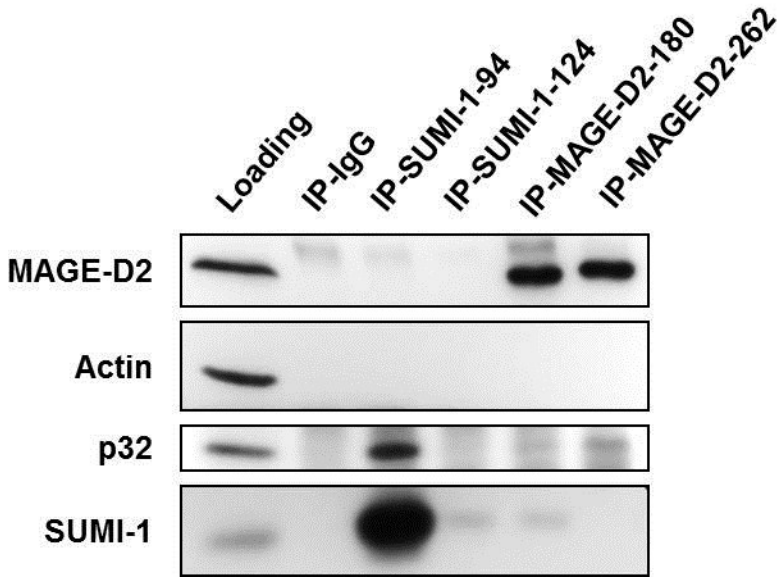

Figure 2-5. Endogenous binding between p32-MAGED2 and p32-SUMI-1. Western blot showing interaction between endogenous proteins. Lysates from untransfected U2OS cells were immunoprecipitated with indicated antibodies (IgG, negative control) and resolved by SDS-PAGE. Loading is shown on left. Note that the SUMI-1-94 antibody is effective for immunoprecipitation, while the SUMI-1-124 is not. MAGE-D2 could be immunoprecipitated with both antibodies, and a p32 band could be observed for each MAGE-D2 IP.

CHAPTER III

LOCALIZATION AND FUNCTIONAL STUDIES OF THE UNCHARACTERIZED MELANOMA ANTIGEN FAMILY PROTEIN, MAGE-D2

Introduction and Background

The initial members of the human MAGE (melanoma antigen family) genes to be identified are silent in normal adult tissues and expressed only in the male germ line and tumor cells. These proteins—the MAGE-A, MAGE-B, and MAGE-C subfamilies—are located in clusters on the X chromosome and are each encoded by a single exon. Because of their tumor-specific expression, these proteins have generated interest as potential targets for cancer immunotherapy. Now, the MAGE family has been expanded to include more than 25 members, and some of these are expressed in normal tissues (Chomez et al., 2001). Among these are the MAGE-D subfamily, comprised of MAGE-D1/NRAGE, MAGE-D2, MAGE-D3, and MAGE-D4, each of which contains both a MAGE homology domain (MHD, or MHD I) and a MAGE homology II domain (MHD II). The MHD is found in all MAGE proteins, while the MHD II is shared only by Type II MAGE proteins, which include MAGE-D1-4, MAGE-E1, and MAGE-L2. The MAGE-D subfamily is also unique from the MAGE-A, -B, and -C families in that each member is encoded by multiple exons rather than a single exon (Chomez et al., 2001). The functions of MAGE family proteins are not well-

known, although roles have been uncovered for Type II MAGE proteins in cell survival, cell cycle progression, and apoptosis (Barker and Salehi, 2002).

Because there is known to be extensive functional redundancy among MAGE proteins, examination of other MAGE-D family members can yield clues to potential functions and mechanisms for MAGE-D2. Of the MAGE-D subfamily, only MAGE-D1 has been well-characterized. MAGE-D1 shares 41% amino acid identity with MAGE-D2 and has been reported to regulate apoptosis through several mechanisms. MAGE-D1 interacts with the p75 neurotrophin receptor (p75NTR), which is a member of the TNF (tumor necrosis factor) family of proteins, and co-expression of MAGE-D1 with p75NTR greatly enhances neurotrophin-receptor-mediated apoptosis (Salehi et al., 2000). Overexpression of MAGE-D1 alone was also found to be sufficient to induce apoptosis (Barker and Salehi, 2002; Salehi et al., 2000) by activating c-Jun N-terminal kinase (JNK), leading to phosphorylation of c-Jun, release of cytochrome c, and Caspase activation (Salehi et al., 2002). MAGE-D1 also interacts with several homeodomain family transcription factors that regulate development through control of cell cycle and apoptosis—Msx2, Dlx7, and Dlx5—and MAGE-D1 was shown to be required for Dlx5-dependent transcription (Masuda et al., 2001). MAGE-D1 has also been identified as a binding partner for the anti-apoptotic proteins XIAP and ITA, both members of the IAP (inhibitor of apoptosis) family of proteins (Jordan et al., 2001). IAP proteins block apoptotic cell death by binding to and inhibiting activated Caspases. MAGE-D1 appears to interact with XIAP to accelerate apoptosis induced by IL-3 withdrawal in IL-3-dependent 32D cells.

The exact mechanism is unclear but appears to involve formation of a transient complex between MAGE-D1 and XIAP that may lead to XIAP's degradation and inactivation (Jordan et al., 2001). MAGE-D1-induced apoptosis and cell cycle arrest have both been shown to require activation of the tumor suppressor p53 (Kendall et al., 2005; Wen et al., 2004), which is contrary to the roles of several anti-apoptotic Type I MAGE proteins that have been shown to inhibit p53's transcriptional activity (Doyle et al., 2010; Marcar et al., 2010; Monte et al., 2006; Yang et al., 2007).

MAGE-D2 is not well-characterized but has been identified in several screens for genes with altered expression in cancers. The gene encoding MAGE-D2 is located at chromosome Xp11.2, a hot-spot for x-linked mental retardation, and yields 3 known transcripts. The MAGE-D2 protein is encoded by 11 exons and contains 606 amino acids, with a predicted molecular weight of 65 kD. It contains two known domains, MHD I and MHD II (Figure 3-1), and an arginine-rich region from aa 215-258. The protein is highly conserved in mammals, with 87% amino acid identity in mice (*mus musculus*). In zebrafish (*danio rerio*) and the fruit fly (*drosophila melanogaster*), a single MAGE gene is orthologous to the entire human MAGE family; human MAGE-D2 retains 38% amino acid identity to this gene in zebrafish and 24% identity to the fruit fly ortholog (data obtained from HomoloGene). Like MAGE-D1, human MAGE-D2 is expressed ubiquitously in adult tissues, and its expression is higher in certain brain regions and in the interstitium of the testes (Langnaese et al., 2001). In mice, semiquantitative mRNA dot-blot analysis revealed the presence of MAGE-D2 transcripts in all

adult tissues tested; its expression increases steadily during embryonic development, reaching a maximum just before birth; and mouse embryonic tissues contain a higher level of MAGE-D2 expression than do adult tissues (Chomez et al., 2001). The expression of human MAGE-D2 is elevated in a number of cancers including those derived from the breast (fresh breast cancer tissue, but not breast cancer cell lines) (Hudelist et al., 2006), appendix (Modlin et al., 2006), stomach (Kidd et al., 2006b), and small intestine (Kidd et al., 2006a). Its overexpression is also associated with cancer progression and metastasis—It is elevated 5-10 fold in Type III/IV gastrointestinal cancers but not in Type I/II tumors (Kidd et al., 2006b), it is associated with progression of appendiceal tumor malignancy (Modlin et al., 2006), and it is expressed to a significantly higher degree in colon cancer tumors with liver metastasis than those that have not metastasized (Li et al., 2004).

The functions of MAGE-D2 are unknown, and no studies have been published, to date, regarding its functions. Its elevated expression in cancers and association with cancer progression could implicate MAGE-D2 in a variety of potential roles such as cell proliferation, evasion of apoptosis, cell migration, or cell adhesion. It can be phosphorylated at multiple serine residues (Matsuoka et al., 2007; Olsen et al., 2006), and a screen for substrates of ATM and ATR in the DNA damage response found that MAGE-D2 is phosphorylated by ATM/ATR at specific serine residues (SER-146, SER-162, SER-190, SER-191, and SER-194) following DNA damage (Matsuoka et al., 2007), suggesting that it may be an effector of the ATM- and ATR-mediated DNA damage response pathway. In this

study, we sought to characterize the subcellular localization of MAGE-D2 and investigate whether it plays a role in apoptotic cell death.

Generation of Antibodies for Study of Endogenous MAGE-D2

When we began our research on MAGE-D2, no antibodies were available for biochemical analyses such as western blotting, immunoprecipitation, and immunofluorescence staining of endogenous MAGE-D2. In order to carry out these studies, we generated two rabbit polyclonal antibodies toward MAGE-D2, each targeting a different region of the protein. Various features of the amino acid sequence were assessed in order to identify optimal regions of approximately 12-16 amino acids in length to use as antigens. The most suitable antigens have low hydrophobicity (and are, therefore, more likely to be exposed at the protein surface), high complexity (e.g. beta-turn tendency), high antigenicity, and minimal sequence similarity to other proteins (in order to increase specificity). An additional cysteine must be placed on one terminus in order to conjugate the peptide to the immunogenic protein, KLH (keyhole limpet cyanin), which enhances the immune response in the host. Therefore, no internal cysteines can be present in the selected antigen region. Based on careful analysis of the MAGE-D2 sequence according to the above parameters, two peptide antigens were selected: MD2-180 (corresponding to amino acids 180-194; VKHLDGEEDGSSDQS), and MD2-262 (amino acids 262-276; LQSSQEPEAPPPRDV) (Figure 3-2). The peptides were sent to PRF&L for immunization of rabbits, and serum containing polyclonal antibodies toward the

antigens was shipped to our laboratory for purification. Antibodies were affinity-purified in columns conjugated with the associated peptide antigen and tested in our lab by western blotting for effectiveness and specificity. Each antibody detected both endogenous and ectopically-expressed MAGE-D2 and was specific to MAGE-D2 (Figure 3-3).

MAGE-D2 Localizes to the Mitochondria, Nucleus, and Nucleoli

To gain additional clues regarding its functions, we first explored the subcellular localization of MAGE-D2. Plasmids were generated for expression of N-terminally Myc-tagged, C-terminally Flag-tagged, and C-terminally EGFP-tagged MAGE-D2 fusion proteins. U2OS cells were transfected with the various tagged proteins, and cells were fixed after 18 hours and immunofluorescence stained for Myc or Flag. All three proteins were found to localize primarily to the nucleoli and the nucleus, with the strongest staining apparent in the nucleoli (Figures 3-4 and 3-5). In cells transfected with MAGE-D2-Flag or EGFP-MAGE-D2, faint staining could also be observed in the cytoplasm. Transfection with EGFP-MAGE-D2 appeared toxic to cells, with many transfected cells dying (Figure 3-5). Many of the remaining EGFP-MAGE-D2-expressing cells exhibited abnormal nuclear morphology (Figure 3-5, phase-contrast image and top right panel). It is not clear whether this change in nuclear structure represents apoptosis-induced nuclear fragmentation.

Next, using antibodies that we generated for MAGE-D2, we were able to examine the localization of the endogenous protein. U2OS cells were fixed and

immunofluorescence stained with MAGE-D2 (MD2-262) antibody. As observed with the ectopically expressed proteins, endogenous MAGE-D2 localized primarily to the nucleoli, followed by the nucleus (Figure 3-6). However, a small amount of cytoplasmic staining was also detected in a pattern reminiscent of mitochondria. To determine whether this indeed represented mitochondrial staining, we co-stained cells with MitoTracker™ dye and observed co-localization (Figure 3-6), suggesting that a portion of endogenous MAGE-D2 localizes to the mitochondria. Interestingly, the localization of endogenous MAGE-D2 appears quite heterogeneous, with some cells exhibiting primarily nucleolar and nuclear staining, while other cells have stronger staining in the mitochondria, and others have staining that appears diffuse throughout the nucleus and cytoplasm (Figure 3-7).

The ectopically expressed, tagged MAGE-D2 proteins did not appear to localize to the mitochondria, but it is not uncommon for protein tags to disrupt mitochondrial targeting. An epitope placed at the N-terminus of p32 or SUMI-1, for example, blocks mitochondrial import of these proteins (Figure 4-6E and data not shown). It is possible that the mitochondrial staining detected by the MAGE-D2 antibody represents a nonspecific protein, but this is not likely, as the antibody appears highly specific to MAGE-D2—No other bands were observed on a whole-membrane western blot using the MD2-262 antibody (Figure 3-3, right panel). MAGE-D2 does not contain an obvious mitochondrial targeting signal; however, mitochondrial targeting is often directed by a cryptic combination of N-terminal sequence features such as secondary structure,

enrichment of certain types of residues, number of acidic residues, hydrophobicity, and isoelectric point (Claros and Vincens, 1996). According to MitoProt II, a prediction program for mitochondrial localization that takes into account 47 sequence parameters affecting mitochondrial targeting, the probability that MAGE-D2 is exported to mitochondria is low (0.0452) (Claros and Vincens, 1996). It is possible, however, that the association of MAGE-D2 with mitochondria is based on interaction with another mitochondria-localized protein. This scenario seems plausible, as MAGE-D2 interacts with the mitochondrial protein p32. Immunogold-electron microscopy data shows that a portion of p32 localizes to the mitochondrial outer membrane (data not shown), where it could interact with MAGE-D2 following translation of the protein in the cytoplasm.

Altogether, based on detection of ectopic and endogenous MAGE-D2 with three different antibodies, it is clear that MAGE-D2 localizes to the nucleoli and nucleus, and immunofluorescence staining of endogenous MAGE-D2 also suggests that a subset of MAGE-D2 may localize to the mitochondria and to the cytoplasm. These findings could be further examined with additional experiments such as subcellular fractionation.

Exploring a Potential Role for MAGE-D2 in Regulating Apoptotic Cell Death

Because MAGE-D2 interacts with the pro-apoptotic protein p32, we examined whether MAGE-D2 might also regulate apoptosis. First, we overexpressed MAGE-D2 and examined the effect on cells with and without additional apoptotic stimuli. U2OS cells were transfected with MAGE-D2-Flag

DNA or a control vector, and 24 hours later cells were treated with UV to induce apoptosis. After 18 hours, cells were examined. Ectopic expression of MAGE-D2-Flag appeared to have little effect on cells in the absence of UV but appeared to sensitize cells to UV-induced cell death, as indicated by fewer of the MAGE-D2-transfected cells surviving UV treatment (Figure 3-8). To obtain a quantitative measure of the effect of MAGE-D2 expression on cell death, flow cytometry analysis of cell death was performed. U2OS cells were treated as above except that 18 hours after UV treatment, cells were collected, fixed, and stained with propidium iodide for flow cytometry assessment of DNA content. Cells in the G1 phase of the cell cycle have a diploid (2n) DNA content, while cells in G2 have duplicated their DNA in preparation for cell division and therefore contain a tetraploid (4n) quantity of DNA. Cells that are undergoing apoptosis contain DNA that has partially degraded; thus, any cells whose DNA content is less than that of the G1 peak ("sub-G1," or sub-diploid) are considered to be apoptotic. MAGE-D2 expression alone did not significantly increase the percentage of sub-G1 cells in the absence of apoptotic stimuli (2.2% of cells in sub-G1, compared to 1.4% for vector alone), but MAGE-D2 sensitized cells to UV-induced cell death (25% of cells in sub-G1 compared to 11% for vector alone) (Figure 3-9). These data suggest that, while MAGE-D2 expression alone is not sufficient to induce apoptosis in U2OS cells, MAGE-D2 might have an apoptosis-promoting function, sensitizing cells to apoptotic stimuli. Additional studies must be carried out to determine definitively whether MAGE-D2 regulates apoptotic cell death.

Summary and Discussion

MAGE-D2 is an uncharacterized MAGE (melanoma antigen) family protein that, unlike the majority of MAGE family members, is ubiquitously expressed in normal adult tissues. MAGE-D2 is a Type II MAGE protein, meaning that in addition to sharing the MAGE homology domain (MHD I) with all MAGE proteins, it also shares a MAGE homology domain II (MHD II) with a subset of MAGE proteins, including the MAGE-D subfamily. The physiological functions of MAGE proteins are mostly unknown, but roles have been reported in the regulation of cell survival, cell proliferation, ubiquitin ligase activity, and apoptosis (Barker and Salehi, 2002; Doyle et al., 2010). The closest homolog of MAGE-D2, MAGE-D1/NRAGE, regulates apoptosis through several distinct mechanisms, but the functions of MAGE-D2 are unknown. In order to explore a potential function for MAGE-D2 in regulation of apoptosis, we generated several tools for its study, including tagged proteins for ectopic expression and antibodies for biochemical analyses of endogenous MAGE-D2 in cells.

Using these tools combined with immunofluorescence imaging, we first examined the subcellular localization of MAGE-D2 and determined that it resides in the nucleus, nucleoli, and possibly mitochondria, and that its expression is heterogeneous among cells, with some cells harboring a greater proportion of MAGE-D2 in the nucleoli and the nucleus, and with other cells showing mostly mitochondrial staining. However, as the tagged, ectopically-expressed MAGE-D2 proteins did not also localize to the mitochondria, additional studies are needed to determine whether the apparent mitochondrial localization could represent an

experimental artifact due to recognition of a nonspecific protein by the MAGE-D2 antibody. One method for answering this question is through knockdown of MAGE-D2 with RNAi followed by immunofluorescence staining with MAGE-D2 antibody to determine whether the mitochondrial signal disappears. If RNAi reduces the mitochondrial staining, we can conclude that the apparent mitochondrial localization is genuine. Another means to confirm the localization of MAGE-D2 is through subcellular fractionation, such as the differential detergent mechanism that was utilized in Chapter IV (Figure 4-7) to assess the localization of SUMI-1.

The subcellular localization of a protein can provide clues to its function. Ectopic and endogenous MAGE-D2 were both observed to reside in the nucleus and nucleoli. The nucleus is a membrane-bound organelle containing the cell's chromosomes. The primary functions that take place inside the nucleus are gene transcription and pre-mRNA processing. Nuclear proteins have widely varying roles such as regulation of gene expression, modulation of chromatin structure, sensing and repair of DNA damage, and cell cycle control. It is possible that MAGE-D2 might carry out one of these functions, such as responding to DNA damage and/or regulating transcription, in order to mediate apoptosis or another cellular process. Other MAGE proteins have been reported to regulate gene expression, many of them by modulating the transcriptional activity of the tumor suppressor p53 (Barker and Salehi, 2002). MAGE-D2 was also reported to interact with p53 in screen for novel p53 binding partners using a yeast p53-dissociation assay (Papageorgio et al., 2007), although the function for this

interaction has not been determined. The nucleolus is a sub-nuclear body whose main functions are to carry out synthesis of ribosomal RNA (rRNA) and assembly of ribosomes—complexes consisting of proteins and RNA that translate proteins from mRNA sequences. Many proteins found in the nucleolus are components of the ribosomes themselves, and others regulate ribosomal biogenesis or rRNA synthesis, but a number of proteins in this compartment have no known ties to nucleolar functions. It has been proposed that the nucleolus might act as a storage area for proteins, keeping them inactive until they are required elsewhere in the cell (Pederson and Tsai, 2009). Immunofluorescence staining of endogenous MAGE-D2 suggests that it may also reside in the mitochondria. Inside this organelle, ATP is produced by oxidative phosphorylation, providing most of the energy supply for the cell. Mitochondria also play an important role in the intrinsic apoptotic pathway. During apoptosis, the mitochondrial outer membrane is permeabilized, releasing cytochrome *c* and other contents of the mitochondrial intermembrane space, leading to Caspase activation and execution of apoptosis (Chipuk et al., 2010). Thus, it is possible that MAGE-D2 mediates apoptosis through its association with the mitochondria.

We examined a role for MAGE-D2 in regulating apoptosis, and we found that overexpression of MAGE-D2-Flag sensitized cells to UV-induce apoptosis. While this preliminary result suggests that MAGE-D2 may have an apoptosis-promoting function, it is possible that this result is an artifact of protein overexpression. In order to determine whether MAGE-D2 has a physiologically-relevant role in apoptosis regulation, additional studies are required. For

example, it can be determined whether knockdown of MAGE-D2, such as with siRNA, affects apoptosis. One complication is that extensive redundancy is thought to exist among MAGE family members, so knockdown of one MAGE protein may be compensated for by another. It may be necessary to inhibit more than one MAGE protein (e.g. MAGE-D2 and MAGE-D1) to see an effect. Mechanistic studies can also help determine whether MAGE-D2 has a bona-fide role in regulating apoptosis. In addition, we have not demonstrated that overexpression of MAGE-D2 increases apoptosis, *per se*, rather than another form of cell death. While quantification of apoptosis by assessing the percentage of cells with sub-G1 content is highly precise for cells that are not actively cycling, such as thymocytes, this method is not flawless for analysis of cycling cells, as it does not discriminate between apoptotic cells, fragmented cells, and other debris—a clear peak representing apoptotic cells cannot be observed in cycling cells. Other assays must be carried out to examine other markers of apoptosis, such as western blotting for PARP cleavage or Caspase-3 activation.

Interestingly, we observed several phenomena suggesting that MAGE-D2 might regulate, or be regulated by, the cell cycle and/or cell proliferation. First, the subcellular localization of MAGE-D2 appears heterogeneous from cell to cell, and it is possible that its location may change during cell cycle progression. To test this, the cell cycle could be synchronized with cycloheximide, and cells could be fixed at different time points for immunofluorescence analysis of MAGE-D2 localization. Second, in confluent U2OS cells, MAGE-D2 expression seems to disappear in patches of cells (Figure 3-10). In U2OS cells fixed for

immunofluorescence, confluent regions contained patches of cells expressing little to no endogenous MAGE-D2. It would be interesting to determine whether expression of MAGE-D2 is linked to cell proliferation and/or cell cycle control.

Materials and Methods

Cell Culture, transfection, and apoptotic treatments. U2OS cells were obtained from ATCC and cultured in a 37°C incubator with 5% CO_2 in DMEM supplemented with 10% FBS, 100 U/ml penicillin, and 100 g/ml streptomycin. DNA transfections were carried out with Effectene® (Qiagen) according to the manufacturer's instructions. Apoptosis treatments included UVC radiation (dosage as indicated) using a Stratalinker® UV Crosslinker (Stratagene) and cisplatin (10 µg/ml).

SDS-PAGE and western blotting. Cells were lysed in 0.1% NP-40 lysis buffer, and samples were resolved by SDS-PAGE using a 12.5% or 15% polyacrylamide gel and transferred onto a 0.2 µM nitrocellulose membrane. Membranes were blocked for a minimum of 30 minutes in phosphate-buffered saline with 0.1% Tween-20 (PBST) and 5% nonfat dried milk. Membranes were incubated for 2 hours to overnight in primary antibody, incubated for 1-2 hours in secondary HRP-conjugated antibody, and exposed with Supersignal West Pico (Pierce).

DNA plasmids. N-terminally Myc tagged and C-terminally Flag-tagged MAGE-D2 were cloned into a pcDNA3.1 vector (Invitrogen). MAGE-D2 was cloned into a pEGFP-N1 vector (Clontech) to generate a MAGE-D2-EGFP fusion protein. All plasmids were confirmed by restriction digest and DNA sequencing.

Generation of antibodies. Rabbit anti-MAGE-D2 antibodies were produced by immunizing rabbits (performed by PRF&L, Canadensis, PA) with KLH-conjugated peptide antigens corresponding to amino acids 180-194 (MD2-180) and 262-278 (MD2-262) of MAGE-D2. Sera were affinity purified, and antibody specificity was tested by western blotting (Figure 3-2).

Flow cytometry analysis. Cells were trypsinized, washed in PBS, and fixed in cold 70% ethanol. Cells were treated with RNAse A and stained with propidium iodide. Cells were analyzed using a FACSCalibur flow cytometer (BD Biosciences) at the UNC Flow Cytometry Core Facility, and data were analyzed with Dako software.

Immunofluorescence imaging. Cells were fixed in 4% paraformaldehyde for 10 minutes at room temperature and permeabilized in 0.2% Triton X-100 for 5 minutes at 4°C. Fixed and permeabilized cells were blocked for 30 minutes in 0.5% BSA blocking buffer in PBS, incubated in primary antibody overnight at 4°C with rocking, and incubated with secondary antibodies (anti-mouse or –rabbit rhodamine red) for 30 minutes at room temperature with rocking. Nuclei were

stained with DAPI (diamidino-2-phenylindole), and mitochondria were visualized with MitoTracker™ Red (Invitrogen) where indicated. Cells were mounted in fluorescence mounting medium (Dako) and analyzed using an Olympus IX81 inverted microscope combined with a SPOT™ digital microscope camera and imaging software (SPOT™ Imaging Solutions).

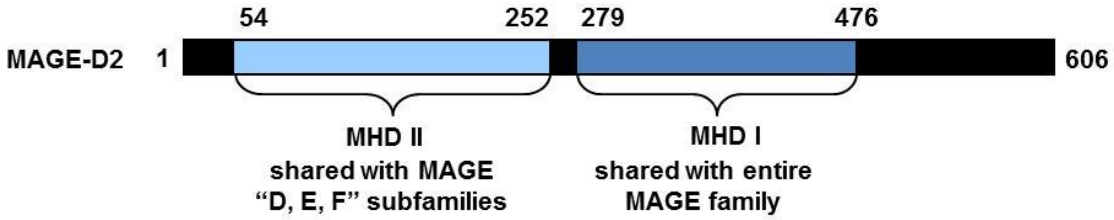

Figure 3-1. Domain structure for MAGE-D2.
MAGE-D2 contains two known functional domains. MHD I (MAGE homology domain 1), which extends from amino acids (aa) 279 to 476, is shared by all MAGE family proteins. MHD II (Mage homology domain II), extending from aa 54-252, is shared by Type II MAGE proteins, including all members of the MAGE-D subfamily. The functions for these domains are not known.

A

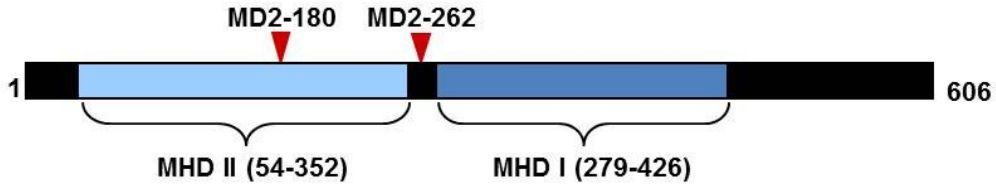

B

MSDTSESGAGLTRFQAEASEKDSSSMMQTLLTVTQNVEVPETPKASKALEV
SEDVKVSKASGVSKATEVSKTPEAREAPATQASSTTQLTDTQVLAAENKSL
AADTKKQNADPQAVTMPATETKKVSHVADTKVNTKAQETEAAPSQAPADEP
EPESAAAQSQENQDTRPKVKAKKARK**VKHLDGEEDGSSDQS**QASGTTGGRR
VSKALMASMARRASRGPIAFWARRASRTRLAAWARRALLSLRSPKARRGKA
RRRAAK**LQSSQEPEAPPPRDV**ALLQGRANDLVKYLLAKDQTKIPIKRSDML
KDIIKEYTDVYPEIIERAGYSLEKVFGIQLKEIDKNDHLYILLSTLEPTDA
GILGTTKDSPKLGLLMVLLSIIFMNGNRSSEAVIWEVLRKLGLRPGIHHSL
FGDVKKLITDEFVKQKYLDYARVPNSNPPEYEFFWGLRSYYETSKMKVLKF
ACKVQKKDPKEWAAQYREAMEADLKAAAEAAAEAKARAEIRARMGIGLGSE
NAAGPCNWDEADIGPWAKARIQAGAEAKAKAQESGSASTGASTSTNNSASA
SASTSGGFSAGASLTATLTFGLFAGLGGAGASTSGSSGACGFSYK

Figure 3-2. Antibody design for MAGE-D2.
A) MAGE-D2 protein sequence showing approximate location of peptide antigens selected for production of MAGE-D2 rabbit polyclonal antibodies Red triangles indicate the approximate positions of the selected peptides relative to MAGE homology domains (MHD) I and II.
B) The MAGE-D2 protein sequence with the two selected peptide antigens (MD2-180 and MD2-262) shown in red and underlined.

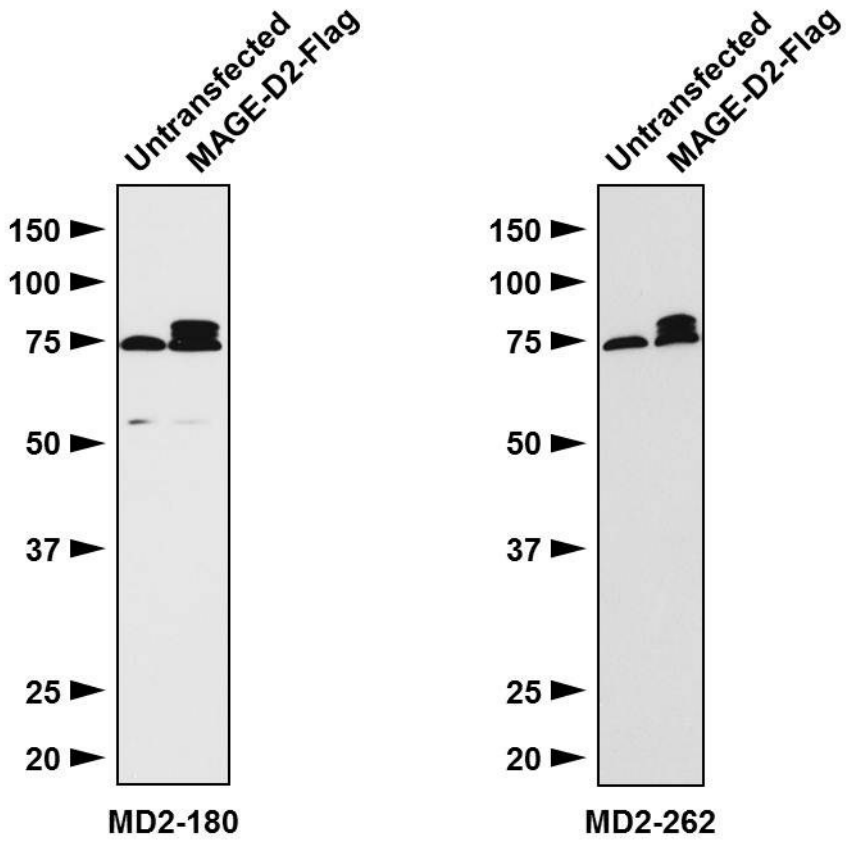

Figure 3-3. MAGE-D2 antibody effectiveness and specificity.
Whole-membrane western blots showing specificity and effectiveness for antibodies targeting two different regions of MAGE-D2 (MD2-180, aa 180-194; MD2-262, aa 262-276). Endogenous MAGE-D2 and Flag-tagged MAGE-D2 are detected by both MAGE-D2 antibodies

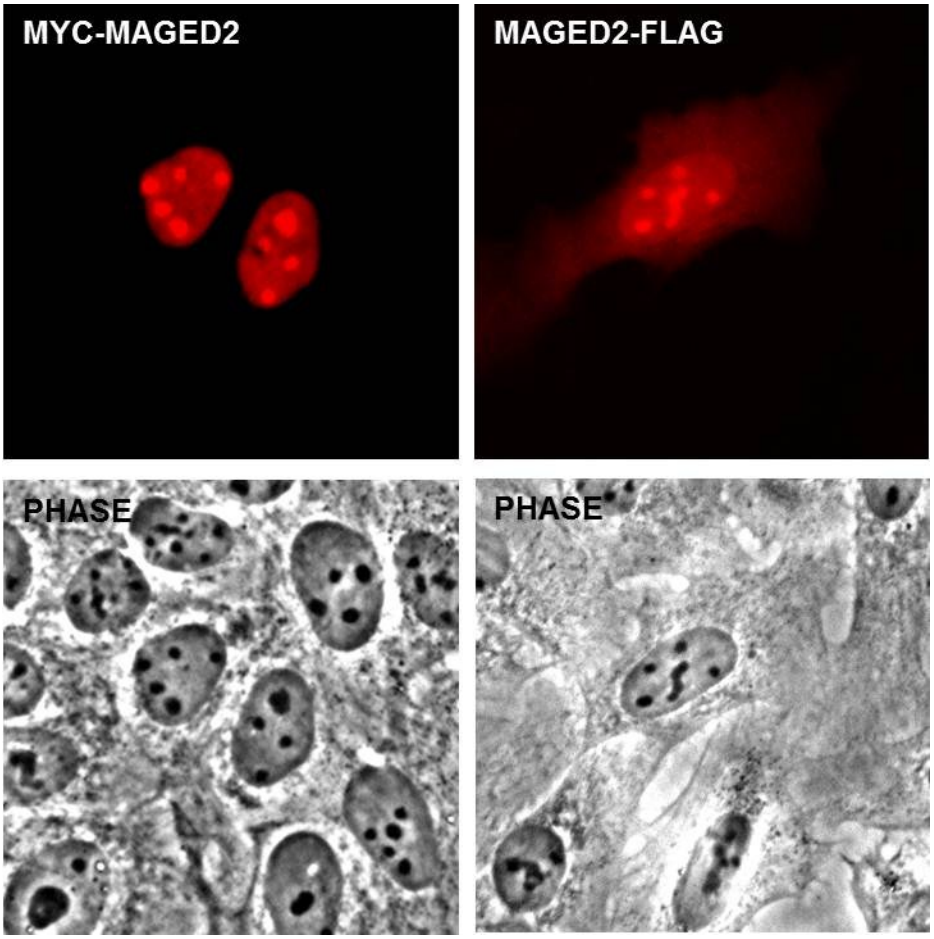

Figure 3-4. Ectopically-expressed tagged MAGE-D2 localizes to nuclei and nucleoli.
Immunofluorescence staining shows MAGE-D2 localization primarily in the cell's nucleus and nucleoli. U2OS cells were transfected with indicated plasmids and fixed after 24 h for immunofluorescence staining with Flag or Myc antibodies. MAGE-D2 that is fused with an N-terminal Myc3 tag (top left panel) can be seen exclusively in the nucleoli and nucleus. C-terminally-tagged MAGE-D2-FLAG can be seen primarily in the nucleoli and nucleus, with faint staining also detectable in the cytoplasm. Corresponding phase-contrast images are shown below.

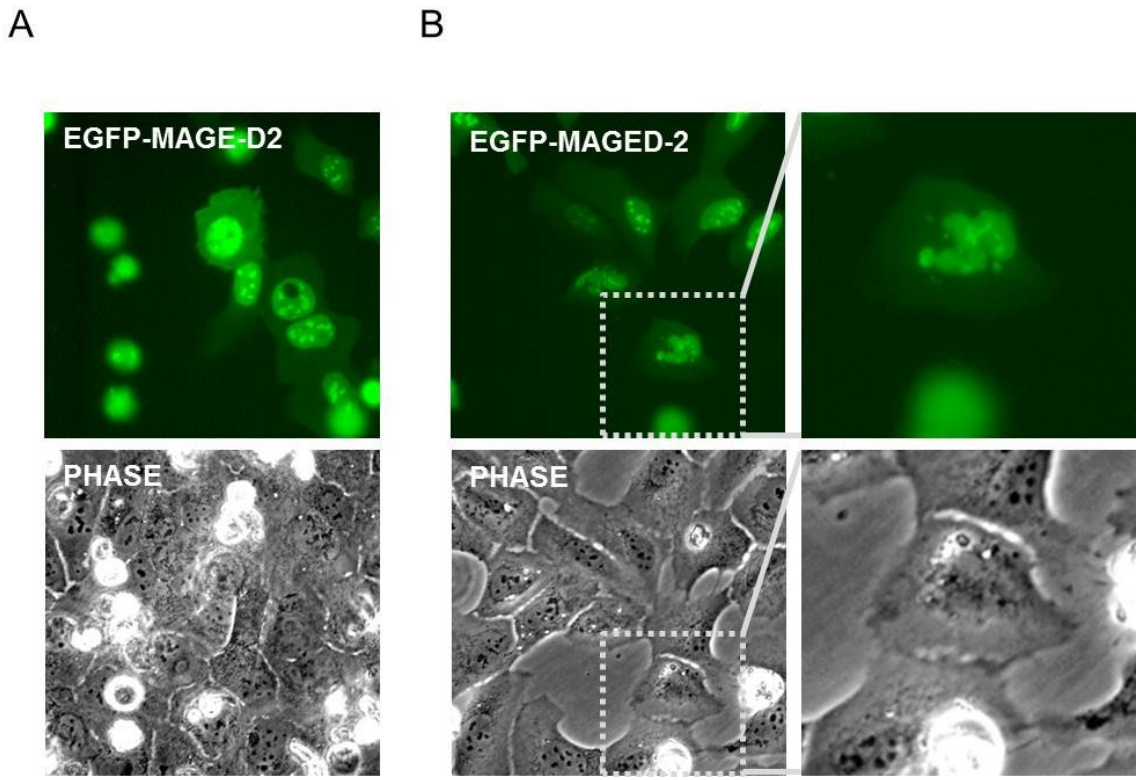

Figure 3-5. Expression of EGFP-tagged MAGE-D2 is toxic to cells and disrupts nuclear and nucleolar morphology.
A) Live-cell fluorescence imaging of U2OS cells transfected with N-terminally-EGFP-tagged MAGE-D2 shows that expression of this construct is toxic to cells, with many transfected cells dying (observed as shrunken, white floating cells in phase-contrast image).
B) Effect of EGFP-MAGE-D2 on cell morphology shown in fixed cells. U2OS cells were transfected with EGFP-MAGE-D2, fixed after 18 h, and visualized by fluorescence microscopy. Many nuclei of transfected cells appear fragmented, and nucleoli appear abnormal (see close-up in panels on right).

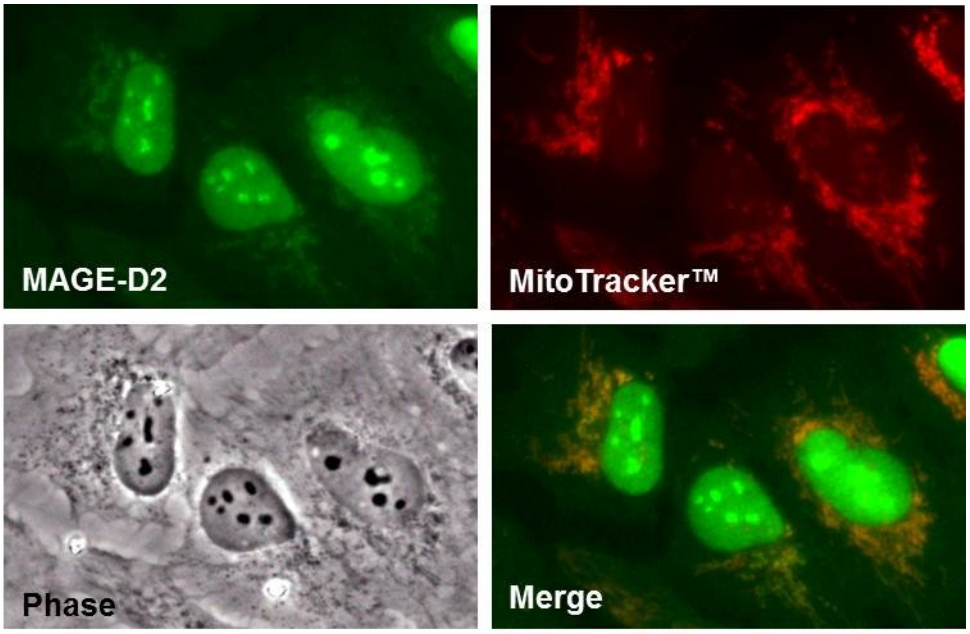

Figure 3-6. Endogenous MAGE-D2 localizes to the nucleoli, nuclei, and mitochondria.
Untransfected U2OS cells were immunofluorescence stained for MAGE-D2 (MD2-262 antibody). Endogenous MAGE-D2 is observed in the nucleoli and nucleus. MAGE-D2 staining was also observed at the mitochondria, as indicated by colocalization with the mitochondrial marker MitoTracker.

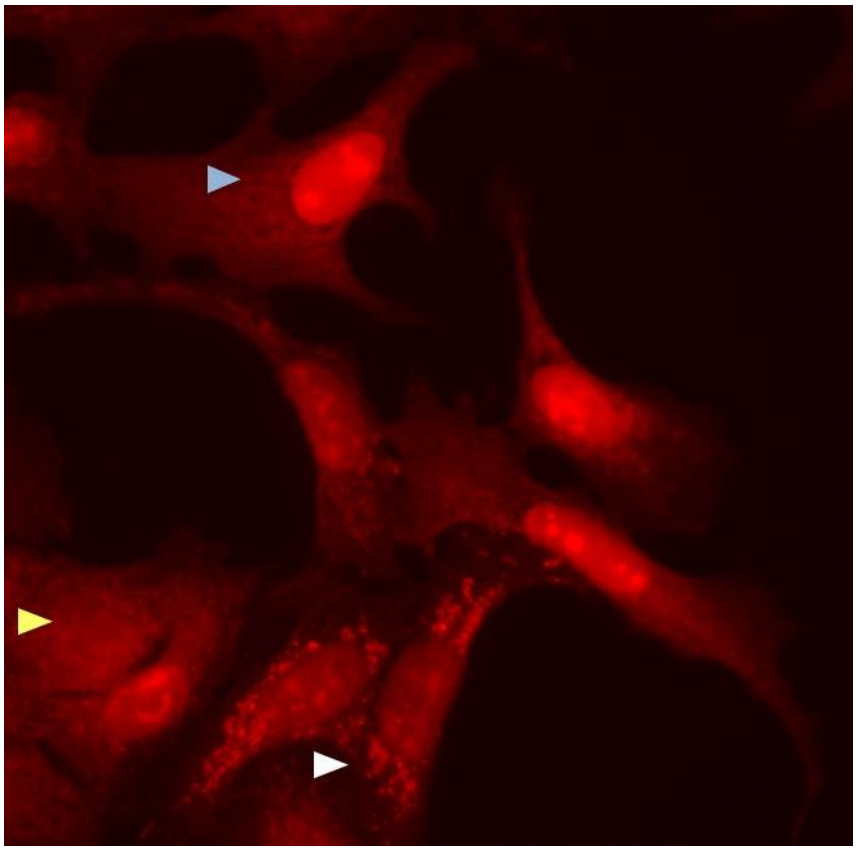

Figure 3-7. Localization of endogenous MAGE-D2 is heterogeneous.
The localization of MAGE-D2 varies significantly from cell to cell. Untreated U2OS cells were immunofluorescence-stained for endogenous MAGE-D2 with antibody MD2-262. Some cells exhibit primarily mitochondrial staining (white arrow), some cells show primarily nucleolar and nuclear staining (blue arrow), and some cells exhibit diffuse cytoplasmic and nuclear staining (yellow arrow).

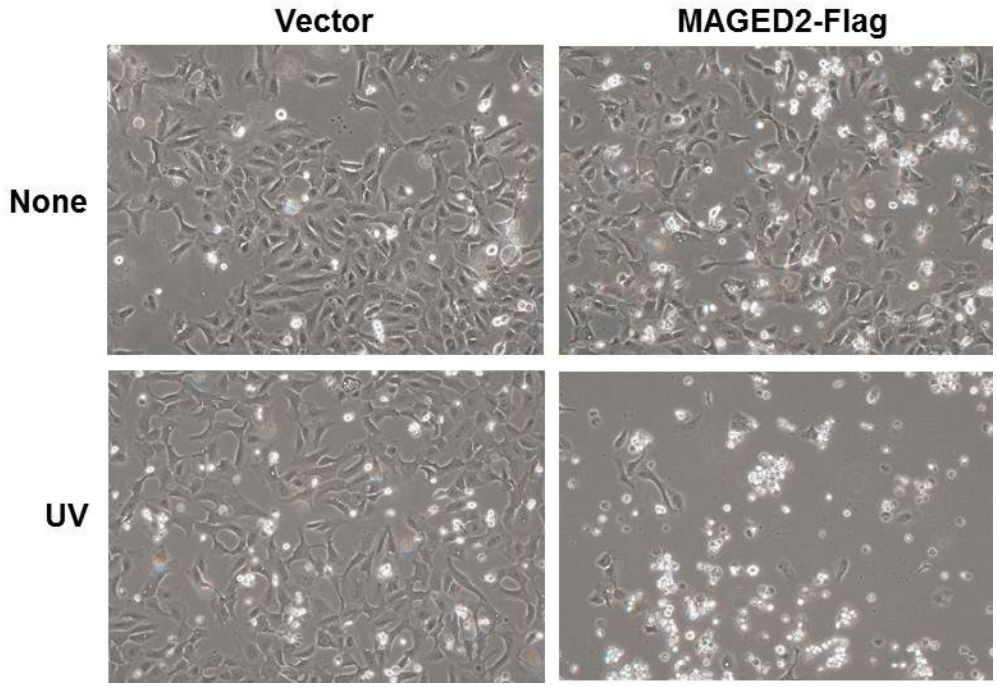

Figure 3-8. Overexpression of MAGE-D2 sensitizes cells to UV-induced cell death.
U2OS cells were transfected with pcDNA3 vector alone or pcDNA3-MAGE-D2-Flag3, as indicated. After 24 hours, cells were either left untreated (None) or treated with 6 mJ/cm^2 UV for 18 hours. Apoptotic cells appear shrunken, rounded, and white, and eventually detach from the plate. Many of the cells treated with both MAGE-D2-Flag and UV (bottom right panel) have detached from the substrate and appear in clusters.

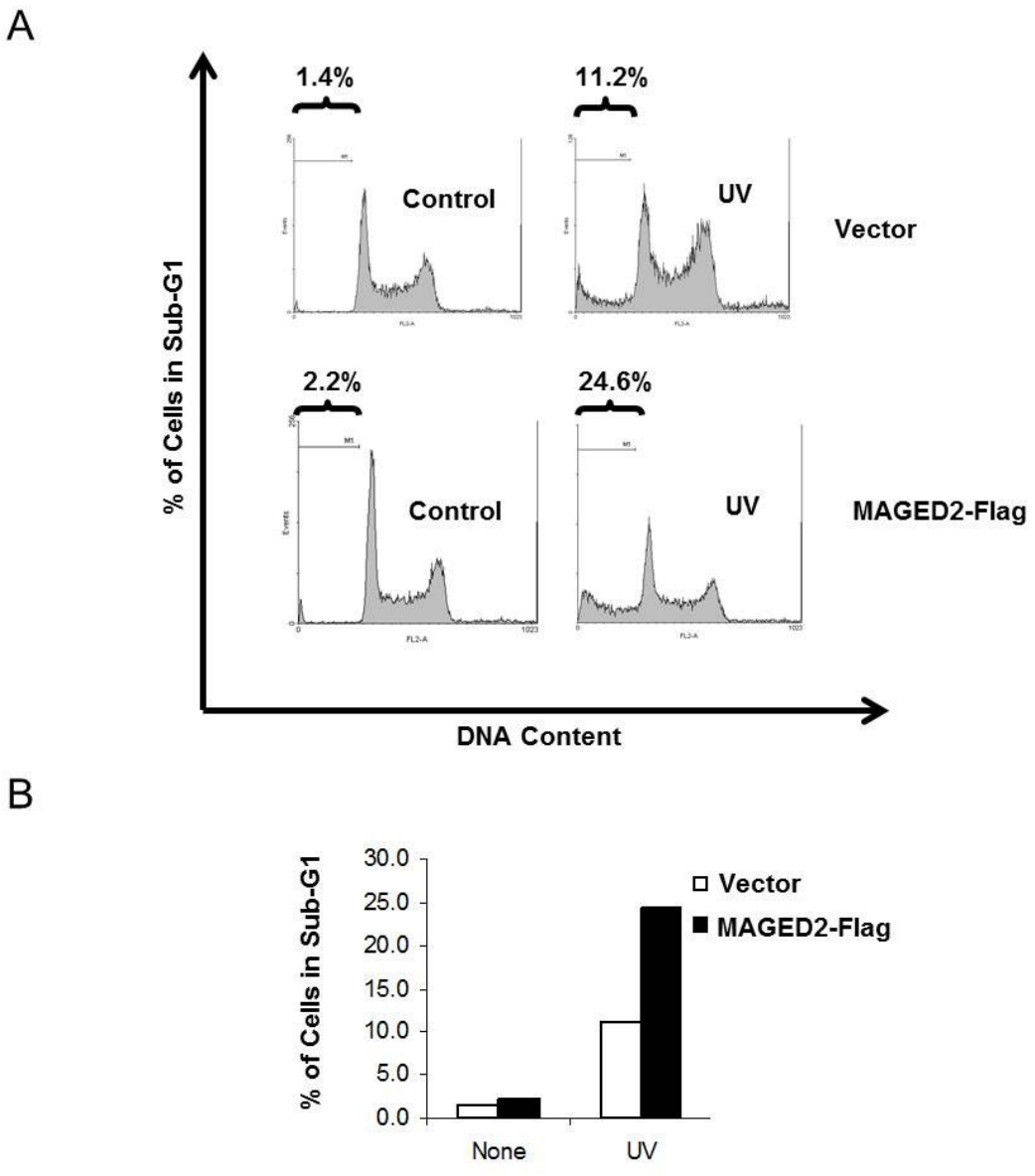

Figure 3-9. Flow cytometry analysis of effect of MAGE-D2 expression on UV-induced apoptosis.

A) Flow-cytometry analysis shows that ectopic expression of MAGE-D2 sensitizes cells to UV-induced cell death. U2OS cells were transfected with MAGED2-Flag DNA, treated 24 h later cells with UV (6 mJ/cm^2) where indicated to induce apoptosis, and were fixed 18 h later in ethanol, stained with propidium iodide, and analyzed by flow cytometry for DNA content.

B) Graphical representation of data from (A).

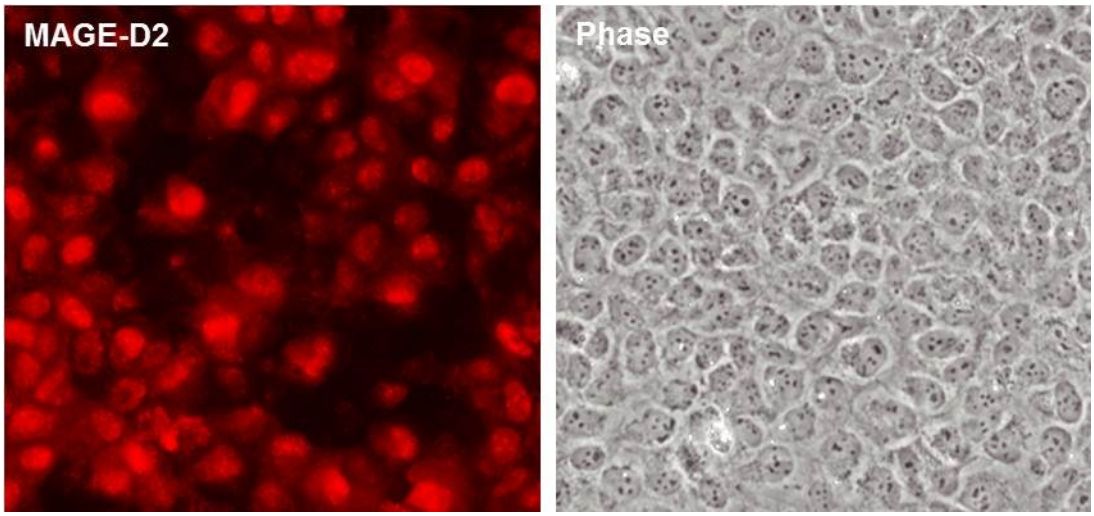

Figure 3-10. Endogenous MAGE-D2 expression is absent in patches of confluent cells.
In confluent U2OS cells immunofluorescence-stained for endogenous MAGE-D2 with MD2-262 antibody, patches of cells are observed with greatly-reduced MAGE-D2 expression. Note that the phase-contrast image on the right shows that the entire field is filled with cells, yet areas are observed in the immunofluorescence image that lack MAGE-D2 expression.

CHAPTER IV

SUMI-1 IS A NOVEL REGULATOR OF MITOCHONDRIAL FISSION-FUSION DYNAMICS AND BAX-MEDIATED APOPTOSIS[1]

Introduction

A critical control point during apoptosis is mitochondrial outer membrane permeabilization (MOMP), during which mitochondrial contents such as cytochrome c are released in order to initiate apoptosis. As MOMP is often the "point of no return" during apoptosis, much research is currently devoted to understanding this process. Our knowledge of MOMP remains incomplete but can be enhanced by identification of novel proteins involved in its regulation. Here, we characterize a small protein, "SUMI-1," that resides at the mitochondrial outer membrane and inhibits apoptosis. We show that early in apoptosis, SUMI-1 translocates from the mitochondria, promoting BAX oligomerization, MOMP, and cytochrome *c* release. We also show that SUMI-1 controls mitochondrial fusion/fission dynamics, providing a mechanism for its regulation of apoptosis. Furthermore, SUMI-1 is overexpressed in many cancers, and knockdown of SUMI-1 sensitizes cancer cell lines to chemotherapeutic drugs, suggesting that SUMI-1 is a potential target for chemosensitizing therapeutics.

---

[1]This chapter is based, with modifications, on a manuscript submitted for publication (Clegg et al.) and includes data generated by Yong Liu, Jiehui Di, Laura A. Tollini, Yizhou He, Aiwen Jin, and Paula Miliani de Marval.

Background

Apoptosis, or programmed cell death, is a critical process during vertebrate development and is abnormally regulated in a diverse array of diseases. Apoptosis can occur through two pathways—receptor-mediated (extrinsic) apoptosis, and mitochondria-mediated (intrinsic) apoptosis. The extrinsic pathway is activated by interaction of extracellular ligands with death receptors, while the intrinsic pathway is triggered by intracellular stresses such as DNA damage and is modulated by the cell's mitochondria. Both pathways converge upon activation of cysteine proteases (Caspases), which cleave downstream substrates to induce the physiological and morphological changes associated with apoptosis such as membrane blebbing, DNA fragmentation, and cell shrinkage.

The intrinsic pathway is regulated largely by pro- and anti-apoptotic BCL-2 family proteins, which together dictate whether a cell undergoes mitochondrial outer membrane permeabilization (MOMP). During MOMP, which is often the point of no return for cells undergoing apoptosis, pro-apoptotic BCL-2 effector proteins BAX and/or BAK oligomerize on the mitochondrial outer membrane, releasing cytochrome *c* and other mitochondrial intermembrane space contents into the cytoplasm to induce apoptosis. The decision to undergo MOMP is also influenced by non-BCL-2 proteins and by mitochondria themselves. Mitochondrial fission-fusion dynamics have recently emerged as a means by which apoptosis is modulated. Mitochondria are dynamic, continually dividing and merging with one another. During apoptosis, mitochondria become fragmented prior to MOMP, due

to an increase in fission and/or a decrease in fusion. Overexpression of fusion-promoting proteins MFN1 or MFN2 protects cells from apoptosis (Brooks et al., 2011), while inhibition of fission-mediating DRP1 partially inhibits mitochondrial fragmentation while delaying MOMP and apoptosis (Brooks et al., 2011). Recently, it was shown that DRP1-induced mitochondrial fragmentation promotes apoptosis by stimulating BAX oligomerization (Montessuit et al., 2010). Despite advances that have been made in our understanding of MOMP, much remains unknown about the mechanisms leading to BAX activation and oligomerization, especially the roles that mitochondria and their associated proteins play in this process. Identification of novel proteins that regulate MOMP can significantly aid in our understanding of this process.

Here, we characterize a small, mitochondria-localized protein that we call SUMI-1 for survival-promoting mitochondrial protein 1 (also known as CHCHD2 for coiled-coil-helix coiled-coil helix domain-containing 2) as a novel regulator of mitochondrial dynamics and mitochondria-mediated apoptosis. We initially identified SUMI-1 as an interacting partner for the pro-apoptotic protein p32/C1QBP; however, this study focuses on characterizing SUMI-1's apoptosis-regulating function, while subsequent studies will be devoted to its interaction with p32. SUMI-1 was recently detected in screens for proteins regulating cellular metabolism and migration (Baughman et al., 2009; Seo et al., 2010), but its functions have not been well-characterized. Here, we report that SUMI-1 acts as a guardian of mitochondrial membrane integrity by inhibiting BAX-induced mitochondrial outer membrane permeabilization. We also show that SUMI-1

regulates mitochondrial fusion in order to maintain a balance between fusion and fission, providing a mechanism for SUMI-1's regulation of BAX and MOMP. Furthermore, most of these experiments were carried out in intact cells using endogenous rather than overexpressed proteins, and our results are therefore likely to be physiologically relevant. Finally, we observed that SUMI-1 expression is upregulated in cancer cell lines, and data obtained from Oncomine™ demonstrates that SUMI-1 is indeed overexpressed in multiple cancers, consistent with SUMI-1's anti-apoptotic function. This study identifies a novel regulator of apoptosis, sheds light on previously-unexplained mechanisms governing mitochondrial dynamics, MOMP, and BAX activation in regulating apoptotic cell death, and provides a potential therapeutic target for chemosensitization in cancer treatment.

SUMI-1 is a Highly-Conserved CHCH-Domain-Containing Protein

The *CHCHD2* gene encoding SUMI-1 spans 4921 base pairs, contains 4 exons, and is located on chromosome 7p11.2, a region amplified in glioblastomas (Arslantas et al., 2004). The protein encoded by this gene is expressed broadly in adult tissues (Shmueli et al., 2003) and is a relatively small protein, comprised of 151 amino acids. SUMI-1 is relatively well-conserved, with 87% amino acid identify in mice, and is conserved through yeast (Table 4-1, Figure 4-1). SUMI-1 contains three functional domains: a putative mitochondrial targeting signal at the N-terminus (Claros and Vincens, 1996), a predicted transmembrane domain (TMBASE), and a C-terminal CHCH (coiled-coil helix-

coiled-coil helix) domain. SUMI-1 also contains a consensus sequence for import into the mitochondrial intermembrane space (ITS) mediated by another CHCH-domain-containing protein, Mia40 (Figure 4-2).

The CHCH domain is characterized primarily by four cysteine residues spaced exactly 10 amino acids apart (a C-X9-C motif) (Schultz et al., 1998). Pairs of cysteines in this domain typically form covalent disulfide bonds, eliciting changes in tertiary protein structure or facilitating oligomerization and/or interactions with other CHCH domain-containing proteins (Arnesano et al., 2005). Analysis of the SUMI-1 sequence with an intramolecular disulfide connectivity prediction program, *DiANNA 1.1*, predicts that a bond may form between cysteines 1-3 and another bond between cysteines 2-4 in the CHCH domain to create a loop structure at the C-terminus (Figure 4-3) (Ferre and Clote, 2005a, b).

The function of the CHCH domain is not well understood, and the few characterized proteins that carry this domain have diverse functions; these proteins include Cox12, Cox17, Cox19, Cox23, Mia40/Tim40, C2360, and MRP10. The yeast protein Cox12 is part of the COX (cytochrome *c* oxidase) complex, which is the final enzyme in the respiratory electron transport chain (LaMarche et al., 1992). Cox17, Cox19, and Cox23 play roles in assembly of the COX complex; specifically, they are thought to feed copper ions into the complex during assembly, and their CHCH domains may be important for copper ion binding (Arnesano et al., 2005; Barros et al., 2004; Nobrega et al., 2002). Of these proteins, Cox17 has been studied the most extensively, and its function in

COX assembly has recently been shown to be mediated by its interaction with SCO-1 (Banci et al., 2008a). Mia40/Tim40 assists in transporting proteins into the mitochondrial intermembrane space by forming temporary disulfide bonds with cysteine-containing proteins as they are imported (Chacinska et al., 2004; Hofmann et al., 2005; Sideris et al., 2009). C2360 is expressed only in human proliferative cytotrophoblasts and not in adult tissues; its function is unknown (Westerman et al., 2004). Finally, the yeast protein MRP10 is a component of the mitochondrial ribosomal 37S subunit, which mediates translation of proteins (Jin et al., 1997). The function of the CHCH domain has been studied most extensively in Cox17, where the domain was shown to change configuration based on oxidative-reductive status, and is thought to regulate homo-oligomerization (Arnesano et al., 2005). The CHCH domain in SUMI-1 is well-conserved across species: The four cysteines comprising the domain are present in 8 of the 9 orthologs shown in Figure 4-1.

Generation of Antibodies for Study of Endogenous SUMI-1

At the onset of our study, no antibodies were available for biochemical analyses of endogenous SUMI-1. Thus, we designed two rabbit polyclonal antibodies as described in Chapter III in order to study endogenous, untagged SUMI-1, avoiding potential artifacts introduced by protein tags and overexpression. Antigen options were limited because SUMI-1 is a small protein (151 amino acids) and consists of a predicted mitochondrial targeting signal at the N-terminus, a putative transmembrane domain in the center of the protein,

and CHCH domain comprised of four cysteines spaced 10 amino acids apart at the C-terminus. These features made the majority of the sequence unsuitable or undesirable because the mitochondrial targeting region could potentially be cleaved off the protein upon mitochondrial translocation, the transmembrane region is hydrophobic (meaning it is not likely to be exposed at the protein surface), and the closely-spaced cysteines in the CHCH domain precluded any antigens longer than 10 amino acids due to the need to have either zero or one terminally-located cysteine and no internal cysteines in the antigen sequence. The regions selected were SU-94 (amino acids 94-108; RPDITYQEPQGTQPA), located adjacent to the central transmembrane domain, and SU-124 (amino acids 124-133; CAQNQGDIKL), located within the CHCH domain (Figure 4-4). The second antigen was shorter than desired (10 amino acids) in order to ensure that no internal cysteines were present in the sequence. The peptides were used to immunize rabbits, and the resulting serum containing polyclonal antibodies was affinity-purified as described in Chapter III. The purified antibodies were then tested by western blotting and immunofluorescence for effectiveness and specificity. The antibody generated with the SU-94 antigen is highly specific to SUMI-1 and can be used for western blotting, immunofluorescence, and co-immunoprecipitation (Figures 4-5 and 2-5).

SUMI-1 Localizes to the Mitochondria

SUMI-1 is predicted by MitoProt to localize to mitochondria, with the first 51 amino acids serving as a putative mitochondrial targeting sequence (Claros

and Vincens, 1996). To determine whether SUMI-1 indeed localizes to the mitochondria, we examined its subcellular localization by immunofluorescence. We transfected U2OS cells with plasmids expressing C-terminal Flag-tagged SUMI-1, fixed the cells after 24 hours, and carried out immunofluorescence staining for Flag. SUMI-1-Flag localized primarily to mitochondria, as indicated by co-staining with MitoTracker™ dye (Figure 4-6A).

Next, we examined the localization of endogenous SUMI-1 by immunofluorescence staining with SUMI-1 antibody in unstressed U2OS cells. Like SUMI-1-Flag, endogenous SUMI-1 was observed to localize primarily to mitochondria, as indicated by co-staining for the mitochondrial marker cytochrome *c* (Figure 4-6B). This localization was also observed in HeLa cells (Figure 4-6C) and mouse embryo fibroblasts (MEFs) (Figure 4-6D). The mitochondrial localization of SUMI-1 was further confirmed by a differential detergent subcellular fractionation method, with SUMI-1 appearing in the mitochondria-enriched heavy membrane fraction, consistent with our immunofluorescence results (Figure 4-7). To examine the submitochondrial localization of endogenous SUMI-1, we carried out immunogold staining in which gold beads were conjugated to SUMI-1 antibody and applied to formaldehyde-fixed U2OS cells before or after paraffin embedding. Using a pre-embedding staining method, endogenous SUMI-1 could be observed by electron microscopy (EM) around the perimeter of the mitochondria, suggesting that SUMI-1 resides at the mitochondrial outer membrane (Figure 4-8). Using a pre-embedding staining method, SUMI-1 was similarly detected at the mitochondrial outer

membrane and could also be observed inside the mitochondria, although the sub-mitochondrial localization (i.e. matrix, inner membrane, or intermembrane space) was not clear (Figure 4-8). Thus, SUMI-1 appears to reside both inside the mitochondria and at the outer mitochondrial membrane. SUMI-1 contains a consensus ITS (intermembrane targeting sequence) that directs Mia40-mediated import of proteins into the mitochondrial intermembrane space. It is possible that upon import, a subset of SUMI-1 is retained in the mitochondria (either in the intermembrane space or embedded in the inner membrane) while another subset becomes anchored via the transmembrane domain into the mitochondrial outer membrane.

Another study that identified SUMI-1 in a screen for novel mediators of cell migration also examined the subcellular localization of SUMI-1 and reported that SUMI-1 resides in the cytoplasm. However, the authors examined only the sub-cellular localization of N-terminally tagged protein, and an N-terminal tag often disrupts mitochondrial localization in proteins containing an N-terminal MTS. We also examined the localization of N-terminally tagged Myc-SUMI-1 by immunofluorescence, and as expected, the mitochondrial localization was lost, with the N-terminally-tagged protein appearing primarily in the cytoplasm and nucleus (Figure 4-6E).

Thus, based on immunofluorescence imaging of C-terminally tagged and endogenous SUMI-1, subcellular fractionation, and immunogold-EM imaging, we conclude that in healthy, unstressed cells, SUMI-1 resides primarily in the

mitochondria, with a subset of SUMI-1 located within the mitochondria and another portion associated with the mitochondrial outer membrane.

SUMI-1 Inhibits Apoptotic Cell Death

We next sought to determine whether SUMI-1 plays a role in regulating apoptotic cell death. We first analyzed whether SUMI-1 knockdown affects apoptosis, using two different siRNA duplexes targeting different regions of SUMI-1 mRNA. We treated cells with nonspecific control siRNA (NS) or two different SUMI-1 siRNA species as indicated for 48 hours and subjected cells to various apoptosis-inducing treatments to determine whether a reduced SUMI-1 level could affect response to the treatments. SUMI-1 knockdown alone caused little to no increase in cell death in the absence of apoptotic stimuli (average 95% of control), SUMI-1 knockdown sensitized cells to apoptosis as measured by quantification of cells surviving treatment with cisplatin (27% of control), UV radiation (64% of control), doxorubicin (54% of control), and staurosporine (69% of control) (Figure 4-9A). Additionally, we tested the effect of SUMI-1 knockdown in HeLa cells treated with UV radiation and cisplatin. Consistent with the U2OS data, SUMI-1 siRNA did not significantly affect apoptosis in the absence of apoptotic stimuli (92% of control) but sensitized HeLa cells to cell death induced by cisplatin (34% of control) and UV (43% of control) (Figure 4-9B). The pattern we observed here was similar to that observed with knockdown of known anti-apoptotic proteins such as BCL-2, BCL-xL, and MCL-1; inhibition of these proteins alone does not usually cause cell death, but sensitizes cells to apoptotic

stimuli (Chipuk et al., 2010). To confirm whether the decrease in cell number resulting from these treatments was indeed due to apoptosis, we carried out western blotting to examine the level of cleaved poly (ADP-ribose) polymerase (PARP) and Caspase-3, both indicators of apoptosis (Simbulan-Rosenthal et al., 1998). Cells treated with UV exhibited PARP and Caspase-3 cleavage, and this was augmented by pre-treatment with SUMI-1 siRNA (Figure 4-10). In addition, apoptosis-associated morphological changes (cell shrinkage, detachment, rounding, and membrane blebbing) were observed in cells treated with apoptotic agents, and these features were enhanced upon SUMI-1 knockdown (example shown in Figure 4-11). U2OS cells were treated with the indicated siRNA for 48 hours followed by UV radiation (6 mJ/cm^2) where indicated, and images were taken at 10x magnification. Membrane blebbing can be observed clearly in a higher-magnification (40x) image of U2OS cells treated with SUMI-1 siRNA and UV (Figure 4-11). Together, these data show that SUMI-1 knockdown sensitizes cells to apoptotic cell death, implicating SUMI-1 as a negative regulator of apoptosis.

We then tested whether overexpression of SUMI-1 could protect cells from apoptosis. U2OS cells were treated with adenovirus expressing either untagged SUMI-1 (Ad-SUMI-1) or GFP as a negative control (Ad-Ctl), and sensitivity to apoptosis was assessed both with and without apoptosis-inducing UV treatment. Overexpression of SUMI-1 had no significant effect on unstressed cells, with similar survival between cells treated with control adenovirus (normalized to 100%) and those treated with SUMI-1 adenovirus (106% of control), whereas

SUMI-1 overexpression protected UV-treated cells from apoptosis (89% survival compared to 51% for control) (Figure 4-12A). SUMI-1 overexpression also reduced PARP cleavage during UV-induced apoptosis as determined by western blotting (Figure 4-12B). Together with the SUMI-1 knockdown experiments, these data strongly suggest that SUMI-1 is an inhibitor of apoptosis.

SUMI-1 Translocates From Mitochondria Prior to Cytochrome *c*

We next sought to identify the mechanism by which SUMI-1 regulates apoptosis. We had observed by immunofluorescence staining that endogenous SUMI-1 translocates from the mitochondria during apoptosis (Figure 4-13A). We co-stained cells for cytochrome *c*, which is itself released from mitochondria at an early stage during apoptosis. Interestingly, a subset of cells was observed in which SUMI-1 had translocated yet cytochrome *c* was still retained in the mitochondria (Figures 4-13B and 4-14), while no cells were observed to contain both released cytochrome *c* and mitochondrial SUMI-1. Thus, it appeared that SUMI-1 may translocate from the mitochondria prior to cytochrome *c*. To further test this, we examined cytochrome *c* and SUMI-1 localization over a time course in UV-treated U2OS cells and quantified the percentage of cells with released SUMI-1 at each time point, and the percentage of cells with released cytochrome *c*. Before administering UV irradiation, cells were pretreated with the pan-Caspase inhibitor Q-VD-OPh (abbreviated QVD) to prevent cell death downstream of cytochrome *c* release, thereby preserving cells with released cytochrome *c* and allowing them to be visualized. Cells were treated with UV (25

mJ/cm^2) and fixed for immunofluorescence staining at the indicated time points. At each time point, we observed a greater percentage of cells with SUMI-1 release than with cytochrome c release, indicating that SUMI-1 translocates from the mitochondria prior to cytochrome *c*. Four hours post-UV, 12% of cells had released SUMI-1, while 7.6% had released cytochrome *c*; eight hours post-UV, 40% and 23% of cells had released SUMI-1 or cytochrome *c*, respectively; and 16 hours post-UV, 87% and 78% of cells had released SUMI-1 or cytochrome *c*, respectively (Figure 4-14B). These data indicate that SUMI-1 translocates from the mitochondria prior to cytochrome *c*.

SUMI-1 Regulates Mitochondrial Outer Membrane Permeabilization (MOMP) and BAX Activation

Our data show that SUMI-1 translocates from the mitochondria at an earlier time point than cytochrome *c*. Because cytochrome *c* release is a standard readout for MOMP (Arnoult, 2008), these data imply that SUMI-1 translocates from the mitochondria prior to the onset of mitochondrial permeabilization. Therefore, we hypothesized that SUMI-1 may regulate MOMP—That is, SUMI-1 may protect healthy cells from apoptosis by inhibiting MOMP, and during apoptosis, SUMI-1 may translocate from the mitochondria, releasing this inhibition and allowing MOMP to proceed. In this case, inhibition of SUMI-1 by siRNA would be expected to promote MOMP. To evaluate this, we treated cells with either nonspecific or SUMI-1 siRNA for 48 hours, induced apoptosis with UV and performed immunofluorescence to visualize cytochrome *c*

release. Cells in which cytochrome *c* was released (staining appeared diffuse throughout the cell) were quantified. SUMI-1 knockdown significantly increased the kinetics with which cytochrome *c* was released, with a greater percentage of cells observed with released cytochrome *c* in si-SUMI-1-treated cells compared to si-NS-treated cells at 1 hour (3.9% and 1.2%, respectively), 2 hours (14% and 5%, respectively), and 4 hours post-UV (35% and 7.5%, respectively) (Figure 4-15), indicating that endogenous SUMI-1 inhibits MOMP.

We next examined potential mechanisms by which SUMI-1 might regulate MOMP. While the exact mechanisms governing MOMP are not entirely clear, MOMP is known to occur when BAX and/or BAK—two pro-apoptotic BCL-2 family proteins—oligomerize on the mitochondrial outer membrane (Chipuk et al., 2010). As BAX is one of the primary inducers of MOMP, we sought to determine whether SUMI-1 might regulate this protein. BAX continually cycles between the mitochondria and cytosol (Edlich et al., 2011). During apoptosis, BAX accumulates at the mitochondria, becomes activated, and forms oligomers on the mitochondrial outer membrane, inducing membrane permeabilization (Edlich et al., 2011; Wolter et al., 1997). Active BAX can be detected by immunofluorescence with BAX 6A7 antibody, which recognizes an N-terminal epitope that is hidden in the inactive protein but is exposed upon conformational changes during activation of BAX. Generally, positive staining with BAX 6A7 indicates the presence of BAX that is both activated and oligomerized in clusters on the mitochondrial outer membrane.

To determine whether SUMI-1 inhibits BAX activation, we treated cells with SUMI-1 siRNA for 48 hours, induced apoptosis with UV, and examined BAX activation by immunofluorescence staining with BAX 6A7 antibody. Cells were pre-treated with QVD to inhibit apoptotic events downstream of cytochrome *c* release, preserving cells with activated BAX. Consistent with the experiments examining sensitivity to apoptosis and cytochrome *c* release, SUMI-1 knockdown alone did not induce BAX activation (Figure 4-16A, top two panels), but greatly increased BAX activation in UV-treated cells, as indicated by a stronger signal from BAX 6A7 antibody (Figure 4-16A, lower panels). We also noted that in U2OS and HeLa cells induced to undergo apoptosis with UV radiation, BAX activation was observed only in cells with released SUMI-1, with no active BAX observed in cells retaining mitochondrial SUMI-1 (Figure 4-16B). Thus, BAX activation/oligomerization correlated with SUMI-1 translocation in cells undergoing apoptosis. To examine BAX oligomerization by another method, purified mitochondria were treated with trypsin, which easily degrades BAX monomers but not oligomers (Lucken-Ardjomande et al., 2008). The trypsin-treated mitochondria were lysed and resolved by SDS-PAGE and blotted for BAX. Any resulting signal detected by BAX antibody represents trypsin-resistant, oligomerized BAX (designated as TR-Bax). SUMI-1 knockdown augmented UV-induced BAX oligomerization (Figure 4-17), consistent with the immunofluorescence data using BAX 6A7 antibody. Together, these data suggest that SUMI-1 regulates MOMP during apoptosis by suppressing BAX activation.

SUMI-1 Does Not Regulate BCL-xL Deamidation

We next examined potential mechanisms by which SUMI-1 could regulate BAX activation. During apoptosis, activation and oligomerization of BAX are mediated in part by pro- and anti-apoptotic BCL-2 family members, as described in Chapter I. Thus, we carried out co-immunoprecipitation experiments to determine whether SUMI-1 interacts with any BCL-2 family proteins during apoptosis, including BAX itself. U2OS cells were lysed in 0.1% NP-40 lysis buffer and immunoprecipitated with SUMI-1 antibody or an isotype (IgG) antibody as a negative control. No interactions were detected between SUMI-1 and BCL-2 or BIM (Figure 4-18A, left panel). Other BCL-2 family proteins were also blotted for, including BAX and BAK, but no signal was observed in the loading controls (data not shown). BAX and BAK can be artificially induced to oligomerize in lysates containing NP-40 detergent and may not be detected at the expected size by SDS-PAGE and western blotting. To avoid this issue, cells can be lysed by alternate means such as with CHAPS lysis buffer. Thus, a co-IP looking for an interaction between SUMI-1 and BAX was repeated using CHAPS buffer. Here, Bax could be observed in the loading samples, but was not found to co-immunoprecipitate with SUMI-1 (data not shown).

An apparent interaction was detected between SUMI-1 and a pro-survival BCL-2 family protein, BCL-xL (Figure 4-18A, right panel). To ensure that the binding was not due to nonspecific interaction between BCL-xL and the SUMI-1 antibody, the experiment was repeated using cells stably-expressing SUMI-1

shRNA as a more stringent control, and two different SUMI-1 antibodies were utilized for the IP. Following incubation with each antibody, an interaction was observed between BCL-xL and SUMI-1. In sh-SUMI-1-expressing cells, less SUMI-1 was immunoprecipitated, and a corresponding decrease was observed in the BCL-xL band (Figure 4-18B).

The bands that were detected by the BCL-xL antibody migrated slightly higher (~34 and 37 kD) than the predicted molecular weight (26 kD) for BCL-xL, and SUMI-1 interacted only with the 34 kD band. BCL-xL is reported to be modified by deamidation during apoptosis, causing a change in conformation and an associated upward shift in migration on SDS-PAGE (Deverman et al., 2002). Deamidation is a process whereby specific asparagine residues are converted, either enzymatically or non-enzymatically, to aspartate or iso-aspartate. In the case of BCL-xL, the majority of deamidated BCL-xL is converted to the iso-aspartate form, and deamidation can occur at one or both of two asparagine residues: N52 and N56. Apoptosis induces deamidation of BCL-xL, and this modification was shown to inhibit BCL-xL's ability to interact with pro-apoptosis BH3-only proteins and its ability to modulate apoptosis. Thus, we hypothesized that SUMI-1 might regulate the deamidation of BCL-xL (either by blocking its deamidation or inducing its re-amidation). To examine this, we treated U2OS cells with SUMI-1 or control siRNA and treated a subset of these cells with UV to induce apoptosis. Knockdown of SUMI-1 led to a decrease in the 34 kD BCL-xL band and a corresponding increase in the 37 kD band. UV radiation induced a similar shift in proportions of the two bands, and SUMI-1 further augmented the

UV-induced change (Figure 4-19). By comparing the migration of these bands with those observed in other publications showing BCL-xL deamidation, it appeared that the 34 kD band might correspond to singly-deamidated BCL-xL, with the 37 kD band corresponding to deamidation at both asparagine residues. To examine this, we generated BCL-xL point mutants to partially mimic deamidation at one or both sites (asparagine is replaced with aspartate: N52D and/or N66D), and other mutants that cannot be deamidated (asparagine is replaced with alanine: N52A and/or N66A). However, the deamidation mimics, while migrating higher than the 26 kD predicted size for BCL-xL, migrated at a lower apparent size than the 34 kD and 37 kD bands that were modulated by RNAi of SUMI-1 (data not shown).

Because the migration of the bands we observed did not match with the predicted molecular weight of BCL-xL or with the migration of deamidation mimic BCL-xL mutants, we began to suspect that the BCL-xL antibody used for the initial co-IP (S-18, Santa Cruz sc-634) might have detected a nonspecific band rather than BCL-xL. To determine whether this band represents BCL-xL, the co-IP was repeated using additional BCL-xL antibodies for blotting after IP, and a reciprocal IP was attempted using several BCL-xL antibodies for the IP and blotting for SUMI-1. However, no other BCL-xL antibodies could detect this interaction, and a reciprocal IP with BCL-xL antibody failed to pull down SUMI-1 (data not shown). Thus, it appeared that the BCL-xL S-18 antibody nonspecifically recognizes a different protein that co-immunoprecipitates with SUMI-1.

SUMI-1 interacts with p32, which is the same molecular weight (34 kD) as the band recognized by the BCL-xL antibody to interact with SUMI-1. To determine whether the 34 kD band recognized by the BCL-xL antibody is p32, a co-IP was done in U2OS cells transfected with either p32 siRNA or with plasmids expressing various p32 proteins (tagged and untagged; full-length and the mature/cleaved form). Whole cell extracts (to represent loading) and samples immunoprecipitated with SUMI-1 antibody were resolved by SDS-PAGE and blotted with the BCL-xL S-18 antibody. Indeed, the BCL-xL antibody recognized tagged and untagged ectopically-expressed p32 and an endogenous band of identical molecular weight (Figure 4-20), indicating that this antibody is capable of detecting p32. The antigen used by Santa Cruz to produce the BCL-xL S-18 antibody is an undisclosed peptide located within the first 50 amino acids of the BCL-xL sequence. Comparison of this N-terminal region of BCL-xL with the p32 sequence revealed an area of homology between these proteins that is located within the BH4 domain of BCL-xL and near the N-terminus of mature (cleaved) p32. This region, which is located within the range of amino acids that Santa Cruz indicated were used for producing the Bcl-xL antibody, could potentially explain the interaction between this antibody and p32. We conclude that the apparent interaction detected between BCL-xL and SUMI-1 was merely an artifact caused by nonspecific interaction of p32 with the BCL-xL antibody.

SUMI-1 Regulates Mitochondrial Fission-Fusion Dynamics

As we did not detect any confirmed interactions between BCL-2 family proteins and SUMI-1, we considered alternative mechanisms by which SUMI-1 might regulate BAX. BAX-mediated MOMP is reported to be regulated by mitochondrial fusion-fission dynamics (reviewed recently by (Martinou and Youle, 2011)). To determine whether SUMI-1 affects these processes, we treated cells with SUMI-1 siRNA and examined the resulting mitochondrial morphology by immunofluorescence staining with the mitochondrial marker Tim23. As shown in Figure 4-22A, SUMI-1 knockdown led to mitochondrial fragmentation, with cells exhibiting smaller, more punctate mitochondria than found in control cells.

We next examined whether SUMI-1 overexpression could protect mitochondria from the fragmentation that occurs during apoptosis. Cells were treated with adenovirus expressing untagged SUMI-1, or empty-vector control, and apoptosis was induced with UV. SUMI-1 overexpression greatly reduced UV-induced mitochondrial fragmentation (Figure 4-22B). Together, these data suggest that SUMI-1 inhibits mitochondrial fragmentation. To determine whether the fragmentation induced by SUMI-1 loss resulted from increased fission or decreased fusion, we carried out a cell hybrid assay to examine the effect of SUMI-1 knockdown on mitochondrial fusion (Figure 4-23A). In this assay, cells were first treated with NS or SUMI-1 siRNA. One group of U2OS cells was transfected with mt-RED (mKate2 fused with a mitochondrial targeting signal), while another group of cells were transfected with mt-GREEN (GFP fused with a mitochondrial targeting signal) in order to label mitochondria red or green,

respectively. The two groups of cells were then seeded together in the same plate, and PEG was applied for 5 minutes to induce fusion of cells. This process creates hybrid cells in which a cell with red-labeled mitochondria is merged with a cell with green-labeled mitochondria, allowing the two separately-labeled mitochondrial groups to intermingle in an intact cell. Under conditions of normal mitochondrial fusion, red and green mitochondria fuse, resulting in yellow mitochondria (Figure 4-23B, left panel). Without fusion, red and green mitochondria remain distinct (Figure 4-23B, right panel). The numbers of hybrid cells with and without mitochondrial fusion were tallied and the results plotted. SUMI-1 knockdown impaired fusion in the absence of apoptotic stimuli (66% of hybrids exhibited fusion compared to 97% for control cells). Consistent with previous reports (Lee et al., 2004), we observed a decrease in fusion when cells were treated with UV to induce apoptosis (82% of hybrids with fusion), and SUMI-1 knockdown augmented UV-induced inhibition of fusion (19% of hybrids displayed fusion) (Figure 4-23C). These results suggest that SUMI-1 regulates mitochondrial dynamics by inhibiting mitochondrial fusion, providing a plausible mechanism for SUMI-1's regulation of BAX-mediated MOMP and apoptosis.

Discussion

Mitochondrial outer membrane permeabilization (MOMP) is a critical control point during apoptosis and is often the "point of no return," as cells usually proceed to die upon the resulting release of cytochrome c and other mitochondrial proteins. For this reason, regulation of MOMP has been an area of

intense research, with particular interest in the mechanisms leading to BAX and BAK activation and oligomerization. Elucidating these mechanisms may aid in our discovery of therapeutics for apoptosis-associated diseases such as immune disorders, neurodegenerative disease, and cancer. Identifying novel proteins regulating MOMP can enhance our understanding of this process.

This study establishes SUMI-1 as a novel anti-apoptotic protein residing at the mitochondria, where it regulates mitochondrial dynamics, BAX activation, and MOMP during apoptosis. Based on the data presented here, we propose a model (Figure 4-23) in which SUMI-1 resides on the mitochondria of healthy cells, where it protects cells from unnecessary apoptosis by promoting normal mitochondrial fusion and inhibiting apoptotic-stimuli-induced BAX activation and/or oligomerization. Shortly after treatment with apoptotic stimuli, BAX translocates to mitochondria, while SUMI-1, presumably independently, translocates from the mitochondria. This exodus of SUMI-1 triggers mitochondrial fragmentation, promoting BAX oligomerization and allowing MOMP and apoptosis to proceed. These findings provide a localization and function for a protein that was previously not well-characterized, contributing to our knowledge of the physiological events that take place at the mitochondria to regulate BAX-mediated MOMP during apoptosis.

During apoptosis, SUMI-1 translocates from the mitochondria to the cytoplasm and nucleus. It is unknown what signal induces this translocation, and this would be an interesting area of further investigation. It is also possible that SUMI-1 may have an additional role in the cytoplasm and/or nucleus post-

translocation. Non-mitochondrial SUMI-1 is not required for apoptosis, however, as demonstrated by two pieces of evidence. First, transfection with N-terminally-tagged SUMI-1, which lacks mitochondrial localization (Figure 4-6E), does not appear to influence apoptosis (data not shown). More importantly, knockdown of SUMI-1 with siRNA promotes rather than inhibits apoptosis, indicating that cytoplasmic SUMI-1 is not required for this process. Instead, it is possible that non-mitochondrial SUMI-1 may carry out a pro-apoptotic, rather than anti-apoptotic, function in the cytoplasm and/or nucleus, or it may contribute to biochemical or morphological changes observed during apoptosis such as phosphatidylserine flipping.

Evasion of apoptosis is one of the hallmarks of cancer, and cancers often exhibit reduced expression of pro-apoptotic proteins and/or enhanced expression of anti-apoptotic proteins (Hanahan and Weinberg, 2000, 2011). According to mRNA microarray expression data mined from Oncomine, SUMI-1 is overexpressed in a number of cancers derived from different tissues, including those of the breast, prostate, lung, kidney, skin, cervix, brain, mesothelium, head/neck, pancreas, and in myeloma, lymphoma, and two types of leukemias (Table 4-2) (Albino et al., 2008; Andersson et al., 2007; Gordon et al., 2005; Haqq et al., 2005; Landi et al., 2008; Pei et al., 2009; Pyeon et al., 2007; Sorlie et al., 2003; Storz et al., 2003; Tomlins et al., 2007; Yusenko et al., 2009; Zhan et al., 2007). Graphs of these data for three cancers are shown in Figure 4-24. Consistent with these reports, we observed increased expression of SUMI-1 protein in cancer cell lines compared to non-transformed cells (Figure 4-25). This

upregulation of SUMI-1 in cancers, along with our data showing that SUMI-1 knockdown sensitizes cancer cells to chemotherapeutic agents, suggests that further research may be warranted to investigate SUMI-1 as a diagnostic marker in cancers or as a potential chemosensitizing drug target to enhance current cancer therapies.

Interestingly, expression of SUMI-1 was reported to be significantly downregulated in Alzheimer's Disease, which is characterized by increased apoptosis (Blalock et al., 2004). It is unknown whether this altered expression of SUMI-1 contributes to or is merely a consequence of the increased apoptosis that occurs in this neurodegenerative disorder, and it is also unknown where SUMI-1 might fit into apoptosis pathways that are altered in Alzheimer's Disease. β-amyloid aggregates are thought to induce neuronal apoptosis in part through generation of oxidative stress (Ethell and Buhler, 2003). Because SUMI-1 contains a CHCH domain, which is regulated by redox status in other proteins, it is conceivable that SUMI-1 might respond to this change in oxidative stress. Future studies may be able to determine whether SUMI-1 plays a causative role in Alzheimer's or other neurodegenerative disorders.

Materials and Methods

Cell Culture, transfections, and apoptotic treatments. U2OS and HeLa cells were obtained from ATCC, and mouse embryo fibroblasts were harvested at E13.5. All cells were cultured in a 37°C incubator with 5% CO_2 in DMEM

supplemented with 10% FBS, 100 U/ml penicillin, and 100 g/ml streptomycin. DNA transfections were carried out with Fugene-6 or Fugene-HD (Roche), and siRNA transfections were performed with Oligofectamine (Invitrogen), according to the manufacturers' instructions. Apoptosis treatments included UVC radiation (dosages as indicated) using a Stratalinker® UV Crosslinker (Stratagene), cisplatin (10 μg/ml for U2OS and HeLa), doxorubicin (7.5 μM for U2OS), and staurosporine (20 μM for U2OS). Where indicated, cells were pretreated for 1 hour with pan-Caspase inhibitor Q-VD-OPh (R&D Systems, 10 μM for U2OS and 30 μM for HeLa cells). Subcellular fractionation was carried out as described previously (Itahana and Zhang, 2008).

DNA plasmids, adenoviruses, and siRNA. Full-length SUMI-1 cDNA was purchased from Open Biosystems (Genbank accession number NM_016139.2), and untagged, C-terminally Flag-tagged, and N-terminally Myc-tagged SUMI-1 were cloned into a pcDNA3.1 vector (Invitrogen). All cloned constructs were confirmed by DNA sequencing. Recombinant adenoviruses carrying untagged SUMI-1 or GFP were produced using the AdEasy™ XL Adenoviral Vector System (Stratagene) according to the manufacturer's protocol. siRNA duplexes targeting SUMI-1 were obtained from Invitrogen (Stealth RNAi™ #HSS167117 and HSS167119), and nonspecific control siRNA was manufactured by Dharmacon.

SDS-PAGE, co-immunoprecipitation, and western blotting. Cells were lysed in 0.5% NP-40 buffer for straight westerns and either 0.1% NP-40 or 1% CHAPS lysis buffer, where indicated, for co-immunoprecipitation (co-IP). Lysates for co-IP were pre-cleared for 30 minutes with CL-4 beads and incubated in primary antibody for 4 hours to overnight followed by incubation in Protein A beads for 1 hour. Beads were washed 3x, and protein complexes were eluted using 1x SDS-PAGE sample buffer. Samples were resolved by SDS-PAGE on a 15% polyacrylamide gel and transferred onto a 0.2 μM nitrocellulose membrane. Membranes were blocked for a minimum of 30 minutes in phosphate-buffered saline blocking buffer with 0.1% Tween-20 (PBST) and 5% nonfat dried milk. Membranes were incubated for 2 hours to overnight in primary antibody, incubated for 1-2 hours in secondary HRP-conjugated antibody, and exposed with Supersignal West Pico or Dura (Pierce).

Immunofluorescence imaging. Cells were fixed in 4% paraformaldehyde for 10 minutes at room temperature and permeabilized in 0.2% Triton X-100 for 5 minutes at 4°C. Fixed and permeabilized cells were blocked for 30 minutes in 0.5% BSA blocking buffer in PBS, incubated in primary antibody overnight at 4°C with rocking, and incubated with Alexa Fluor® secondary antibodies (488 and 594 donkey anti-rabbit and donkey anti-mouse) for 30 minutes at room temperature with rocking. Nuclei were stained with DAPI (diamidino-2-phenylindole), and mitochondria were visualized with MitoTracker™ Red (Invitrogen) or other mitochondrial markers where indicated. Cells were mounted

in fluorescence mounting medium (Dako) and analyzed using an Olympus IX81 inverted microscope combined with a SPOT™ digital microscope camera and imaging software (SPOT™ Imaging Solutions).

Antibodies. Rabbit anti-SUMI-1 antibody was produced by immunizing rabbits (performed by PRF&L, Canadensis, PA) with a KLH-conjugated peptide antigen corresponding to amino acids 94-108 of SUMI-1. Serum was affinity purified, and antibody specificity was tested by western blotting and immunofluorescence staining with SUMI-1 knockdown (Figure 4-5). The following antibodies were purchased commercially: actin (Chemicon), PARP (C2-10, BD Pharmingen), HSP70/GRP75 (H-155, Santa Cruz), cytochrome *c* (6H2.B4, BD Pharmingen), Tim23 (BD Transduction Laboratories), Active BAX (6A7, BD Biosciences), BIM (C34C5, Cell Signaling), BCL-2 (50E3, Cell Signaling), BAX (Cell Signaling, D2E11), and BCL-xL (S-18, Santa Cruz sc-634; 54H6, Cell Signaling).

Immunogold electron microscopy. Experiments were carried out by the Microscopy Services Laboratory in the Department of Pathology and Laboratory Medicine at the University of North Carolina at Chapel Hill. Cells grown on Nunc Permanox chamberslides were fixed with 4% paraformaldehyde in 0.15 M sodium cacodylate, pH 7.4, for 1 hour. Using a pre-embedding immunogold/silver staining protocol (Yi et al., 2001), cells were incubated in primary antibody (1:50 dilution of rabbit anti-SUMI-1), followed by secondary antibody incubation in goat anti-rabbit IgG 0.8nm immunogold (Aurion, Electron Microscopy Sciences). After

silver enhancement, cells were processed and embedded in Polybed 812 epoxy resin (Polysciences, Inc., Warrington, PA). 70 nm ultrathin sections were cut, mounted on copper grids, and post-stained with 4% uranyl acetate and Reynolds' lead citrate (Reynolds, 1963). Sections were observed using a LEO EM-910 transmission electron microscope operating at 80kV (LEO Electron Microscopy, Thornwood, NY), and images were taken using a Gatan Orius SC1000 CCD camera with Digital Micrograph 3.11.0 (Gatan, Inc., Pleasanton, CA).

Organism	% Amino acid identity to human
Chimpanzee *(Pan troglodytes)*	100%
Dog *(Canis familiaris)*	91%
Rat *(Rattus norvegicus)*	89%
Mouse *(Mus musculus)*	87%
Chicken *(Gallus gallus)*	83%
Fruit fly *(Drosophila melanogaster)*	56%
Worm *(Caenorhabditis elegans)*	54%
Yeast *(Saccharomyces cerevisiae)*	44%

Table 4-1. Conservation among SUMI-1 orthologs.
Percentage of amino acid identity is shown for eight orthologs of the SUMI-1 protein.

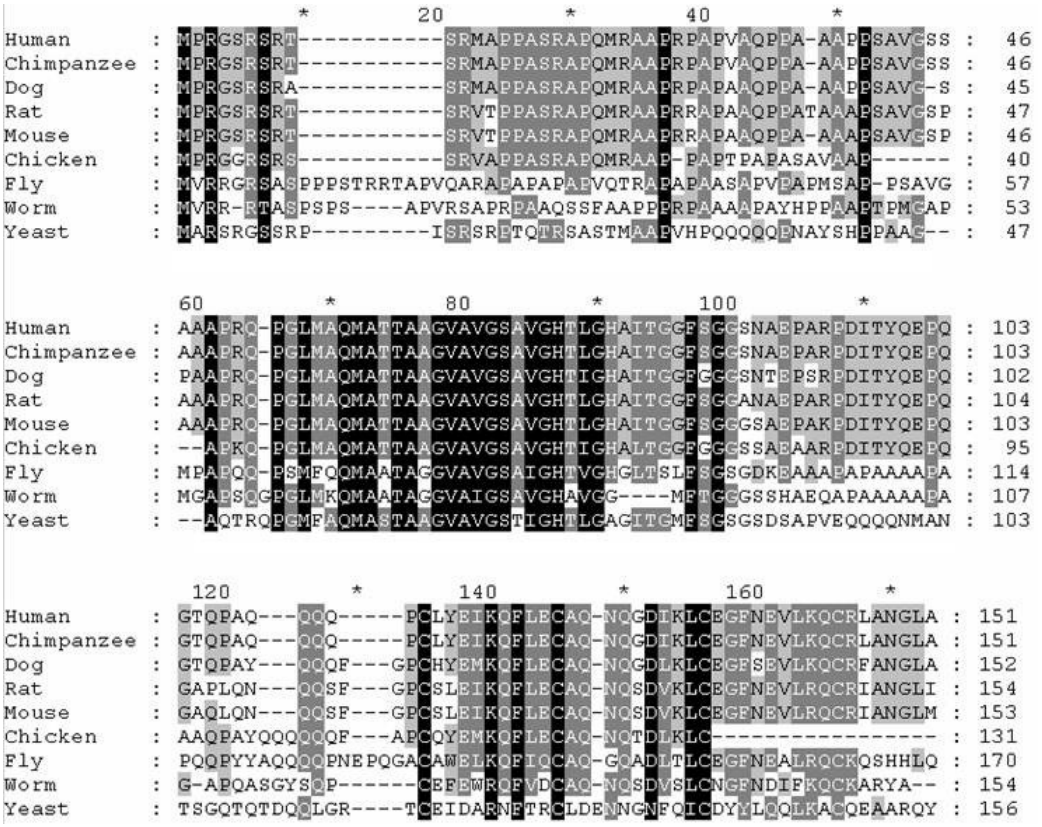

Figure 4-1. Sequence alignment for SUMI-1 orthologs.
CLUSTALW protein sequence alignment of human SUMI-1 protein and SUMI-1 orthologs in the eight species shown in Table 4-1. Darker shading indicates greater sequence similarity.

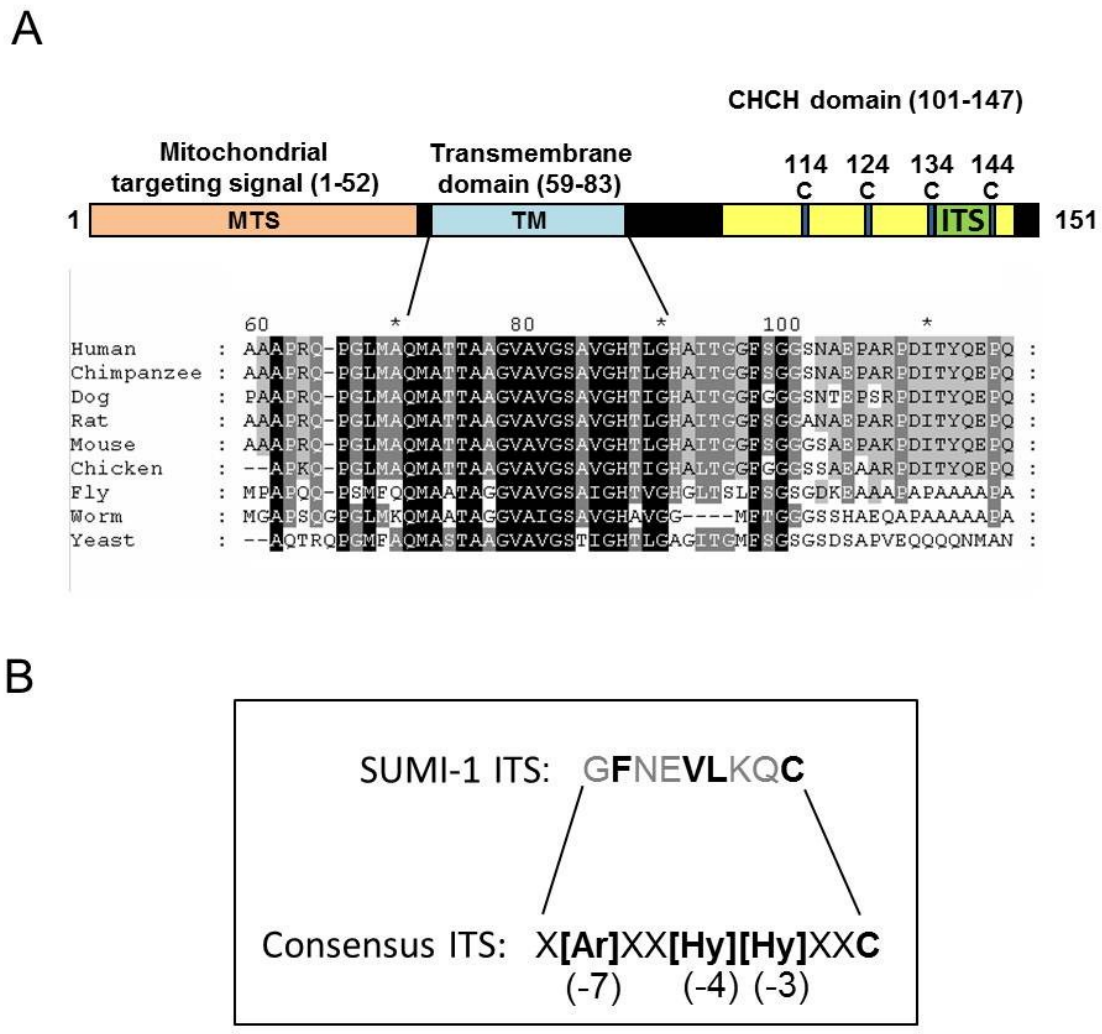

Figure 4-2. Domain structure of SUMI-1.
A) Schematic representation of the SUMI-1 protein, with putative mitochondrial targeting signal (MitoProt), transmembrane domain (TMpred), CHCH (coiled-coil-helix coiled-coil-helix) domain, and intermembrane space targeting sequence (ITS) shown. The transmembrane domain is highly conserved across SUMI-1 orthologs. The CHCH domain is comprised of four evenly-spaced cysteines, with positions indicated. The predicted transmembrane domain is located in a highly-conserved region of the SUMI-1 protein.
B) The SUMI-1 mitochondrial intermembrane space targeting signal (ITS) and the consensus ITS for Mia40-mediated intermembrane space import.

Figure 4-3. Predicted intramolecular disulfide bond formation for SUMI-1. Analysis of the SUMI-1 amino acid sequence by *DiANNA 1.1* predicts the formation of intramolecular disulfide bonds between cysteines 1 and 3 (C1-C3) of the CHCH domain, and between cysteines 2 and 4 (C2-C4), creating a loop in the CHCH domain as illustrated above (drawing not to scale).

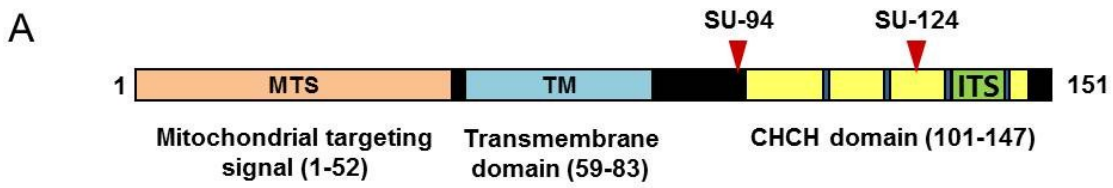

B

MPRGSRSRTSRMAPPASRAPQMRAAPRPAPVAQPPAAAPPSAVGSSAAAPRQPG
LMAQMATTAAGVAVGSAVGHTLGHAITGGFSGGSNAEPA**RPDITYQEPQGTQPA**
QQQQPCLYEIKQFLEC**AQNQGDIKLC**EGFNEVLKQCRLANGLA

Figure 4-4. Antibody design for SUMI-1.
A) Schematic of SUMI-1 protein showing approximate location of the peptide antigens (SU-94 and SU-124) selected for production of SUMI-1 rabbit polyclonal antibodies. Red triangles indicate the approximate positions of the selected peptides.
B) The SUMI-1 protein sequence with the two selected peptide antigens shown in red and underlined.

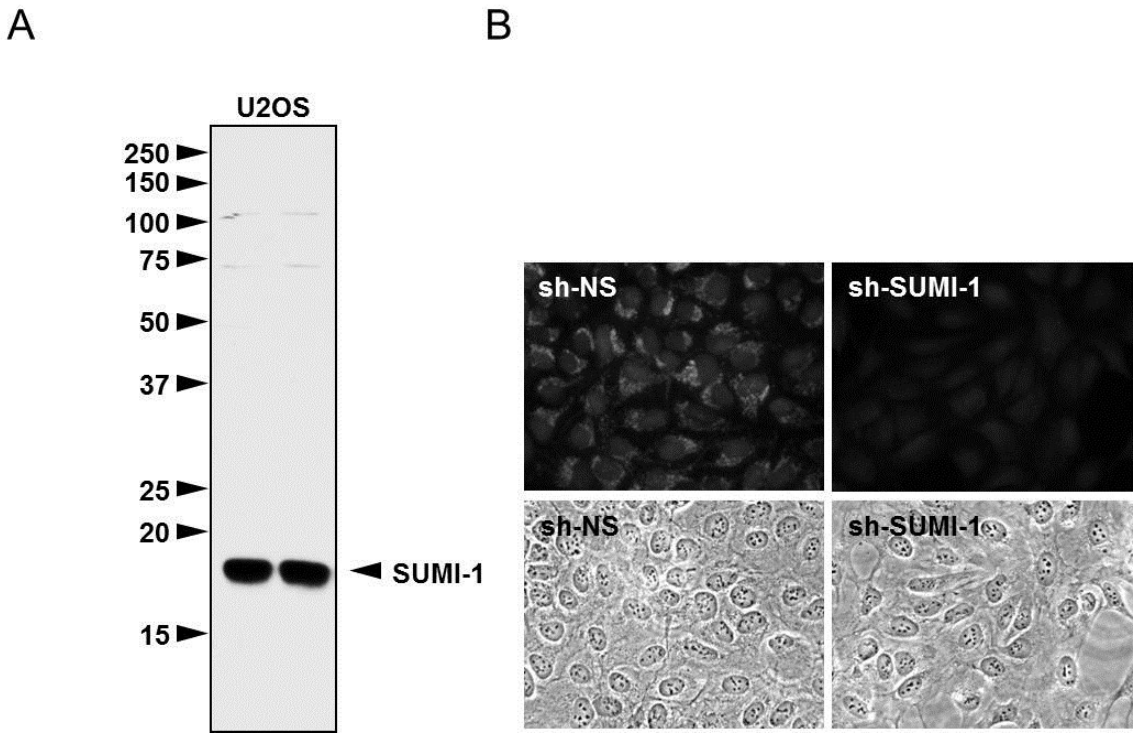

Figure 4-5. SUMI-1 antibody effectiveness and specificity
A) Whole-membrane western blot showing specificity and effectiveness for purified rabbit polyclonal antibody targeting SUMI-1 (SU-94).
B) Immunofluorescence signal detected with SUMI-1 antibody is specific to SUMI-1. Cells were treated with either control lentivirus (sh-NS) or lentivirus expressing SUMI-1 shRNA (sh-SUMI-1), fixed with formaldehyde, permeabilized, and immunofluorescence-stained with SUMI-1 antibody. Phase-contrast images are shown below. Note that fluorescence signal is greatly diminished upon SUMI-1 knockdown (top right panel).

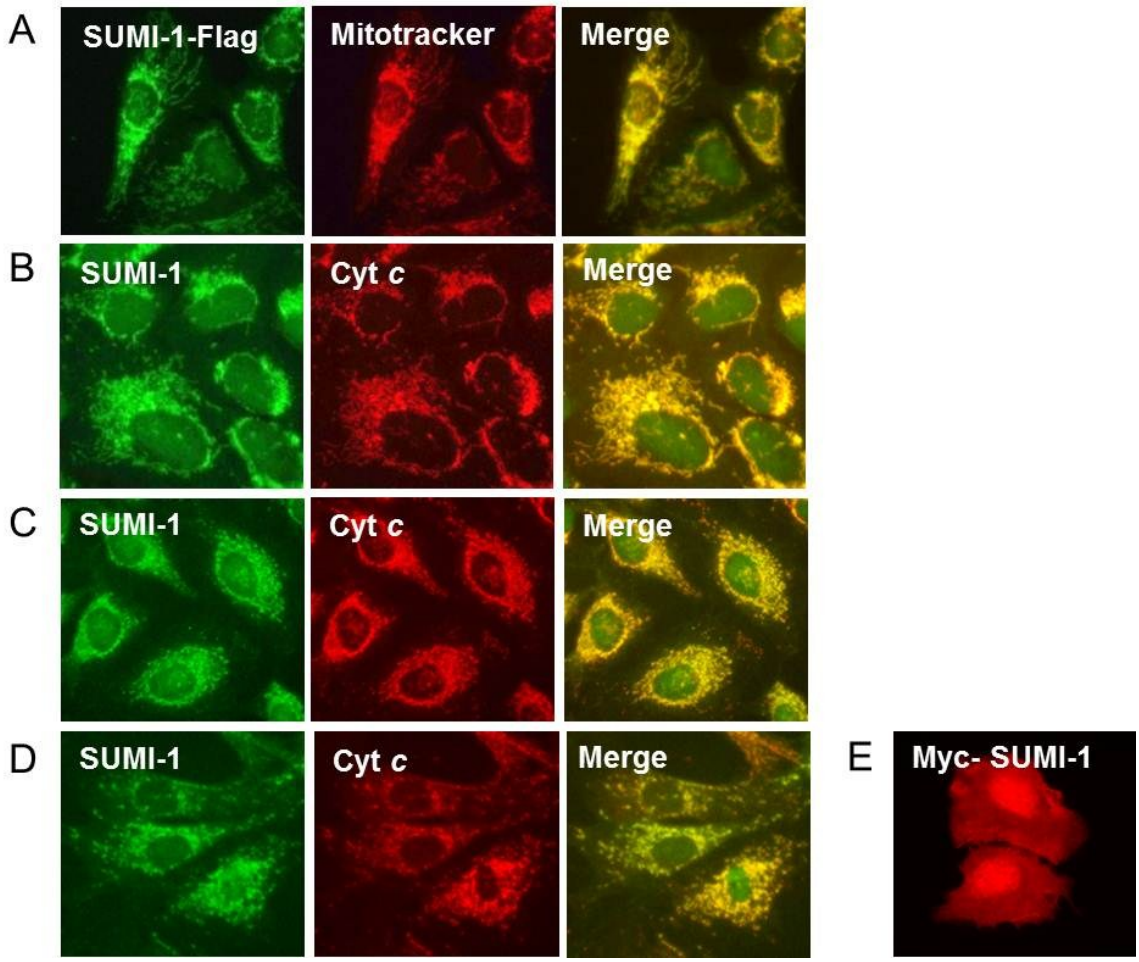

Figure 4-6. Immunofluorescence imaging demonstrates mitochondrial localization of SUMI-1.

A) C-terminally-tagged SUMI-1-Flag localizes to the mitochondria, as indicated by costaining with MitoTracker™ dye. SUMI-1-Flag was detected by immunofluorescence with Flag antibody.

B) Mitochondrial localization of endogenous SUMI-1 in U2OS cells detected by immunofluorescence with SUMI-1 antibody, demonstrated by costaining for mitochondrial marker cytochrome *c.*

C) Mitochondrial localization of SUMI-1 in HeLa cells detected as in (B).

D) Mitochondrial localization of SUMI-1 in MEF (mouse embryo fibroblast) cells detected as in (B).

E) Presence of an N-terminal tag disrupts mitochondrial localization of SUMI-1. Cells were transfected with Myc-SUMI-1 and stained with anti-Myc antibody.

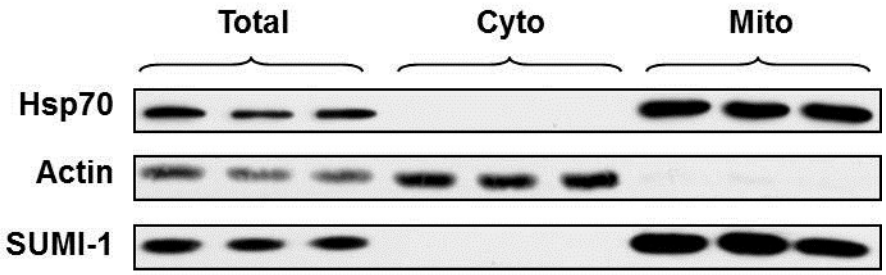

Figure 4-7. Subcellular fractionation of SUMI-1.
Untreated U2OS cells were fractionated using a differential detergent method. SUMI-1 is present in the mitochondria-enriched heavy membrane fraction, with three replicates shown for each fraction. Hsp70 is a marker for the mitochondrial fraction, and actin is a marker for the cytoplasmic fraction (Cyto, cytoplasm; Mito, mitochondria).

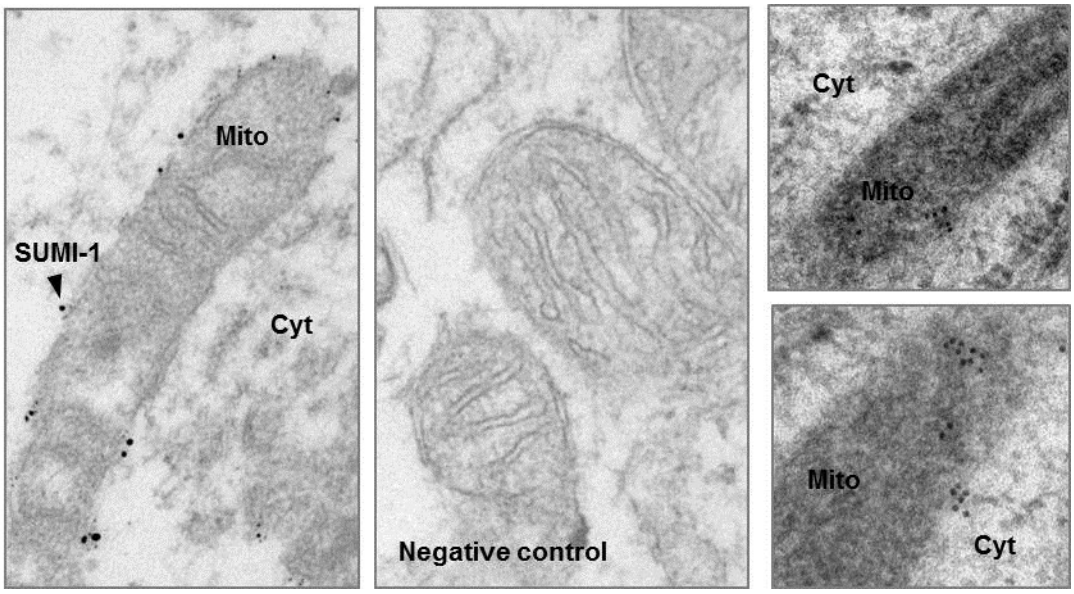

Figure 4-8. Immunogold-EM localization of SUMI-1.
(Left) Pre-embedding immunogold staining of endogenous SUMI-1 visualized by electron microscopy. Gold beads corresponding to endogenous SUMI-1 can be seen around perimeter of mitochondria. One example is designated with an arrow. (Cyt, cytoplasm; Mito, mitochondria). (Center) Immunogold staining with an isotype antibody is shown as a negative control. (Right) Post-embedding immunogold staining shows that endogenous SUMI-1 is also present inside the mitochondria as well as along the outer membrane.

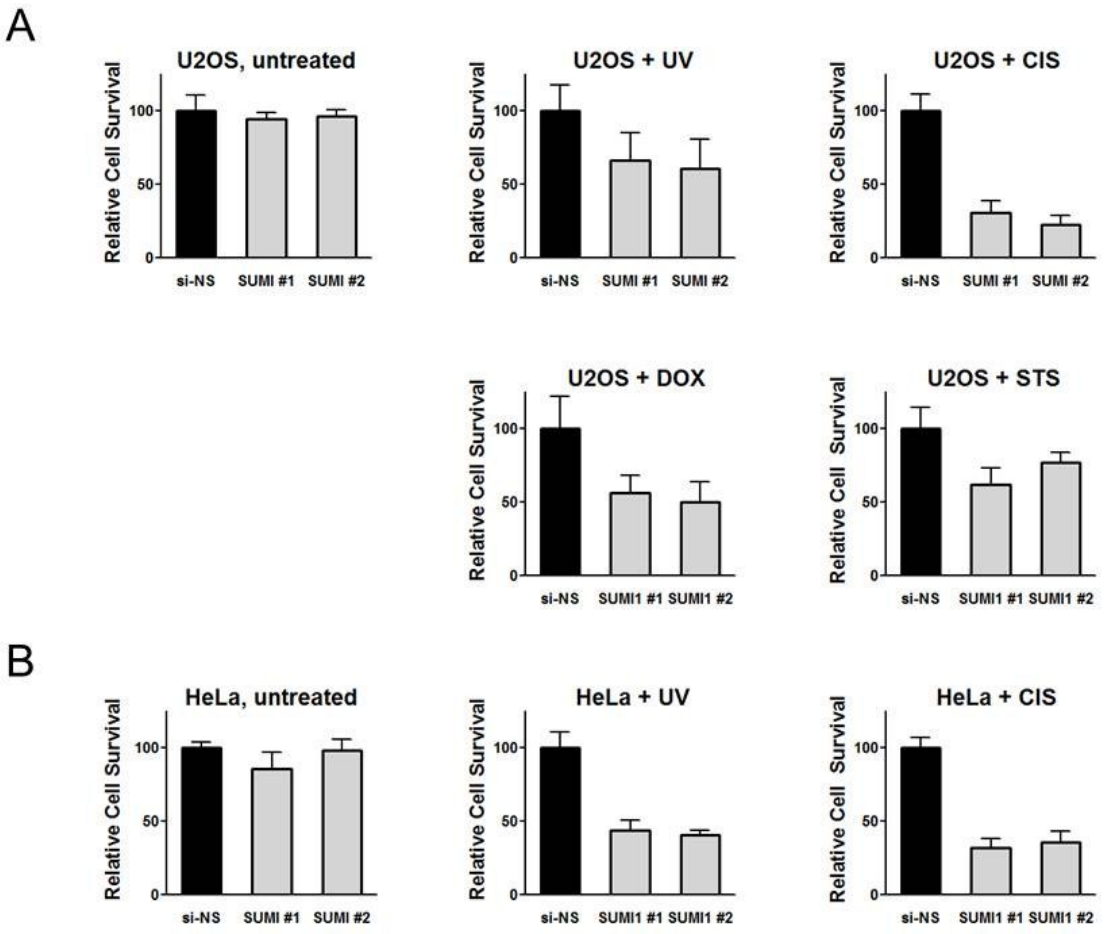

Figure 4-9. SUMI-1 knockdown promotes apoptotic cell death.
A) SUMI-1 knockdown sensitizes U2OS cells to apoptosis induced by a variety of agents. Cells were treated with indicated siRNA for 48 hours and treated to induce apoptosis with cisplatin (CIS, 10 µg/ml for 18 h), UV (25 mJ/cm^2 for 4 h), doxorubicin (DOX, 7.5 µM for 18 h), or staurosporine (STS, 20 µM for 18 h). The number of cells surviving each treatment is shown as a percentage of si-NS control and is an average of cells counted from at least 4 fields for each condition. Error bars indicate standard deviation.
B) SUMI-1 knockdown sensitizes HeLa cells to apoptosis induced by cisplatin (CIS, 10 µg/ml for 18 h) and UV (2.5 mJ/cm^2 for 18 h). Cells were treated and quantified as in (A).

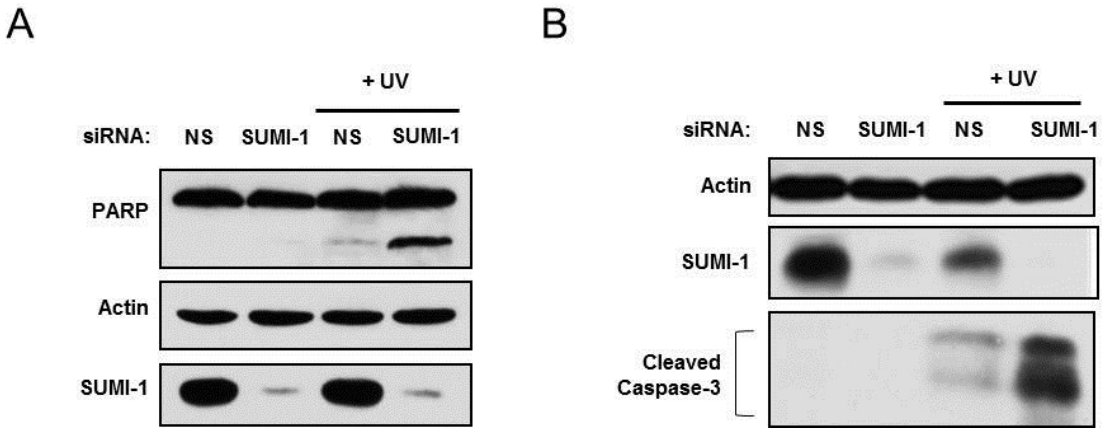

Figure 4-10. SUMI-1 knockdown enhances cleavage of PARP and Caspase-3.

A) SUMI-1 knockdown enhances PARP cleavage during apoptosis. HeLa cells were treated with indicated siRNA for 48 h and treated where indicated with UV (3 mJ/cm^2 for 18 h) to induce apoptosis. Actin is shown as a loading control.

B) SUMI-1 knockdown increases cleavage of Caspase-3 during apoptosis. U2OS cells were treated with indicated siRNA for 48 h and treated where indicated with UV (6 mJ/cm^2 for 18 h) to induce apoptosis. Actin is shown as a loading control.

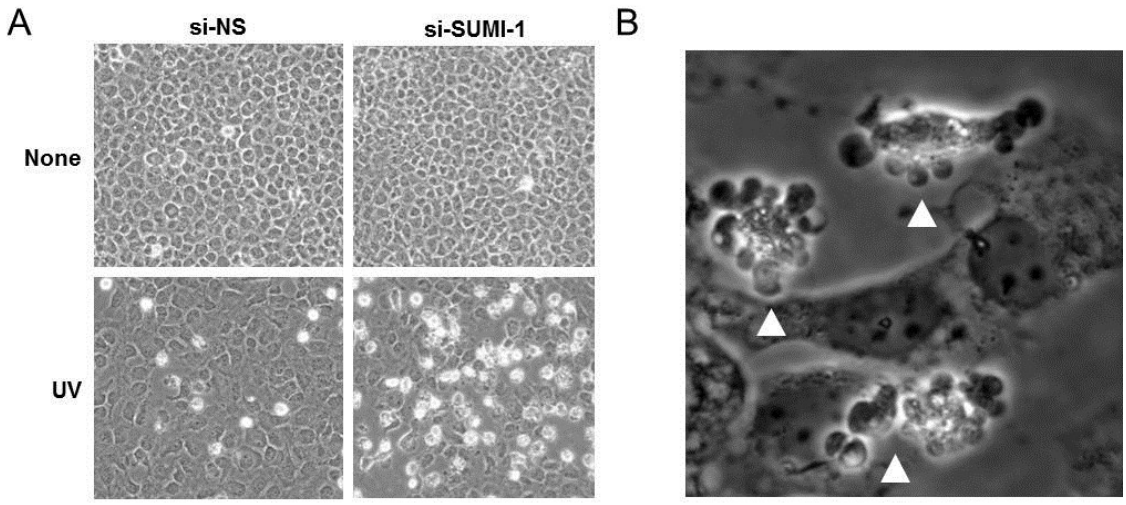

Figure 4-11. SUMI-1 knockdown promotes apoptotic cell death.
(A) SUMI-1 knockdown sensitizes U2OS cells to UV-induced cell death. Phase-contrast images (10x) are shown of cells treated for 48 hours with nonspecific siRNA (si-NS) or SUMI-1 siRNA (si-SUMI-1), with or without UV treatment (25 mJ/cm^2 for 3 hours). Floating (dead) cells appear rounded and white.
(B) Apoptotic membrane blebbing is evident at higher magnification (40x) in cells from (A) treated with SUMI-1 siRNA and UV. Cells displaying blebbing are indicated with arrows.

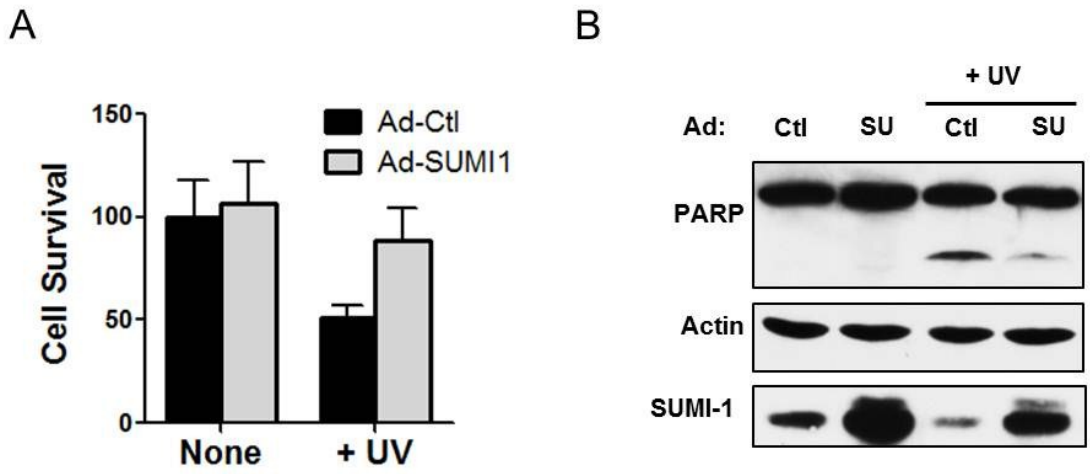

Figure 4-12. SUMI-1 overexpression protects against apoptotic cell death.
A) Overexpression of untagged SUMI-1 protects U2OS cells from apoptosis. Cells were treated for 24 h with control adenovirus (expressing GFP) or adenovirus expressing untagged SUMI-1 and then treated with UV to induce apoptosis (25 mJ/cm^2 for 8 hours). The number of cells surviving is shown as a percentage of Ad-GFP control.
B) SUMI-1 overexpression inhibits PARP cleavage during apoptosis. HeLa cells were treated with indicated adenovirus for 24 hours (Ctl, Ad-GFP; SU, SUMI-1) and then treated with UV (25 mJ/cm^2 for 8 hours) to induce apoptosis. Actin is shown as a loading control.

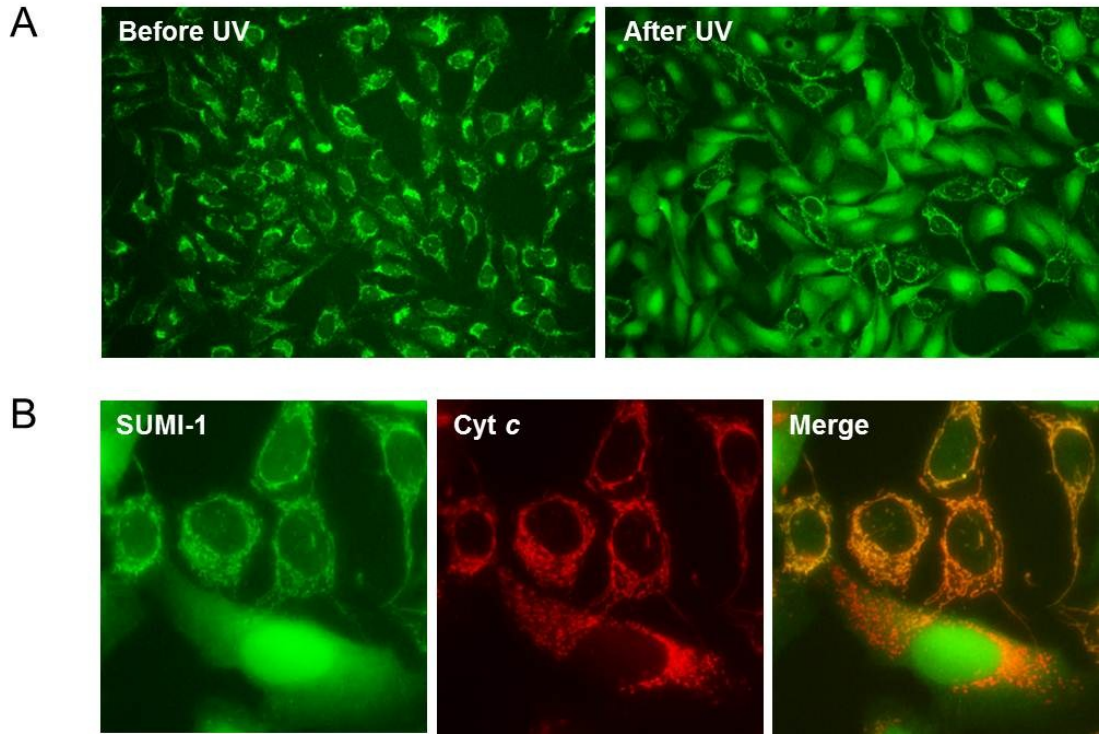

Figure 4-13. SUMI-1 translocates from mitochondria during apoptosis.
A) SUMI-1 translocates from mitochondria during apoptosis. U2OS cells were pretreated with QVD for 1 h and treated with UV to induce apoptosis (6 mJ/cm^2 for 24 h), where indicated. Endogenous SUMI-1 was detected by immunofluorescence staining.
B) A higher-magnification immunofluorescence image of endogenous SUMI-1 (green) and endogenous cytochrome *c* (red) together in UV-treated (6 mJ/cm^2 for 12 h) U2OS cells reveals that cytochrome *c* can be observed in mitochondria from which SUMI-1 has already translocated.

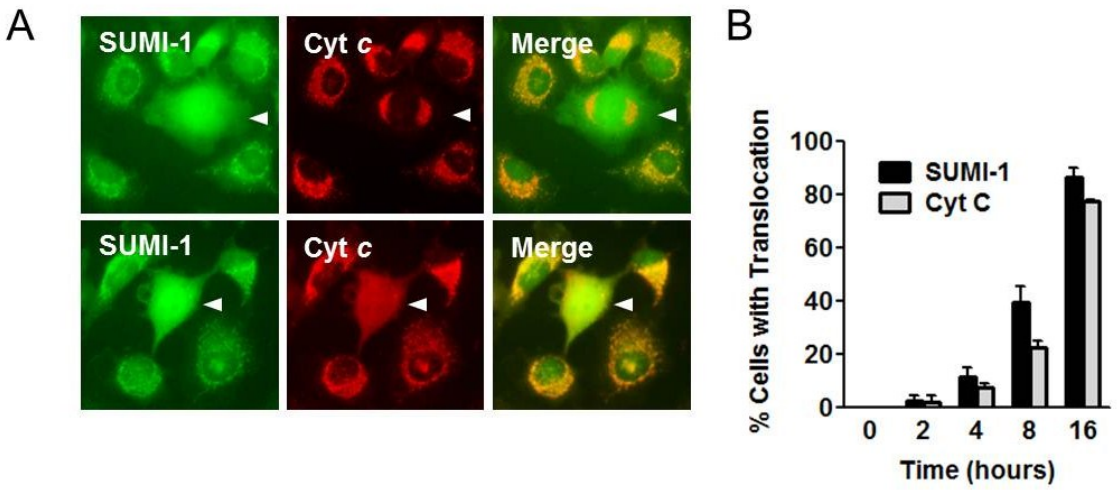

Figure 4-14. SUMI-1 translocates from mitochondria prior to cytochrome *c*.
A) SUMI-1 translocates prior to cytochrome *c* during apoptosis. HeLa cells were treated with UV (6 mJ/cm^2 for 12 h) to induce apoptosis, and immunofluorescence staining was done for endogenous SUMI-1 (green) and endogenous cytochrome *c* (red). Arrows in top row indicate a cell in which SUMI-1 has translocated but cytochrome c is retained in mitochondria. Arrows in bottom row indicate a cell in which both SUMI-1 and cytochrome *c* have translocated from mitochondria.
B) SUMI-1 translocates more rapidly than cytochrome c over a time course. U2OS cells were pretreated with Caspase inhibitor QVD (10 μM for 1 h) to preserve cell survival post-MOMP, treated with UV (25 mJ/cm^2) to induce apoptosis, and fixed at indicated time points. Immunofluorescence staining was done for endogenous SUMI-1 and cytochrome *c*. The percentages of cells with translocated SUMI-1 and cytochrome *c* were quantified at each time point and shown on graph as averages from 4 fields. Error bars indicate standard deviation

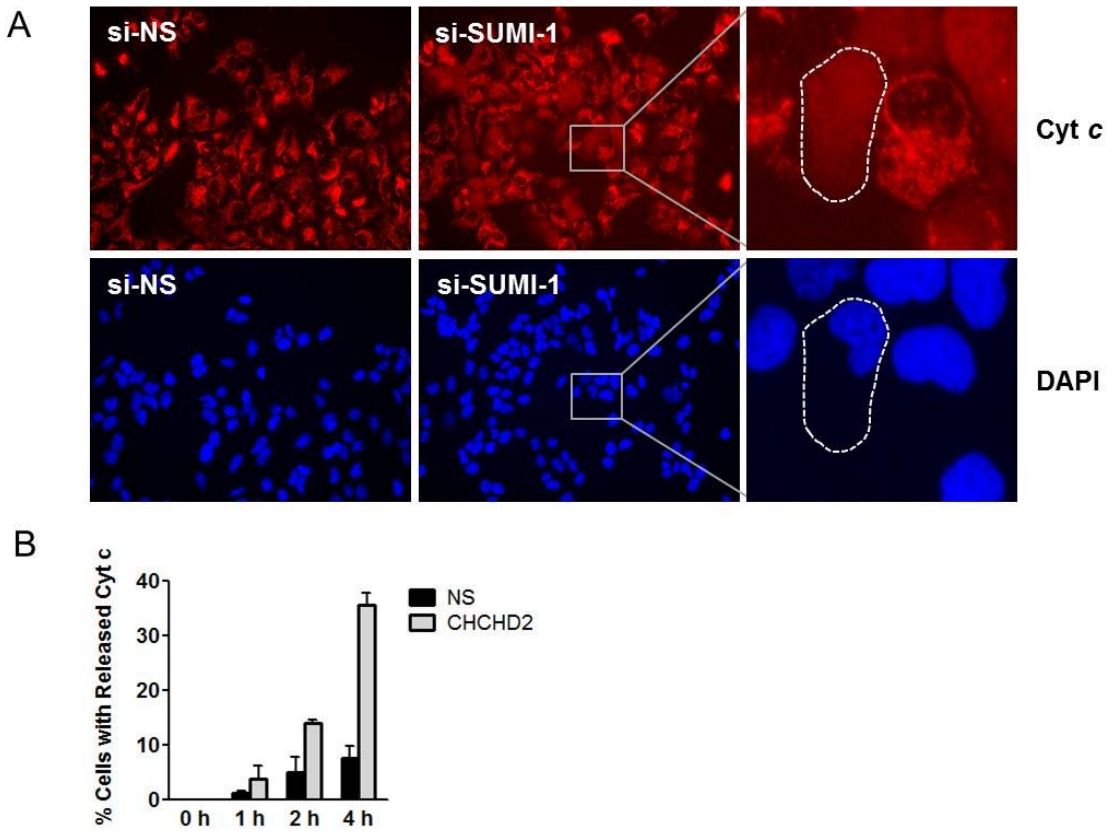

Figure 4-15. SUMI-1 knockdown regulates mitochondrial outer membrane permeabilization.

A) SUMI-1 knockdown increases the kinetics of MOMP as indicated by cytochrome *c* release. U2OS cells were treated with indicated siRNA (NS, nonspecific) for 48 hours, pretreated with Caspase inhibitor QVD to preserve cell survival post-MOMP, and treated to induce apoptosis where indicated (UV, 25 mJ/cm^2 for 4 hours) followed by immunofluorescence staining for endogenous cytochrome *c*. The panel on the right shows an example of a cell (demarcated with dotted line) with released cytochrome c, which appears diffuse throughout the cytoplasm and nucleus. Note that cells treated with SUMI-1 siRNA exhibit a greater proportion of cells with cytochrome *c* release.

(B) SUMI-1 knockdown increases the kinetics of MOMP over a time course. U2OS cells were treated as in (A) and fixed at various time points after UV treatment. Following immunofluorescence staining for endogenous cytochrome *c*, the percentages of cells exhibiting released cytochrome *c* were quantified at indicated time points and shown on the graph as averages from at least 4 fields. Error bars indicate standard deviation.

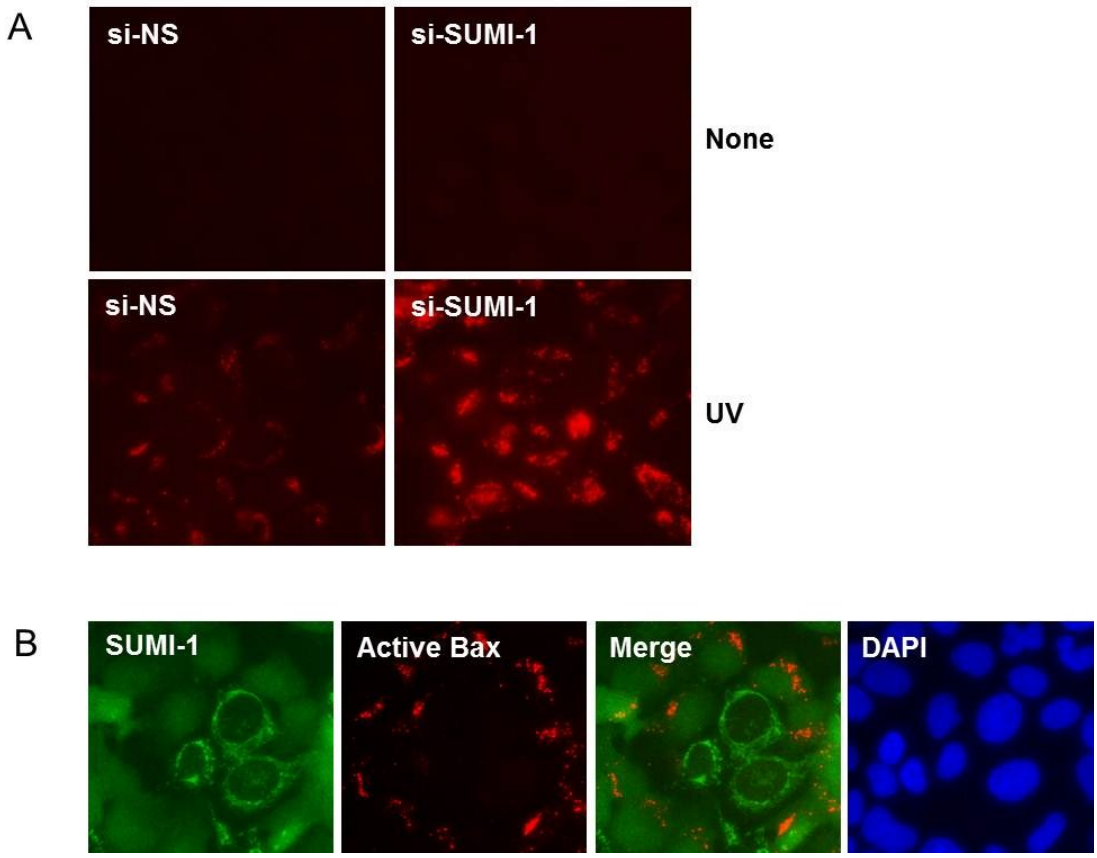

Figure 4-16. SUMI-1 knockdown regulates BAX activation.
A) SUMI-1 knockdown increases Bax activation during apoptosis. U2OS cells were treated with indicated siRNA (NS, nonspecific) for 48 h followed by treatment to induce apoptosis (UV, 6 mJ/cm^2) where indicated. Cells were fixed after 24 h and stained for active Bax (6A7). Red staining indicates presence of active, oligomerized Bax that has accumulated on mitochondria.
B) Bax activation correlates with SUMI-1 translocation in U2OS cells. Cells were treated with UV (6 mJ/cm^2 for 24 h) to induce apoptosis. Immunofluorescence staining was done for endogenous SUMI-1 (green) and active Bax 6A7 (red). Active Bax is observed only in cells in which SUMI-1 has translocated from mitochondria. Nuclei were stained with DAPI.

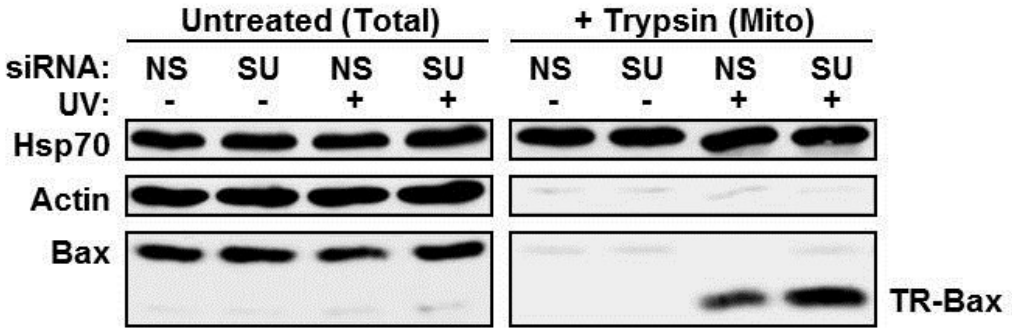

Figure 4-17. SUMI-1 knockdown regulates BAX oligomerization.
SUMI-1 knockdown increases trypsin-resistant, oligomerized BAX (TR-Bax). A trypsin-resistance assay was carried out on isolated mitochondria after treating cells with indicated siRNA for 48 hours followed by UV where indicated. Mitochondria were treated with trypsin to digest monomeric BAX, lysed, resolved by SDS-PAGE and assayed by immunoblotting alongside whole cell lysates.

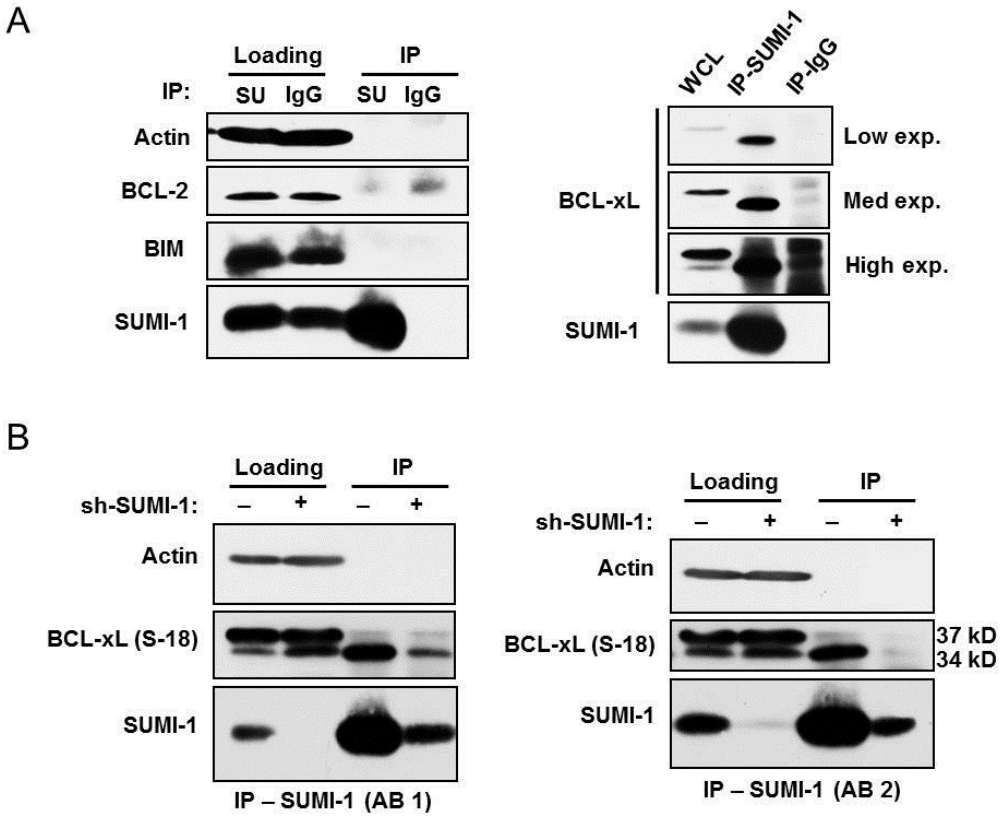

Figure 4-18. SUMI-1 co-immunoprecipitates with a protein recognized by BCL-xL S-18 antibody.

A) Co-immunoprecipitation (co-IP) in untreated cells using SUMI-1 antibody (SU-94, designated as SU above) or IgG control. Complexes were resolved by SDS-PAGE and blotted with indicated antibodies. No interaction was found between SUMI-1 and BCL-2 or BIM, but apparent binding was detected between SUMI-1 and BCL-xL (right panel).

B) Co-IP in untreated U2OS cells or U2OS cells stably-expressing sh-SUMI-1. Complexes were resolved by SDS-PAGE and blotted with indicated antibodies. IP for SUMI-1 with two different antibodies (AB 1, SU-94; AB 2, Proteintech) pulled down a protein migrating at 34 kD that is detected with the BCL-xL S-18 antibody (Santa Cruz, sc-634). Co-immunoprecipitation of this protein was diminished by shRNA inhibition of SUMI-1, demonstrating that the protein does not interact nonspecifically with the SUMI-1 antibodies.

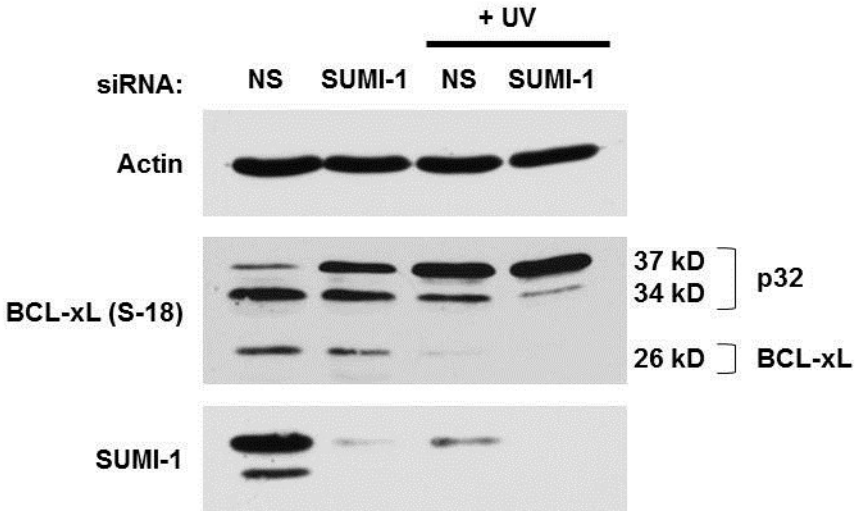

Figure 4-19. SUMI-1 siRNA induces shift in proportion of 34 kD and 37 kD bands detected by BCL-xL S-18 antibody.
U2OS cells were treated with SUMI-1 siRNA or nonspecific (NS) control siRNA and treated with UV where indicated to induce apoptosis. Lysates were resolved by SDS-PAGE and blotted with indicated antibodies. Note that siRNA inhibition of SUMI-1 induces a decrease in the 34 kD band detected by the BCL-xL S-18 antibody, and a corresponding increase in the 37 kD band. The 34 kD and 37 kD bands were later identified to be p32 (Figure 4-19). Apoptosis-inducing UV treatment causes a similar shift, and knockdown of SUMI-1 further augments this shift.

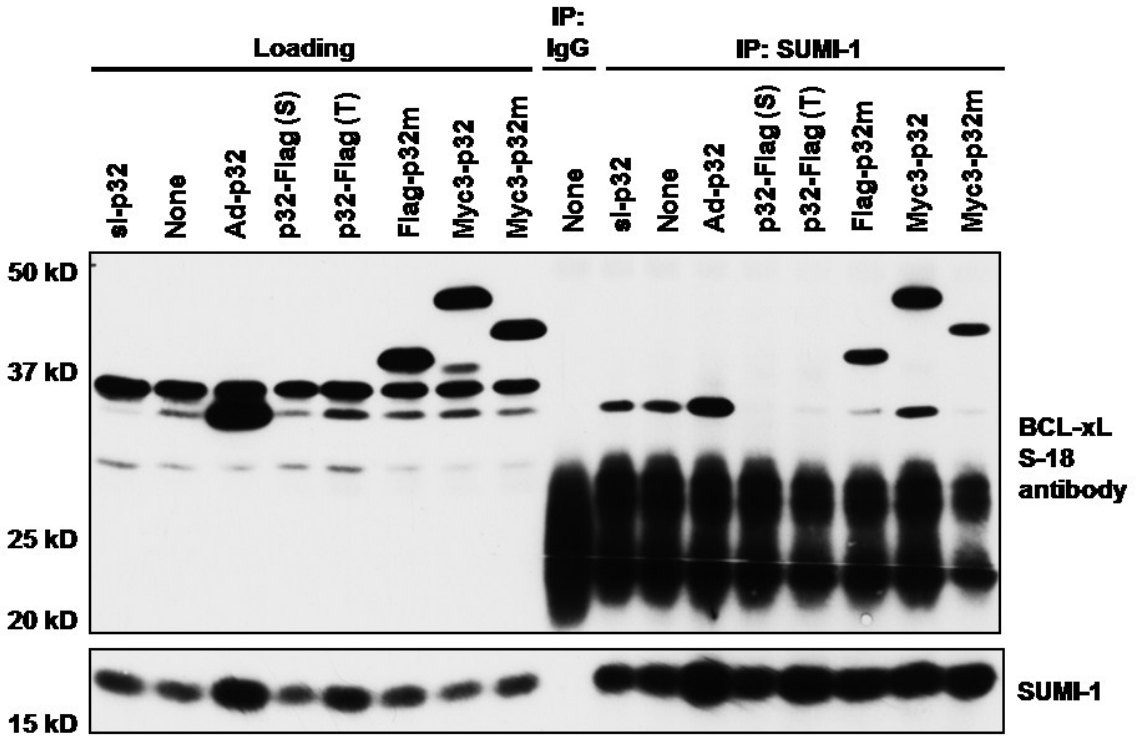

Figure 4-20. Nonspecific band recognized by BCL-xL S-18 antibody is p32. U2OS cells were transfected with various agents to inhibit or overexpress p32 and subjected to IP with SUMI-1 antibody (C-94). Loading and IP samples were resolved by SDS-PAGE and blotted with BCL-xL antibody (S-18, Santa Cruz sc-634). Note that the BCL-xL S-18 antibody recognizes both endogenous p32 and various ectopically-expressed tagged p32 proteins. (si-p32, p32 siRNA; Ad-p32, adenovirus expressing untagged p32; p32-Flag (S), stable transfection of p32-Flag; p32-Flag (T), transient transfection of p32-Flag; Flag-p32m, Flag-tagged mature/cleaved p32; Myc3-p32; Myc3-tagged full-length p32; Myc3-p32m, Myc3-tagged mature/cleaved p32).

This experiment was performed by Yong Liu.

Figure 4-21. Region of homology between p32 and BH4 domain of BCL-xL. CLUSTAL 2.1 sequence alignment indicates a 20-residue region of similarity between p32 and BCL-xL corresponding to the N-terminal BH4 domain of BCL-xL. This region includes a motif (VDFLS) that is identical between the proteins. Dots indicate similarity, and colons indicate strong similarity. (Red = small; blue = acidic; magenta = basic; green = hydroxyl + sulfhydryl + amine + G).

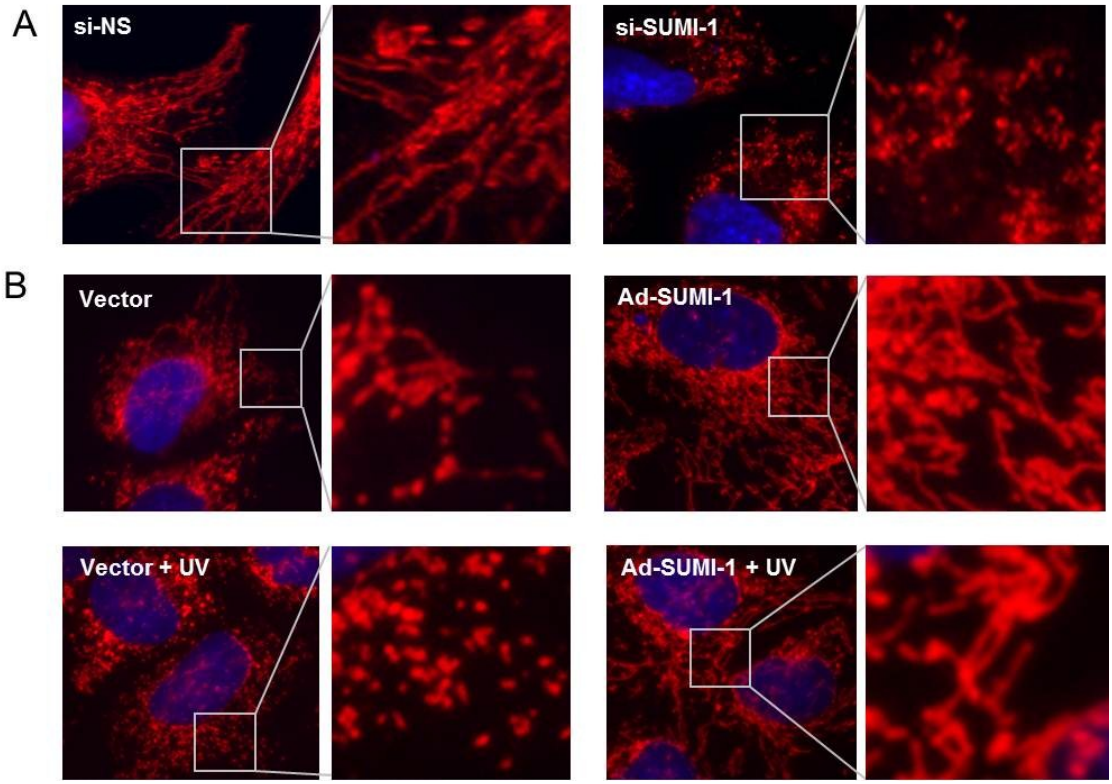

Figure 4-22. SUMI-1 inhibits mitochondrial fragmentation.
A) SUMI-1 knockdown leads to mitochondrial fragmentation. U2OS cells were treated with indicated siRNA for 48 hours and subjected to UV (25 mJ/cm^2 for 3 h) to induce apoptosis. Immunofluorescence staining was carried out for a mitochondrial marker Tim23 (red) and DAPI to indicate nuclei (blue). Cells treated with SUMI-1 siRNA showed increased mitochondrial fragmentation (right).
B) SUMI-1 overexpression protects cells from UV-induced mitochondrial fragmentation. U2OS cells were treated with adenovirus expressing untagged SUMI-1 or empty adenovirus (vector) where indicated, and 24 h later treated with UV (25 mJ/cm^2 for 3 h) where indicated. Note that mitochondria remain elongated in cells overexpressing SUMI-1.

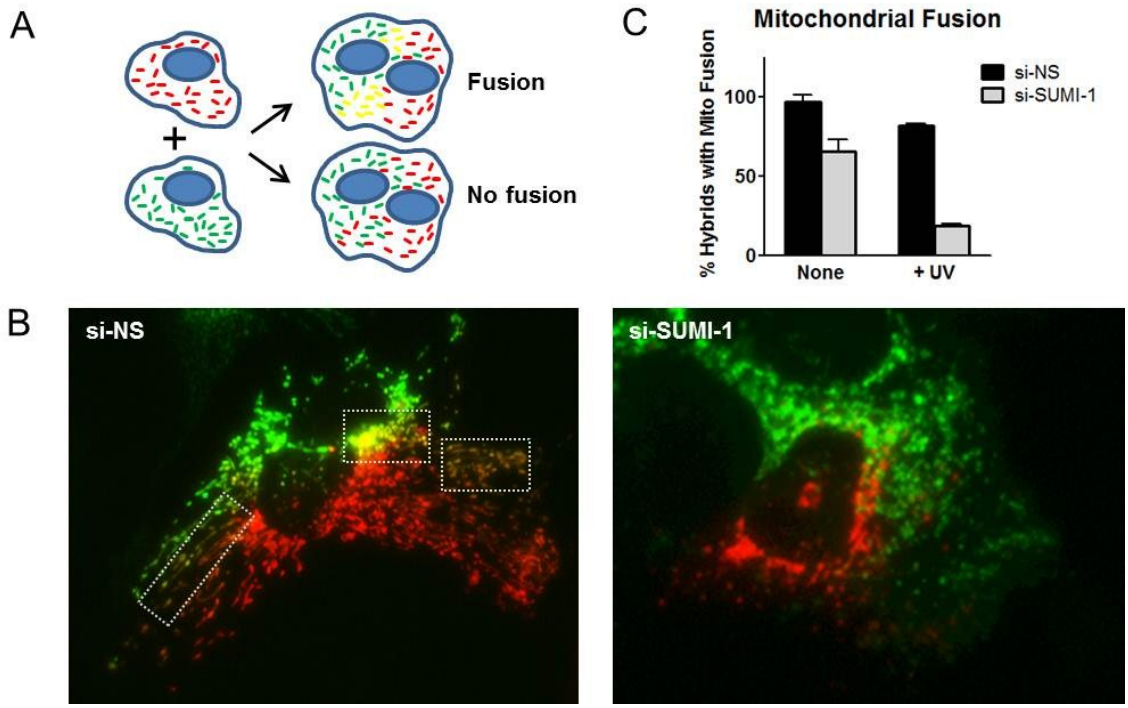

Figure 4-23. SUMI-1 regulates mitochondrial fusion.
A) In a cell hybrid mitochondrial fusion assay, one plate of cells is transfected with mitochondrial-targeted GFP (mt-GFP) to label mitochondria green, and another plate is transfected with mt-mKate2 to label mitochondria red. The cells are then plated together and treated with PEG for five min. to create cell hybrids containing red and green mitochondria. If fusion ensues, regions with yellow mitochondria (containing both red and green fluorescent proteins) are observed. Without fusion, red and green mitochondria remain distinct.
B) SUMI-1 knockdown impairs mitochondrial fusion. Cells were treated with indicated siRNA for 48 hours and treated as described in (A). Cells were treated with UV (25 mJ/m^2) where indicated, fixed after 2.5 h, and analyzed. An example of a cell hybrid exhibiting mitochondrial fusion (contains yellow mitochondria) is shown on the left (boxes enclose areas displaying fused, yellow, mitochondria). A hybrid lacking fusion is shown on the right.
C) Cells were treated as in (B), and hybrids with mitochondrial fusion (determined by presence of yellow color) were quantified and shown on graph as a percentage of total hybrids. Error bars indicate standard deviation.

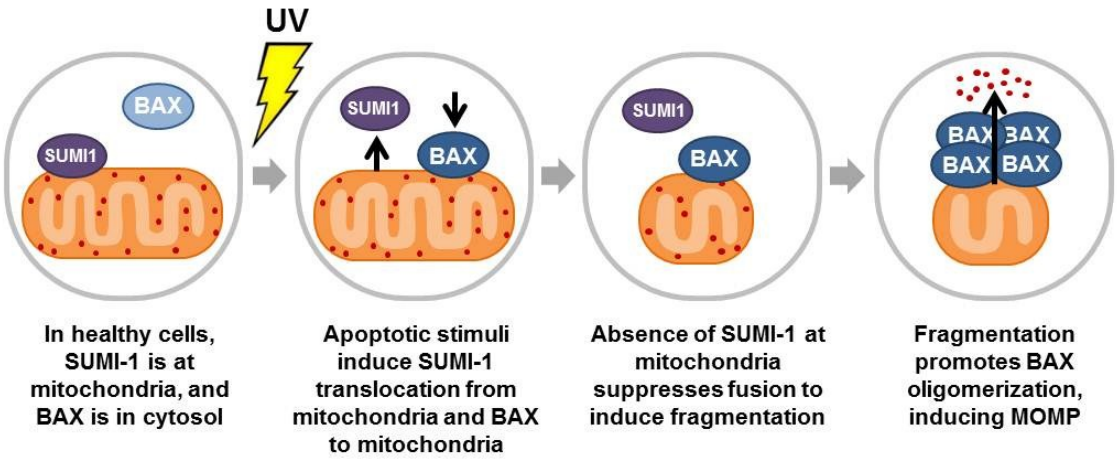

Figure 4-24. Model for regulation of MOMP by SUMI-1.
In unstressed cells, SUMI-1 resides at the mitochondrial membrane, where it keeps mitochondrial fusion-fission dynamics in balance. Upon treatment with apoptotic stimuli such as UV, SUMI-1 translocates from the mitochondria, while Bax becomes activated by BH3-only proteins and accumulates at the mitochondria, likely independent from SUMI-1. Following SUMI-1 translocation, mitochondrial fusion is inhibited while mitochondrial fission continues unperturbed, leading to mitochondrial fragmentation. This fragmentation promotes Bax oligomerization, leading to MOMP, cytochrome *c* release, and ultimately, apoptosis.

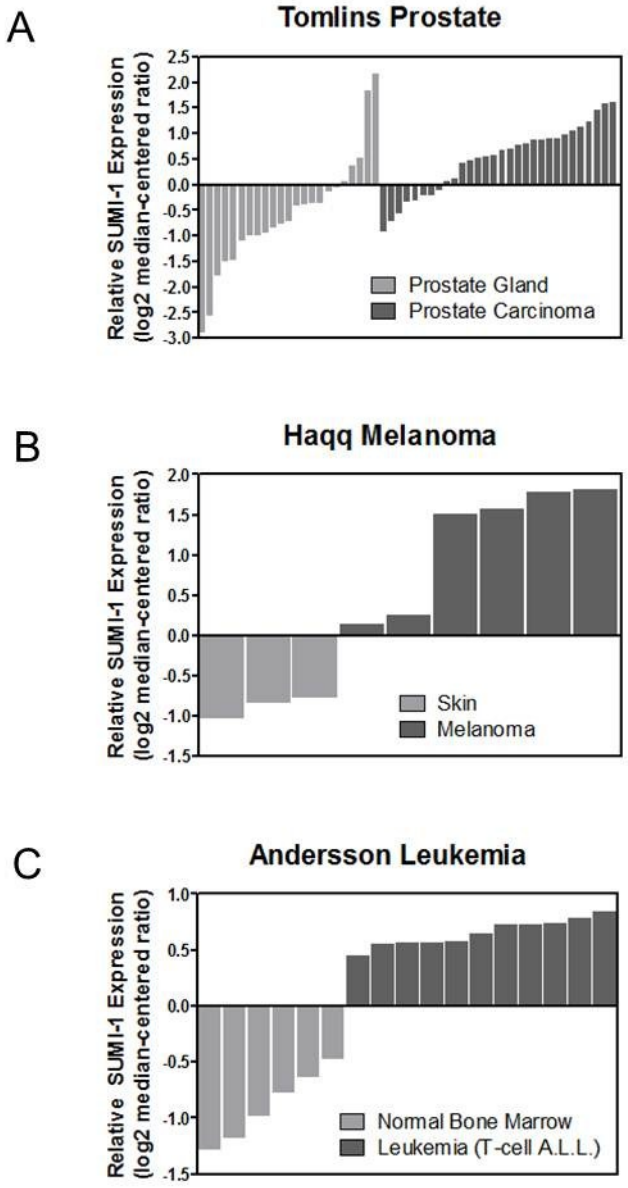

Figure 4-25. Increased expression of SUMI-1 in cancers.
Data obtained from Oncomine for expression of SUMI-1 mRNA in three types of cancer compared to corresponding normal tissues. SUMI-1 expression is represented as a log2 median-centered ratio in normal tissue (light grey bars) and cancerous tissue (dark grey bars). Each bar represents an individual sample.
A) Tomlins Prostate: Average fold change is 2.130, and P-value is 1.98E-4.
B) Haqq Melanoma: Average fold change is 4.163, and P-value is 4.77E-4.
C) Andersson Leukemia: Average fold change is 2.913, and P-value is 1.56E-5.

Cancer Type	Fold Increase	P-Value	Dataset
Breast, ductal carcinoma	1.754	4.10E-10	Sorlie 2003
Cervical cancer	1.656	2.00E-03	Pyeon 2007
Glioblastoma	1.579	5.57E-05	Liang 2005
Leukemia, acute myeloid	2.032	2.16E-05	Andersson 2007
Leukemia, childhood T-cell acute lymphoblastic	2.913	1.56E-05	Andersson 2007
Lung adenocarcinoma	1.564	3.07E-13	Landi 2008
Lymphoma, diffuse B-cell	1.846	1.00E-02	Storz 2003
Melanoma	4.163	4.77E-04	Haqq 2005
Mesothelioma, pleural malignant	2.018	1.62E-06	Gordon 2005
Myeloma, smoldering	2.018	3.23E-05	Zhan 2007
Neuroblastoma	1.755	8.76E-04	Albino 2008
Oral cavity carcinoma	2.827	2.05E-06	Pyeon 2007
Oropharyngeal carcinoma	2.325	3.85E-06	Pyeon 2007
Pancreatic carcinoma	1.520	3.48E-05	Pei 2009
Prostate carcinoma	2.130	1.98E-04	Tomlins 2007
Renal cell carcinoma, papillary	1.591	1.30E-04	Yusenko 2009
Tongue carcinoma	2.231	1.12E-05	Pyeon 2007

Table 4-2. Increased expression of SUMI-1 in cancers.
SUMI-1 mRNA microarray expression data mined from Oncomine for cancerous tissues compared to corresponding normal tissues. Cancers with at least 1.5-fold overexpression of SUMI-1 compared to normal tissue and a P-value ≤ 0.01 are shown.

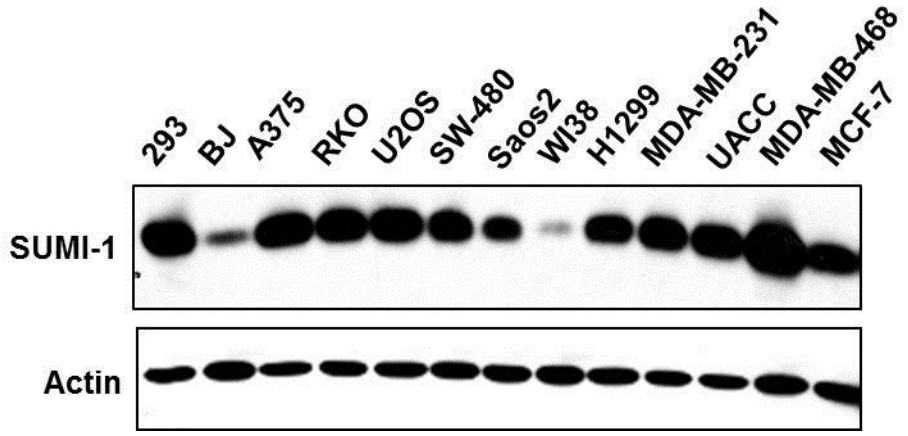

Figure 4-26. Increased expression of SUMI-1 in cancerous compared to non-cancerous cell lines.
Expression of SUMI-1 was assessed in a panel of lysates from cultured human cell lines. Cells were lysed in 0.5% NP-40 lysis buffer, resolved by SDS-PAGE, and blotted with an antibody for SUMI-1 (C-94) and actin as loading control. Note that SUMI-1 expression is lowest in the two non-cancerous cell lines (BJ, normal skin fibroblast; WI38, normal embryonic lung).

CHAPTER V

REGULATION OF SUMI-1 DURING APOPTOSIS

Introduction

We show that SUMI-1 translocates during apoptosis prior to cytochrome *c* release in order to regulate MOMP. However, the SUMI-1 protein level also appears to decrease during apoptosis, suggesting that in addition to translocation, SUMI-1 may be regulated by degradation during apoptosis. Thus, we carried out experiments to determine whether SUMI-1 may be regulated by degradation and/or another mechanism, in addition to translocation, during apoptosis.

Apoptotic Stimuli Reduce Level of Endogenous SUMI-1

In our previous experiments, we observed that the level of endogenous SUMI-1 protein decreases during apoptosis induced by UV radiation and cisplatin. To examine this in more detail, apoptosis was induced in U2OS cells using a variety of agents, and the effect on SUMI-1 level was examined. As shown in Figure 5-1 (left panel), the level of endogenous SUMI-1 in U2OS cells was decreased following administration of UV, staurosporine, doxorubicin, cisplatin, vinblastine, and taxol. To determine whether this effect could be reproduced in another cell type, we examined HeLa cells with and without

apoptosis induced by UV. As in U2OS cells, UV treatment decreased the level of endogenous SUMI-1 (Figure 5-1, right panel).

SUMI-1 is Not Degraded by the Proteasome During Apoptosis

Protein degradation is usually carried out by the proteasome—a large protein complex that breaks down proteins that are no longer needed by the cell or that must be eliminated in order to regulate processes such as cell cycle control or apoptosis. Proteins are targeted for proteasomal degradation by covalent addition of the small protein ubiquitin to specific lysine residues on the target protein, a process carried out by ubiquitin-conjugating enzymes (E1, E2, and E3 ubiquitin ligases). When multiple ubiquitin molecules have been added to a single residue, the resulting polyubiquitin chain directs the target protein to the proteasome, which cleaves the protein into peptides 7 to 8 amino acids in length. These short peptides can be further broken down into individual amino acids and recycled for use in translation of new proteins (Baumeister et al., 1998).

We carried out experiments to determine whether SUMI-1 is degraded proteasomally, using the potent and specific inhibitor MG132, which blocks the ability of the 26S proteasome to degrade proteins (Tsubuki et al., 1996). If SUMI-1 is normally degraded by the proteasome during apoptosis, MG132 should block the associated decrease in SUMI-1 protein level. To test this, we treated U2OS and HeLa cells with MG132 (20 uM) for 1 hour followed by UV (250 J/m^2) for 4 h and examined the level of endogenous SUMI-1 as well as positive controls p53 and Mdm2, which are known to be degraded by the proteasome. While MG132

effectively prevented degradation of p53 and Mdm2, it did not block the decrease in SUMI-1 level observed during UV-induced apoptosis. In fact, MG132 augmented the UV-induced decrease in SUMI-1 level (Figure 5-2, compare lanes 3-4, and 7-8), and treatment with MG132 alone also significantly decreased the SUMI-1 level (Figure 5-2, compare lanes 1-2, and lanes 5-6.). This MG132-induced decrease in SUMI-1 level is not surprising, as MG132 and other proteasome inhibitors are known to induce apoptosis (Drexler, 1997), and, as shown in Figure 5-1, the level of endogenous SUMI-1 decreases during apoptosis. Based on the data presented here, it is unlikely that the apoptosis-associated decrease in SUMI-1 is due to proteasomal degradation.

SUMI-1 is Potentially Regulated by Oligomerization

We next examined oligomerization as a possible explanation for the decrease in SUMI-1 level observed during apoptosis. That is, SUMI-1 may not be degraded but may instead form SDS-resistant oligomers. This phenomenon would reduce the quantity of monomeric (17 kD) SUMI-1 observed by western blotting. Indeed, SUMI-1 contains a CHCH (coiled-coil-helix-coiled-coil-helix) domain that is known to mediate SDS-resistant homo- and hetero-oligomerization in other proteins containing this domain. This oligomer formation is mediated by covalent disulfide bonds between conserved cysteines in the CHCH domain and has been studied most extensively in the CHCH-domain-containing protein Cox17 (Arnesano et al., 2005), which interacts with SCO-1 to feed copper ions into the COX (cytochrome *c* oxidase) complex during COX

assembly (Banci et al., 2008a; Banci et al., 2008b). Another CHCH-domain protein, Mia40, mediates transport of mitochondrial proteins into the intermembrane space by forming transient disulfide-mediated hetero-oligomers with other cysteine-containing proteins as they are imported (Sideris et al., 2009). In both cases, formation of these oligomers depends on the reductive-oxidative (RedOx) status of the proteins' immediate environment (Arnesano et al., 2005), as bond formation requires oxidation of the cysteines' thiol groups. In a fully-reduced environment, cysteines are not capable of forming disulfide bonds with one another, while in a more oxidative environment, bonds can form either between specific cysteines on another protein to mediate homo- or hetero-oligomerization, or between cysteines on the same protein to induce changes in tertiary structure such as hairpin formations. Which of these cysteines interact, and which tertiary or quaternary structure results (i.e. intramolecular folding, homo-oligomerization, or hetero-oligomerization), depends largely on the extent of oxidation (Arnesano et al., 2005) but is also affected by features of the surrounding amino acid sequence such as distance between adjacent cysteines.

To determine whether SUMI-1 might oligomerize during apoptosis, we carried out a whole-membrane western blot with SUMI-1 antibody after treating U2OS cells with increasing doses of UV radiation. As we observed previously, the 17 kD band disappeared upon UV radiation in a dose-dependent manner. Interestingly, we observed a corresponding increase in a higher molecular weight (HMW) band (approximately 65 kD in size) detected by the SUMI-1 antibody (Figure 5-3A). To determine whether the HMW band could represent an SDS-

resistant oligomer of SUMI-1, we assessed whether the band would disappear under harsher denaturing conditions. Often, disulfide bond-mediated oligomers are not reduced by standard SDS-PAGE, even in the presence of denaturing agents such as DTT. In order to reduce this type of oligomer, an additional denaturing agent must typically be applied, such as extended heating, deep-freeze/thaw cycles, or treatment with a denaturing chemical such as urea. Stronger disulfide bonds require harsher denaturing agents, and the type of denaturing agent required to break these bonds can be used as a quantitative measure of the disulfide bond's strength. In the first 2 lanes of Figure 5-3B, U2OS cells were either left untreated or treated with UV (10 mJ/cm^2), with both samples heated in SDS-DTT sample buffer for the standard time (3 minutes). Consistent with our previous observations, UV radiation led to a decrease in the 17 kD band and an increase in the 65 kD band (compare lanes 1 and 2). In the third lane, a portion of the same lysate used for lane 2 (UV-treated) was heated for 60 minutes instead of 3 minutes. This extended heating resulted in a partial decrease in the 65 kD band and a partial increase in the 17 kD band (Figure 5-3B, compare lanes 2 and 3).

In addition, we attempted to determine whether overexpression of SUMI-1 could increase the higher molecular weight bands detected by the SUMI-1 antibody. We transfected cells with a pShuttle plasmid expressing untagged SUMI-1 or an empty vector as a negative control. To our surprise, we did not observe any increase in the 17 kD band, but only in the 65 kD band detected by the SUMI-1 antibody (Figure 5-4). The reason for these results is not clear, but it

is possible that SUMI-1 preferentially takes the oligomerized form and that there is a limit to the quantity of monomeric SUMI-1 that can reside in a cell, or that the experimental conditions (e.g. excessive oxidation of lysis buffer) induced oligomerization. Alternatively, it is possible that the pShuttle vector used for expressing SUMI-1 did not express properly, but this would not explain the increase in the HMW band detected by the SUMI-1 antibody following transfection. This same plasmid was used later to generate adenovirus expressing untagged SUMI-1. This adenovirus successfully expressed the 17 kD SUMI-1 band (Figure 4-12), but its effect on higher molecular weight bands has not yet been examined. The HMW band was also examined after treatment with SUMI-1 siRNA, which failed to decrease this band (data not shown). However, siRNA does not induce complete knockdown of SUMI-1, and it is possible that the oligomerized form is more stable or is the preferred state for SUMI-1, as suggested by the overexpression data.

Together, the experiment showing that the proteasome inhibitor MG-132 does not prevent the decrease in the 17 kD SUMI-1 band, and the data showing that UV induces a dose-dependent increase in a HMW band that corresponds to a decrease in the 17 kD band, partially recovered by further denaturation of the lysate, suggest that SUMI-1 is not proteasomally degraded during apoptosis and may instead form SDS-resistant oligomers. However, additional experiments are needed to confirm this finding or to determine whether SUMI-1 might be regulated in a different manner.

Discussion

The level of SUMI-1 protein visualized by western blotting decreases during apoptosis induced by a variety of apoptotic stimuli. Here, we examined potential reasons for this apparent reduction in SUMI-1 level. We show that this decrease is not affected by the proteasome inhibitor MG132, suggesting that SUMI-1 is not degraded during apoptosis, at least not by the ubiquitin-proteasome pathway. Instead, we observed that a higher molecular weight band (approximately 65 kD) detected by purified SUMI-1 antibody is induced by UV radiation, and this HMW band appears in a dose-dependent manner corresponding to a decrease in the 17 kD band. These data suggest that SUMI-1 may form oligomers during apoptosis. These HMW complexes could represent SUMI-1 homo-oligomers; in this case, the molecular weight (approximately 65-70 kD) appears most consistent with that of a SUMI-1 tetramer, which would be predicted to migrate at approximately 68 kD, although oligomers can potentially migrate more rapidly or slowly than expected. Alternatively, it is possible that SUMI-1 does not homo-oligomerize but forms disulfide-bond mediated complexes with one or more unknown proteins.

It is also possible that the HMW band detected by the SUMI-1 antibody is not oligomerized SUMI-1, but another protein detected nonspecifically by the SUMI-1 antibody. This alternative is unlikely, as it cannot explain our finding that further denaturation of lysate from UV-treated cells caused a partial decrease in the HMW band and a corresponding increase in the 17 kD band (Figure 5-3). Nevertheless, in an attempt to rule out the possibility that this band may

represent a nonspecific protein, we carried out several additional experiments, but results have been inconclusive. SDS-resistant oligomers are notoriously difficult to study—Artificial oligomers can be formed by oxidation of lysates, for example, and oligomerization status can be quite sensitive to conditions of cell culture and lysis. When repeating an experiment under seemingly identical conditions, proportions of oligomers and monomers can change. Sometimes additional bands are observed by western blotting with SUMI-1 antibody, migrating at approximately 40-45 kD and 110-120 kD; we have not been able to discern a pattern for the appearance of these bands. In an attempt to preserve the native status of disulfide bonds in the cell and avoid introducing artificial ones during cell lysis, we attempted to treat cells with N-ethylmaleimide (NEM) upon addition of lysis buffer. NEM is a small alkene that interacts irreversibly with thiols, “capping” them so that they can no longer interact with other cysteines to form disulfide bonds. Thus, addition of NEM during lysis should prevent formation of new disulfide bonds that were not already present in the intact cell. However, when NEM was applied to our lysis buffer prior to SDS-PAGE, we paradoxically observed a dramatic decrease in the 17 kD (monomer) band along with disappearance of the putative oligomer band and appearance of several new HMW band of various sizes (data not shown). We have not been able to explain these results. One possibility is that NEM alters the cell’s redox status by inactivating redox-regulating proteins such as glutathione, many of which contain cysteines, inducing SUMI-1 oligomerization. Another method for determining whether the HMW band is an oligomer is by detecting this band with two different

SUMI-1 antibodies targeting different regions of the protein. We attempted to detect the 65 kD band with another antibody that we produced, and we were unable to detect it. However, the antigen for this antibody is located in the center of the oligomerization (CHCH) domain, which is not likely to be exposed to the antibody when the protein is oligomerized. This issue could potentially be addressed by using another antibody toward SUMI-1. In summary, given our findings that 1) SUMI-1 is not proteasomally degraded during apoptosis, 2) a HMW band is detected by the SUMI-1 antibody in a dose-dependent manner corresponding to a decrease in the 17 kD band, and 3) Additional denaturation of cell lysate causes a partial decrease in the HMW band and a corresponding increase in the 17 kD band, the most logical explanation is that SUMI-1 oligomerizes during apoptosis. Furthermore, the CHCH domain found in SUMI-1 is known to mediate SDS-resistant oligomerization in other proteins. Nevertheless, it remains possible that SUMI-1 is not regulated by oligomerization. Further studies could be carried out to address this issue, such as detecting the same HMW band with another SUMI-1 antibody.

If oligomerization of SUMI-1 does not occur during apoptosis, another mechanism must account for the apparent decrease in the 17 kD band during apoptosis. One alternative is that SUMI-1 is transcriptionally regulated—Signaling pathways induced by apoptotic stimuli may block transcription of SUMI-1 mRNA. While we have not formally examined this idea, it is not likely that SUMI-1 is regulated in this manner, as the existing SUMI-1 in the cell would still have to be degraded in order for impaired transcription to result in reduced

protein so rapidly, and SUMI-1 is too stable for the degradation to occur as rapidly as 18 hours; while a formal half-life assay has not been performed, when SUMI-1 is targeted with RNAi, a significant decrease in SUMI-1 level is not observed until 48 hours after siRNA transfection, indicating that SUMI-1 is a relatively stable. Thus, impaired transcription cannot account for the decrease of SUMI-1 in this time frame unless degradation is also induced. It is possible that SUMI-1 is degraded through an unknown, non-proteasomal, mechanism during apoptosis, or it may be cleaved by a protease. Whole-membrane blotting with SUMI-1 antibody has not detected any low molecular weight cleavage products, although if cleavage occurred inside the antibody recognition site, the antibody may no longer be able to recognize the resulting SUMI-1 fragments.

If SUMI-1 does oligomerize during apoptosis, this phenomenon could be a mechanism to regulate SUMI-1's function. Oxidation-induced oligomerization of SUMI-1 may trigger its translocation from the mitochondria, for example. Apoptosis often involves generation of free radicals, resulting in oxidation that could stimulate disulfide-bond formation and oligomerization. Alternatively, oligomerization of SUMI-1 could occur as a result of its translocation, but this is unlikely, as disulfide bonds do not typically occur in reducing environments such as the nucleus and cytoplasm (although they may remain stable in these locations after being formed elsewhere); such oxidation is only known to occur in specific compartments of the cell such as the endoplasmic reticulum and mitochondria. Thus, oligomerization of SUMI-1 is likely to precede its translocation. SUMI-1 oligomerization may also occur as a side effect of

apoptosis rather than as a regulatory mechanism for SUMI-1; that is, in the absence of oligomerization, SUMI-1 may become inactivated through translocation or another means. The regulation of SUMI-1 is an important area for future studies.

Materials and Methods

Cell culture, transfections, and apoptotic treatments. U2OS and HeLa cells were obtained from ATCC. All cells were cultured in a 37°C incubator with 5% CO_2 in DMEM supplemented with 10% FBS, 100 U/ml penicillin, and 100 g/ml streptomycin. DNA transfections were carried out with Fugene-6 or Fugene-HD (Roche), and siRNA transfections were performed with Oligofectamine (Invitrogen), according to the manufacturers' instructions. Apoptosis treatments included UVC radiation (dosages as indicated) using a Stratalinker® UV Crosslinker, and various reagents and doses as indicated. Where indicated, cells were pre-incubated with MG132 for 1 h before apoptotic treatments.

Adenoviruses. Recombinant adenoviruses expressing untagged SUMI-1 or GFP were produced using the AdEasy™ XL Adenoviral Vector System (Stratagene) according to the manufacturer's protocol.

SDS-PAGE and western blotting. Cells were lysed in 0.5% NP-40 buffer, and lysates were resolved on a 15% polyacrylamide gel and transferred onto a 0.2

μM nitrocellulose membrane. Membranes were blocked for a minimum of 30 minutes in phosphate-buffered saline blocking buffer with 0.1% Tween-20 (PBST) and 5% nonfat dried milk. Membranes were incubated for 2h to overnight in primary antibody, incubated for 1-2 hours in secondary HRP-conjugated antibody, and exposed with Supersignal West Pico or Dura (Pierce).

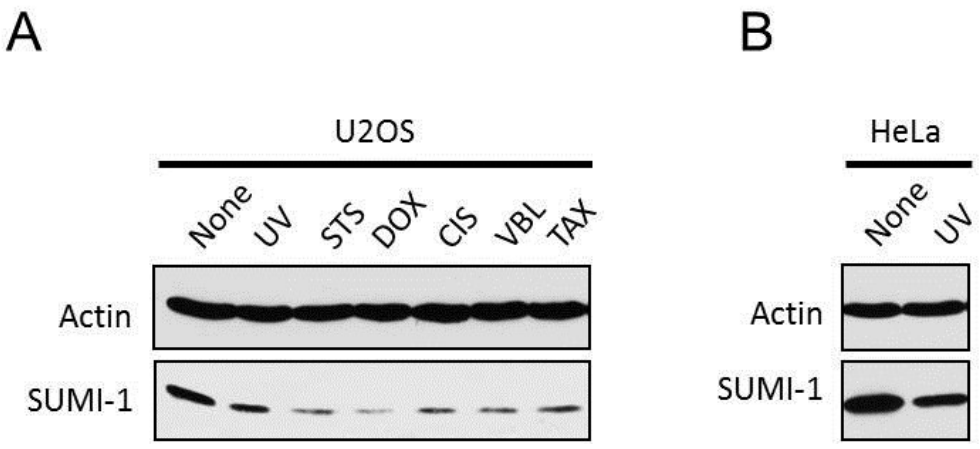

Figure 5-1. Apoptotic stimuli reduce the level of endogenous SUMI-1.
A) U2OS cells were treated with various apoptosis-inducing agents for 18 hours, lysed, resolved by SDS-PAGE, and blotted for actin (loading control) and SUMI-1. UV, 6 mJ/cm^2. Staurosporine (STS), 10 μM. Doxorubin (DOX), 10 μM. Cisplatin (CIS), 10 μg/ml. Vinblastine (VBL), 25 nM. Taxol (TAX), 50 nM.

B) HeLa cells were treated with UV (6 mJ/cm^2) for 18 hours, lysed, resolved by SDS-PAGE, and blotted for actin (loading control) and SUMI-1.

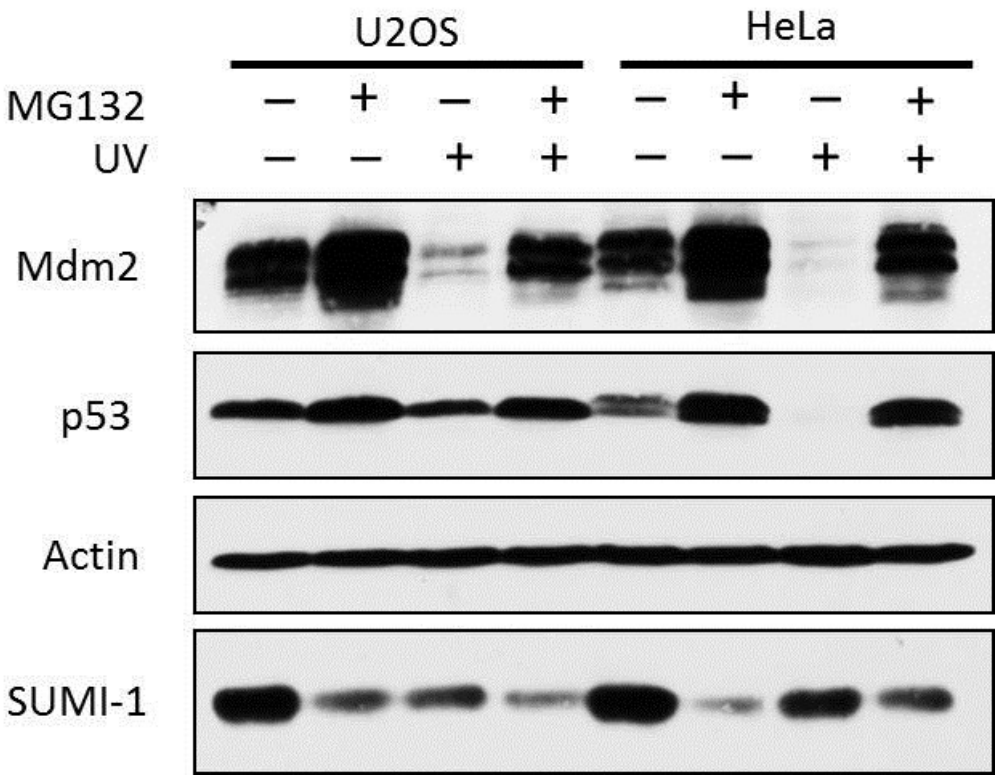

Figure 5-2. Proteasome inhibitor MG132 does not prevent apoptosis-associated reduction in SUMI-1 level.
Where indicated, U2OS and HeLa cells were pre-treated with the proteasome inhibitor MG132 (20 μM for 1 h), followed by treatment with apoptosis-inducing UV radiation (250 J/m^2 for 4 h). Lysates were resolved by SDS-PAGE and blotted for actin (loading control), Mdm2 and p53 (positive controls for suppression of proteasomal degradation by MG132), and SUMI-1. Note that in both cell types, treatment with MG132 did not prevent decrease in SUMI-1 level but did prevent degradation of p53 and Mdm2.

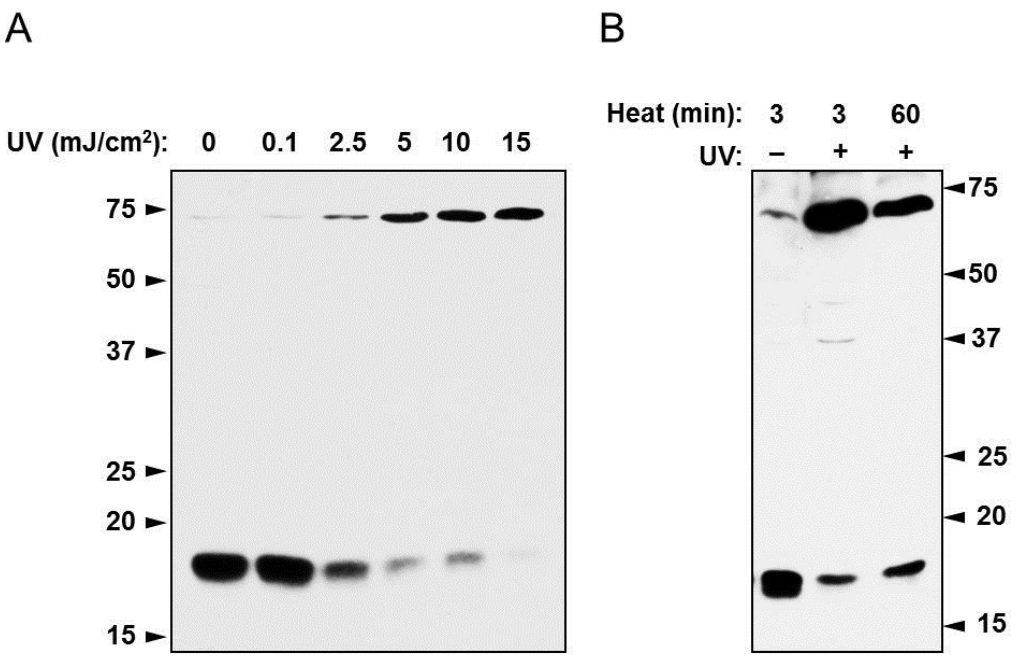

Figure 5-3. High molecular weight bands are detected by SUMI-1 antibody when cells are treated to undergo apoptosis.

A) In U2OS cells treated to undergo apoptosis with increasing doses of UV radiation, a dose-dependent decrease is observed in the 17 kD band, while a corresponding increase is observed for a higher molecular weight band (approximately 65-70 kD) that is detected by the SUMI-1 antibody. Cell lysates were resolved by SDS-PAGE in the presence of DTT.

B) In U2OS cells treated to undergo apoptosis (10 mJ/cm^2 UV), a higher molecular weight (HWM) band detected by the SUMI-1 antibody increased in size while the 17 kD band decreased. Samples in first two lanes were heated for the standard time period (3 minutes) at 95°C in SDS-DTT sample buffer prior to resolving by SDS-PAGE. Heating the lysate from lane 2 for 60 minutes led to a partial decrease in the HWM band and an increase in the 17 kD band.

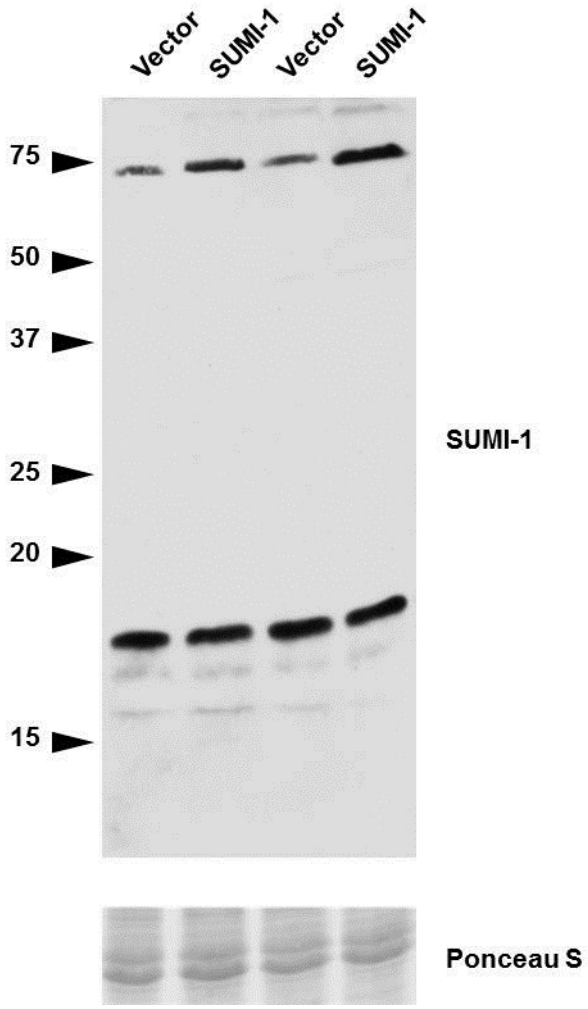

Figure 5-4. Transfection of untagged SUMI-1 increases HMW bands detected by SUMI-1 antibody.
U2OS cells were transfected with pShuttle-SUMI-1 plasmid (expressing untagged SUMI-1) or empty pShuttle plasmid (negative control). Two replicates are shown. Note that the band around 65 kD increases upon transfection with SUMI-1. Ponceau S staining is shown to indicate even loading.

CHAPTER VI

DISCUSSION

Identification of Novel Apoptosis-Regulating Proteins

Apoptotic cell death has been an area of intense investigation in recent years, likely owing to its relevance during development as well as for maintaining homeostasis in adult organisms, and due to its contribution in the etiology of diverse diseases such as developmental and autoimmune disorders, neurodegeneration, and cancer. Research identifying the signaling pathways and biological mechanisms by which apoptosis occurs, especially those mechanisms by which it is regulated, can help us to better understand developmental and homeostasis processes as well as diseases that are affected by dysregulation of apoptosis. Ultimately, this knowledge may aid in the development of diagnostic and therapeutic tools for these diseases.

A critical control point in apoptosis is mitochondrial outer membrane permeabilization (MOMP), as cells that have crossed this threshold do not recover in most cases. Much has been learned about MOMP in recent years, especially the roles of BCL-2 family proteins in regulating this process. However, several questions remain to be fully elucidated: What are the exact biochemical mechanisms governing MOMP? What are the non-BCL-2 proteins that mediate

MOMP? Finally, what is the role of mitochondria, including mitochondria-localized proteins, in regulating MOMP?

In this body of work, we initially sought to identify novel interacting proteins for the pro-apoptotic protein, p32, which was previously determined in our lab to regulate ARF-mediated MOMP and apoptosis through a mechanism that has remained unclear (Itahana and Zhang, 2008). In the process, we identified two novel potential regulators of apoptosis, SUMI-1 and MAGE-D2. This study examined the functions of these two proteins individually, and future studies will explore the interactions between these proteins and p32. Here, MAGE-D2 was found to be localized to the nucleus, nucleolus, and mitochondria, and the preliminary data presented here suggest that MAGE-D2 may regulate cell cycle control and apoptosis, although further studies are necessary to establish a definitive function for this protein. SUMI-1 was characterized much more extensively in this work and was established as a novel, mitochondria-localized inhibitor of apoptosis that functions by regulating mitochondrial dynamics, BAX activation, and mitochondrial outer membrane permeabilization. Identification of these proteins will fill some of the gaps in our knowledge of signaling pathways and mechanisms regulating apoptosis—especially MOMP—and may provide a potential therapeutic target for diseases that are affected by aberrant regulation of apoptosis.

MAGE-D2 Localization and Function

MAGE-D2 is a ubiquitously expressed, uncharacterized member of the MAGE (melanoma antigen) family of proteins, and its increased expression is associated with some cancers. The functions of most MAGE proteins in normal tissues are unclear, but other proteins belonging to the MAGE-D subfamily have been identified to regulate cell cycle progression and apoptosis. In this work, we examined the localization and potential functions for this protein. To study MAGE-D2, several plasmids were generated to express both N-terminally and C-terminally tagged MAGE-D2 fusion proteins, and two rabbit polyclonal antibodies were produced in order to study endogenous MAGE-D2 by western blotting, immunofluorescence, and co-immunoprecipitation.

By examining both ectopically-expressed tagged MAGE-D2 and endogenous MAGE-D2 by immunofluorescence, the localization of MAGE-D2 was determined to be primarily nuclear and nucleolar, with a portion of MAGE-D2 likely residing in or on the mitochondria as well. To determine whether MAGE-D2 indeed localizes to the mitochondria, a subcellular fractionation and western blot could be carried out. Interestingly, the localization of MAGE-D2 was found to be heterogeneous among cells, with some cells exhibiting primarily mitochondrial staining and other cells displaying mostly nuclear or nucleolar staining.

The ability of MAGE-D2 to regulate apoptosis was examined briefly. Cells transfected with MAGE-D2-Flag appeared more sensitive to UV-induced apoptosis as assessed by examining cell number and morphology and through

flow cytometry analysis of DNA content. However, quantification of apoptosis by analysis of sub-G1 DNA content is not necessarily an accurate measurement for cells that are actively cycling, as it is not possible in this type of cells to distinguish apoptotic cells from fragmented cells or other debris. An alternative or additional quantitative measure should be used, such as cell counting, and specific markers of apoptosis should be examined, such as cleavage of PARP or Caspase-3. In addition, overexpression of proteins, especially tagged constructs, can yield data artifacts for various reasons: Relative protein levels may be critical, and the tagged protein may not behave in the same manner as the untagged protein. Stronger evidence of a protein's function can be provided by inhibiting the protein through RNA interference. An experiment examining the effect of MAGE-D2 siRNA on apoptosis would help clarify whether MAGE-D2 is a *bona fide* regulator of apoptosis.

If MAGE-D2 is found to regulate apoptosis, the next step in characterizing this protein would be to determine the mechanism by which it regulates apoptosis. We found MAGE-D2 to be localized in the nucleus, nucleoli, and possibly mitochondria, and this localization does not appear to change during apoptosis (data not shown). It is possible that the apoptosis-regulating function of MAGE-D2 could be carried out in any of these compartments, especially the nucleus and mitochondria, where control of apoptosis is known to take place. In the nucleus, MAGE-D2 could regulate protein transcription. As described in Chapter III, MAGE-D2's closest homolog—MAGE-D1/NRAGE—acts as a transcription cofactor. MAGE-D1 interacts with several transcription factors that

regulate apoptosis and cell cycle control, and is required for Dlx5-dependent transcription (Masuda et al., 2001). MAGE-D1's pro-apoptotic function is also shown to be mediated by the transcription factor p53 (Kendall et al., 2005; Wen et al., 2004). MAGE-D2 has also been reported to interact with p53 (Papageorgio et al., 2007), which becomes activated following extensive DNA damage or other apoptotic signals, leading to transcription of apoptosis-inducing genes such as *NOXA* and *PUMA*. RT-PCR studies with and without MAGE-D2 knockdown and overexpression could be used to determine whether MAGE-D2 affects the ability of p53 to induce these target genes during apoptosis. MAGE-D2 might act as a transcriptional cofactor for p53; that is, if MAGE-D2 promotes apoptosis, it might enhance the ability of p53 to induce transcription of *NOXA*, *PUMA*, or other apoptosis-regulating genes during apoptosis. In this case, one would expect to see increased mRNA transcripts of these genes by RT-PCR when MAGE-D2 is overexpressed, and/or decreased transcription when MAGE-D2 is inhibited with RNAi. Western blotting should also be carried out under these experimental conditions to determine whether the corresponding protein levels are also increased by expression of MAGE-D2. To determine whether any transcription-regulating effect of MAGE-D2 is indeed mediated by p53, these experiments could be performed in both WT and p53-null mouse embryo fibroblasts (MEFs); if MAGE-D2 functions by modulating the activity of p53, it would not be expected to affect gene transcription in p53-null cells. It would also be interesting to determine whether MAGE-D2 affects p53-mediated transcription globally or just for apoptosis-regulating genes. It is also possible that, even though an interaction

was reported between p53 and MAGE-D2, MAGE-D2 may mediate transcription independently of p53, or that MAGE-D2 may interact with mitochondria-localized p53 during apoptosis to affect p53's non-transcription-related functions (such as its interaction with BCL-2 family proteins) at the mitochondria. Alternatively, a luciferase assay using a p53-responsive promoter could be used to examine the effect of MAGE-D2 on p53's transcriptional activity, but the RT-PCR approach has the advantage of assessing multiple p53 targets at once and, importantly, it assesses transcription of endogenous DNA promoters (complete with any associated proteins) and is therefore more likely to accurately recapitulate transcriptional regulation *in vivo*.

The putative interaction between MAGE-D2 and p53 is not well-established, and it is possible that MAGE-D2 regulates apoptosis independently of p53. We found that MAGE-D2 binds with the pro-apoptotic protein p32 and the anti-apoptotic protein SUMI-1, and it is likely that MAGE-D2 modulates apoptosis through its interaction with one or both of these proteins. Potential experiments exploring this possibility will be discussed later in this chapter. Finally, MAGE-D2 could influence apoptosis independently of presently-known interacting proteins. In this case, it might regulate apoptosis through interaction with another binding partner, and a large-scale co-immunoprecipitation to look for novel interacting partners could provide clues for its function. As there is thought to be extensive redundancy among MAGE proteins, it is also reasonable to examine the mechanisms by which other MAGE family members, especially those in the MAGE-D subfamily, regulate apoptosis. As mentioned above, MAGE-D1-

mediated apoptosis is known to require the transcription factor p53, implicating transcriptional regulation as a potential mechanism for MAGE-D2's function. However, MAGE-D1 can also activate c-Jun N-terminal kinase (JNK), leading to MOMP and apoptosis (Salehi et al., 2002), and MAGE-D1 interacts transiently with XIAP and may lead to degradation of this anti-apoptotic protein during apoptosis (Jordan et al., 2001). It is possible that MAGE-D2, which shares extensive sequence homology with MAGE-D1, may regulate apoptosis through one of these mechanisms.

MAGE-D2 may also regulate cell cycle progression. In patches of confluent U2OS cells, MAGE-D2 expression was decreased significantly. This suggests that MAGE-D2 might either regulate, or be regulated by, the cell cycle. Additionally, in a flow cytometry experiment, it was observed that cells transfected with MAGE-D2-Flag yielded a higher peak representing the G1 phase of the cell cycle compared to mock-transfected cells, as determined visually, although the percentages of cells in each phase have not been quantified. It would be interesting to carry out additional experiments to determine whether MAGE-D2 affects cell cycle progression. First, the above-mentioned flow cytometry experiment could be repeated and quantified. siRNA could be used to determine whether MAGE-D2 knockdown causes the opposite effect. That is, can inhibition of MAGE-D2 decrease the proportion of G1 phase cells?

To determine whether MAGE-D2-Flag expression induces cell cycle arrest, cellular proliferation could be monitored to determine whether cell division

slows in MAGE-D2-Flag expressing cells compared to untreated cells. Additionally, a BRDU-incorporation assay could be used to assess whether MAGE-D2-Flag-transfected cells arrest at G1 or progress into S (DNA synthesis) phase. When BRDU (bromodeoxyuridine) is added to cycling cells, it becomes incorporated into the new DNA that is produced during S phase. A decrease of BRDU incorporation indicates that fewer cells are entering S phase, and cell cycle arrest may be occurring. MAGE-D2 expression is heterogeneous from cell to cell in terms of both quantity and localization. That is, cells express varying amounts of MAGE-D2, with localization appearing primarily nuclear/nucleolar in some cells and primarily mitochondrial in other cells. These differences may correspond to cell cycle progression. To determine whether the cell cycle stage affects MAGE-D2 expression and/or localization, cells could be treated with cycloheximide to synchronize the cell cycle and then fixed at various time points to be examined by immunofluorescence (to assess localization) and western blotting (to assess protein level). To determine whether MAGE-D2 expression correlates with a specific cell cycle phase, markers of the various cell cycle phases could be examined simultaneously. These results would yield clues to the mechanism by which MAGE-D2 might regulate, or be regulated by, the cell cycle. The absence of MAGE-D2 in some confluent cells seems contradictory to the data showing that overexpression of MAGE-D2-FLAG might increase the percentage of cells in G1. Again, the tag could be affecting the function of the protein, or overexpression might cause non-physiological results. The experiments described above can help to determine whether MAGE-D2 plays a

role in cell cycle control, and whether it promotes or inhibits cell cycle progression.

The preliminary data presented here suggest that MAGE-D2 may have a pro-apoptotic function and/or a cell-cycle-inhibitory function. However, it must be considered that these experiments were based on ectopic protein overexpression, which can yield artifacts and should be complemented by knockdown data when possible. Ratios among proteins can be critical for normal functioning, and gross overexpression can cause other functions not observed with the endogenous protein, such as aberrant localization or sequestering of another protein. Therefore, knockdown data using RNAi is generally considered more reliable and would greatly aid in determining the true, *in vivo*, functions of MAGE-D2. Tags can also interfere with protein function, and MAGE-D2-Flag may not behave the same as untagged MAGE-D2 in cells. Data from MAGE-D2-Flag overexpression suggest a potential pro-apoptotic or proliferation-inhibitory function. However, expression of MAGE-D2 is elevated in a number of cancers, and this would be more consistent with the opposite role for MAGE-D2 (anti-apoptosis and/or pro-proliferation). It is possible that the Flag tag interferes with the function of MAGE-D2. This issue could be resolved by transfecting cells with untagged MAGE-D2 and/or MAGE-D2 tagged at the other terminus.

Our studies have not addressed how MAGE-D2 itself is regulated during apoptosis and/or cell cycle control, or what upstream signaling pathways may lead to its activation. A large-scale screen for substrates of ATM/ATR found that MAGE-D2 is phosphorylated by these proteins at several serine residues

following DNA damage (Matsuoka et al., 2007). ATM (ataxia telangiectasia, mutated) and ATR (ATM and Rad3-related) are serine-threonine protein kinases that act as key regulators of the DNA damage cell cycle checkpoint. ATM responds to DNA double-strand breaks, while ATR primarily mediates response to UV radiation and stalled DNA replication. Activation of these proteins leads to G1 cell cycle arrest mediated by p53, allowing time for cells to repair DNA damage prior to dividing (Matsuoka et al., 2000; Maya et al., 2001; Shieh et al., 2000). In the event of extensive (irreparable) DNA damage, activation of ATM/ATR, in conjunction with activation of other signaling pathways, can induce apoptosis (Norbury and Zhivotovsky, 2004). To determine whether MAGE-D2 mediates ATM/ATR-induced response to DNA damage by regulating cell cycle arrest and/or apoptosis, the ability of ATM/ATR to regulate these events could be assessed with and without MAGE-D2 knockdown. The four serines in MAGE-D2 that are reported to be phosphorylated by ATM/ATR could be mutated to determine whether the effects of these proteins depend specifically on phosphorylation of MAGE-D2 at these residues.

Overall, the data presented here suggest an interesting potential role for MAGE-D2 in mediating apoptosis and/or a cell cycle checkpoint, and examination of various aspects of MAGE-D2—reported functions of homologs as well as interacting proteins and modifications of MAGE-D2—provides several compelling directions for future research. This work provides a foundation from which to study the functions and mechanisms of MAGE-D2 and provides

valuable tools (expression plasmids and two effective and specific antibodies) with which to carry out these studies.

Regulation of Apoptosis by SUMI-1

In this work, SUMI-1 is characterized as a novel regulator of BAX-mediated apoptosis. We show that in healthy cells, SUMI-1 resides at the mitochondria, where it regulates mitochondrial dynamics. We present a model in which SUMI-1's exodus from mitochondria during apoptosis inhibits mitochondrial fusion, while fission proceeds as normal, resulting in fragmented yet intact mitochondria. This fragmentation promotes oligomerization of BAX, leading to mitochondrial outer membrane permeabilization (MOMP), cytochrome *c* release, Caspase activation, and apoptosis. Data from Oncomine show that SUMI-1 is upregulated in a variety of cancers, consistent with its anti-apoptotic function. Likewise, we show that SUMI-1 is overexpressed in cancerous human cell lines compared to non-transformed cells and that inhibition of SUMI-1 sensitizes cells to chemotherapeutic-induced apoptosis. Together, these data suggest that SUMI-1 may represent a potential chemosensitizing therapeutic target for cancer treatment.

While we show that SUMI-1 regulates mitochondrial dynamics and oligomerization of BAX, the exact biochemical mechanisms of SUMI-1's function remain unknown. Mitochondrial fusion is mediated by Mitofusins 1 and 2 (MFN1 and MFN2), and these Mitofusins on adjacent mitochondria homo-or hetero-dimerize to anchor mitochondria together and induce fusion. SUMI-1 may interact

with one or both Mitofusins in order to promote their function, or it may affect fusion indirectly through another mechanism. BAK, in addition to oligomerizing to induce MOMP during apoptosis, also interacts with Mitofusins and regulates mitochondrial dynamics during apoptosis. During apoptosis, binding between BAK and MFN1 increase, and this interaction inhibits fusion, leading to mitochondrial fragmentation and promoting MOMP (Brooks et al., 2007). Preliminary data show that inhibition of SUMI-1 with RNAi increases the level of BAK protein. Apoptosis induced by UV also increases the level of BAK, and SUMI-1 knockdown augments the UV-mediated BAK increase (data not shown). It is possible that SUMI-1 normally keeps the level of BAK in check, maintaining the ability of mitochondria to fuse. During apoptosis, inhibition of SUMI-1 (such as by translocation from the mitochondria, a decrease in level, and/or oligomerization), may lead to increased BAK levels, thereby inhibiting fusion and sensitizing cells to BAX- and/or BAK-mediated MOMP and apoptosis. Further studies could be carried out to determine whether SUMI-1 indeed regulates BAK, and through what mechanism (e.g. protein degradation or inhibition of transcription) and whether SUMI-1 modulates mitochondrial dynamics and apoptosis through BAK or an alternative mechanism.

It is not known how SUMI-1 itself is regulated during apoptosis. We have shown that SUMI-1 translocates from the mitochondria during apoptosis prior to cytochrome *c* in order to regulate MOMP. However, the stimulus triggering this translocation is unknown. Preliminary data described in Chapter V suggest that SUMI-1 might oligomerize during apoptosis. This oligomerization, mediated by

disulfide bond interactions between cysteines in the CHCH domain, would almost certainly be regulated by RedOx status. Generally, an increase in oxidation induces formation of disulfide bonds, although variations in oxidation might influence whether these bonds form intramolecularly (generating a hairpin or loop in the CHCH domain) or between SUMI-1 molecules to create an oligomer—It is not yet known whether a monomer with intramolecular disulfide bonds or a disulfide-bond-mediated oligomer represents the fully-oxidized state of SUMI-1. This could be explored by altering the RedOx status of cells and examining the effect on development of higher molecular weight SUMI-1 bands by western blotting. Given that free radical production is associated with apoptosis, and that SUMI-1 appears to oligomerize during apoptosis, it is likely that SUMI-1 oligomers represent a more oxidized state than the monomers. One hypothesis for regulation of SUMI-1 during apoptosis is that SUMI-1 responds to changes in RedOx status by forming disulfide-bond-mediated oligomers, inducing its translocation from the mitochondria. Presumably, this RedOx stimulus would be oxidation induced by free radical generation. This idea could be tested by performing a subcellular fractionation to determine the localization of SUMI-1 monomers and putative oligomers during apoptosis. Mutations could be generated in cysteines of the CHCH domain (i.e. cysteine-to-alanine mutations) in order to determine whether translocation of SUMI-1 during apoptosis relies on disulfide bond formation involving two or more of the four cysteines in this domain.

Alternatively, SUMI-1 may be regulated by another mechanism such as phosphorylation. Another CHCH-domain-containing protein, CHCHD3, was recently identified as a substrate for cAMP-dependent protein kinase A (PKA) (Schauble et al., 2007). CHCHD3 was characterized earlier this year as an inner mitochondrial membrane protein that maintains mitochondrial function and crista integrity (Darshi et al., 2011). Upon phosphorylation of CHCHD3 by PKA at Threonine 10 (Thr^{10}), CHCHD3 translocates from the mitochondria to the nucleus, although the function for this PKA-induced translocation is unknown. According to analysis by KinasePhos (Huang et al., 2005), SUMI-1 also contains a predicted PKA phosphorylation site, located at Thr^{9}. Perhaps phosphorylation by PKA at this site might induce translocation of SUMI-1 during apoptosis. PKA can be activated by cyclic AMP (cAMP) to induce mitochondrial outer membrane permeabilization and apoptosis through mechanisms that are not well understood (Zhang et al., 2008). If SUMI-1 is phosphorylated by PKA, leading to its translocation during apoptosis, this would provide a link between PKA activation and sensitivity to mitochondrial outer membrane permeabilization during apoptosis. To determine whether SUMI-1 is a substrate of PKA, an *in vitro* kinase assay could be performed using combinations of SUMI-1, PKA, and radiolabeled ATP. Additional experiments could be carried out in intact cells by adding an inducer of cAMP with and without PKA knockdown and assessing the effect on SUMI-1 phosphorylation.

To assess whether Thr^{9} is indeed the phosphorylation site, a threonine-to-alanine mutation could be generated at residue 9 (T9A) to prevent

phosphorylation. As negative controls, other threonines and serines could be mutated to alanine to generate mutants that can still potentially be phosphorylated at Thr^9. If the phosphorylation site is identified, phospho-specific antibodies could be developed to more easily detect the phosphorylation status of SUMI-1.

To find out whether the translocation of SUMI-1 depends on phosphorylation at Thr^9, a T9A mutation could be generated to prevent phosphorylation. If Thr^9 is required for mitochondrial translocation of SUMI-1, apoptotic stimuli should fail to induce translocation of the T9A mutant. Mutation of threonine to glutamic acid can mimic phosphorylation (Wheatley et al., 2004); a T9E mutation could, therefore, induce SUMI-1 translocation. Together, these data would provide strong evidence that phosphorylation of SUMI-1 at Thr^9 is the trigger for SUMI-1's exodus from the mitochondria.

Experiments to determine how SUMI-1 translocates during apoptosis will provide insight into mechanisms by which SUMI-1's function can be manipulated. This knowledge could aid in the development of chemosensitizing drugs to inhibit SUMI-1, assuming that subsequent studies show that SUMI-1 is a suitable target for inhibition in cancer treatment.

A significant strength of the studies presented here is that they were carried out in intact cells, primarily using endogenous proteins. In the few cases in which ectopic expression was utilized, cells were usually transfected with non-tagged SUMI-1. The importance of these points was highlighted by a recent study reporting SUMI-1 as a modulator of cell migration (Seo et al., 2010). In that

paper, SUMI-1 was identified in a screen for novel cell-migration-regulating proteins, and several experiments were carried out to confirm this function. SUMI-1 was reported in that study to localize to the cytosol rather than the mitochondria, but the authors had assessed localization only by ectopic expression of an N-terminally-tagged SUMI-1 construct. As shown in Figure 4-6E of this work, an N-terminal tag blocks the mitochondrial localization of SUMI-1. Thus, the reported localization of SUMI-1 in the study by Seo et al. does not represent that of the endogenous protein. Furthermore, the authors claimed that co-transfection of p32 with SUMI-1 inhibited SUMI-1's function. However, the authors had transfected cells with an N-terminally tagged p32 whose mitochondrial targeting was also disrupted, causing the tagged p32 to localize to the cytosol rather than mitochondria. This means that both transfected proteins were incorrectly localized and grossly overexpressed, which affects how the data can be interpreted. When localized to a different cellular compartment, the interaction between the proteins may be altered, and overexpression of cytoplasmic p32 might have sequestered the cytoplasmic SUMI-1 or affected SUMI-1 in some manner that does not occur when both proteins are in the mitochondria. For example, the nature of the interaction between p32 and SUMI-1 might be different when SUMI-1 is embedded in the mitochondrial outer membrane as opposed to in its soluble form, and the disulfide bond formation—and therefore the intra- and inter-molecular structure—will differ between the oxidative environment of the mitochondria and the reducing environment of the cytosol.

While the studies here were carried out in intact cells and relying mostly on endogenous proteins—conferring many benefits over *in vitro* and ectopic expression experiments—studies using immortalized cell lines do not always recapitulate what occurs in a live organism. To address this issue, *SUMI-1* knockout mice could be generated for *in vivo* studies. Because SUMI-1 knockdown will probably increase apoptosis in the mouse as it does in human cell culture, it is likely that development will be disturbed by this deletion or that embryonic lethality may result. Further complicating the issue is that SUMI-1 has also been identified in screens for regulators of oxidative phosphorylation and cell migration, and both of these processes are essential during development. In the case of embryonic lethality, a conditional knockout mouse could be generated using a Cre/LoxP system to ablate SUMI-1 in specific mouse tissues. From these mouse knockout studies, we could determine whether SUMI-1 functions similarly in a live organism as in cell culture. The effect of SUMI-1 knockdown on apoptosis *in vivo* can be assessed using TUNEL staining of fixed mouse tissues, or of fixed embryo tissue in the case of embryonic lethality. Mouse embryo fibroblast (MEF) cells generated from these mice can also be used for experiments to assess the role of SUMI-1 in non-cancerous cells. An advantage here is that SUMI-1 expression can be completely ablated. It is difficult to transfect non-cancerous cell lines such as WI38 and BJ cells with siRNA, but SUMI-1-null MEFs should have complete abrogation of SUMI-1 expression and would provide another means by which to study non-transformed cells. These cells could also help answer questions about SUMI-1

oligomerization, as the HMW bands detected by western blotting with SUMI-1 antibody should be completely eliminated in SUMI-1-null MEFs, whereas with siRNA only partial knockdown is achieved, and if the oligomer form of SUMI-1 is favored, it may not disappear with siRNA treatment.

Several data suggest that SUMI-1 may be a candidate drug target for chemosensitizing agents in cancer treatment: SUMI-1 is an anti-apoptotic protein, and evasion from apoptosis is a hallmark of cancer; elevated SUMI-1 expression correlates with transformation of cell lines; SUMI-1 is elevated in a wide variety of human cancers; and inhibition of SUMI-1 sensitizes cancer cell lines to apoptosis induced by chemotherapeutic agents such as doxorubicin and cisplatin. Before SUMI-1 can be considered a valid drug target, additional studies are needed. First it should be determined whether SUMI-1 knockdown promotes shrinkage of tumors in nude or SCID (immune-compromised) mice; based on cell culture data, it is likely that SUMI-1 inhibition will sensitize the ectopic tumors to treatment with chemotherapeutic drugs. It is difficult to utilize siRNA in this type of experiment as the siRNA becomes quite dilute during the initial proliferation of tumor cells. To avoid this issue, a dominant-negative SUMI-1 (SUMI-1 c-terminally tagged with Flag) could be used to inhibit SUMI-1; tumor cells stably-expressing SUMI-1-Flag could be compared with mock-transfected cells.

In summary, the data presented here establish SUMI-1 as a novel regulator of mitochondrial fusion/fission dynamics and BAX-mediated apoptosis, and because the experiments were performed in live cells using mostly endogenous proteins, they are likely to be physiologically relevant. Future studies

can help us to learn the upstream signaling pathways that regulate SUMI-1, to understand whether SUMI-1 functions the same way in a live organism as it does in cell culture, and to determine whether SUMI-1 is a suitable target for cancer therapeutics.

Roles for Interactions Among p32, SUMI-1, and MAGE-D2

In this study, SUMI-1 and MAGE-D2 were both identified as binding partners for p32, and MAGE-D2 and SUMI-1 were also found to interact with each other. The initial rationale behind the search for p32-interacting proteins was to better understand the function of p32; we hoped to find an interaction with a known apoptosis-regulating protein that would provide clues regarding the mechanisms by which p32 regulates apoptosis. No such proteins were found among the eleven putative p32-interacting partners identified, but SUMI-1 and MAGE-D2 appeared to be promising candidates for novel regulators of apoptosis, and we elected to first characterize the functions of these two proteins on their own, independent of their interactions with p32. To understand the mechanisms of these three proteins in more detail, it would be helpful to determine the purpose for their interactions with one another.

Several studies could be carried out to determine the nature of the relationship between SUMI-1 and p32. First, it should be determined whether p32 interacts with SUMI-1 and/or MAGE-D2 to regulate apoptosis, and which protein is upstream and which is downstream in this pathway—that is, does p32 regulate SUMI-1 and MAGE-D2, or *vice versa*? To accomplish this, various

overexpression and knockdown experiments can be utilized. For example, SUMI-1 could be overexpressed with and without p32 knockdown or overexpression, and the ability of SUMI-1 overexpression to inhibit apoptosis could be assessed. If p32 acts downstream of SUMI-1, then its inhibition or overexpression might affect the ability of SUMI-1 overexpression to block apoptosis. By performing various combinations of these experiments, it can be determined whether the p32-SUMI-1 or p32-MAGE-D2 interactions mediate apoptosis, as well as whether p32 lies upstream or downstream of these proteins in the respective pathways. It is also possible, however, that p32 interacts with one or both proteins in a cooperative manner; two of the proteins, or all three, could comprise a complex that regulates apoptosis together—in this case, we might find that none of the proteins modifies the function of another. It is also possible that SUMI-1 and p32 do not interact to regulate apoptosis. Both proteins have reported roles in oxidative phosphorylation, and it is possible that they interact to mediate cellular metabolism, apoptosis, or both processes.

After a purpose for the interaction is established, the mechanism for this regulation can be explored. Mapping experiments indicate which specific domains interact and can often provide leads regarding how one protein might regulate another. Mapping can be accomplished by generating tagged deletion mutants of each protein and carrying out a co-immunoprecipitation to identify which peptides interact. Deletion mutants for p32 are available from a previous lab member, and I have designed and produced six Myc-tagged deletion mutants each for SUMI-1 and MAGE-D2 (Figure 6-1). In addition to mapping, it can be

determined whether inhibition or overexpression of one protein affects the other's expression level or localization. Knockdown of SUMI-1 does not appear to affect the level of endogenous p32 detected by western blotting with a p32 antibody (data not shown). However, another antibody that is marketed as a BCL-xL antibody (Santa Cruz, anti-BCL-x S-18, sc634) recognizes two strong bands (on a western blot) of approximately 34 and 37 kD in size that, surprisingly, represent p32 rather than BCL-xL (Figure 4-20). During apoptosis, these bands shift—the 34 kD band disappears, while the 37 kD band becomes stronger (Figure 4-19). This shift in migration of p32 may represent a modification of p32 that occurs during apoptosis. Interestingly, knockdown of SUMI-1 promotes this shift in migration and even induces a partial shift in the absence of apoptotic stimuli, suggesting that SUMI-1 inhibits this modification of p32. During apoptosis, p32 is released from the mitochondria concurrent with cytochrome *c* (unpublished data from our laboratory), while SUMI-1 translocates prior to cytochrome *c*, suggesting that SUMI-1 translocates before p32 and therefore dissociates from p32 upon its exit from the mitochondria. Translocation of SUMI-1 from the mitochondria (causing its release from p32), might promote p32 modification, allowing MOMP and apoptosis to proceed.

Upon examination of the BCL-xL S-18 antibody and attempts to determine how it recognizes p32, it was found that p32 contains an area of homology with BCL-xL within the N-terminal BH4 domain (Figure 4-21). Apparently, this region of p32 mimics the BH4 domain of BCL-xL well enough to induce strong binding between the BCL-xL antibody and p32. This suggests that p32 might contain a

BH4-mimetic domain. Perhaps p32 can interact with or mimic other BCL-2 family members via this domain. A previous lab member performed a co-immunoprecipitation experiment searching for interactions between p32 and several BCL-2 family members, with inconclusive results (data not shown). It is possible that p32 interacts with one of these proteins transiently, or more likely, that p32 interacts with these proteins only during apoptosis; for example, the potential BH4-mimetic domain could be hidden by SUMI-1 until SUMI-1 translocates from the mitochondria during apoptosis. It would be interesting to explore this hypothesis with additional co-immunoprecipitation experiments in the presence of apoptotic stimuli, using crosslinking to preserve weak or transient interactions if necessary.

Data published by Itahana and Zhang show that p32 regulates apoptosis by recruiting ARF to the mitochondria, inducing a change in mitochondrial membrane potential and sensitizing cells to apoptotic stimuli (Itahana and Zhang, 2008). It is possible that ARF dissociates SUMI-1 from p32, causing SUMI-1 translocation from mitochondria. Alternatively, SUMI-1 might sequester p32, preventing its interaction with ARF until SUMI-1 translocates during apoptosis. It is unknown whether these three proteins can exist in a complex together, or whether SUMI-1 can influence the ability of p32 and ARF to interact together. A sequential co-IP could determine whether the proteins are part of the same complex. To determine whether SUMI-1 affects the p32-ARF interaction, a co-IP between p32 and ARF could be carried out with and without siRNA knockdown of SUMI-1.

Establishing a purpose and mechanism for the interactions among p32, MAGE-D2, and SUMI-1 will provide mechanistic insights into the functions of these proteins and may identify a novel signaling pathway in regulating apoptosis.

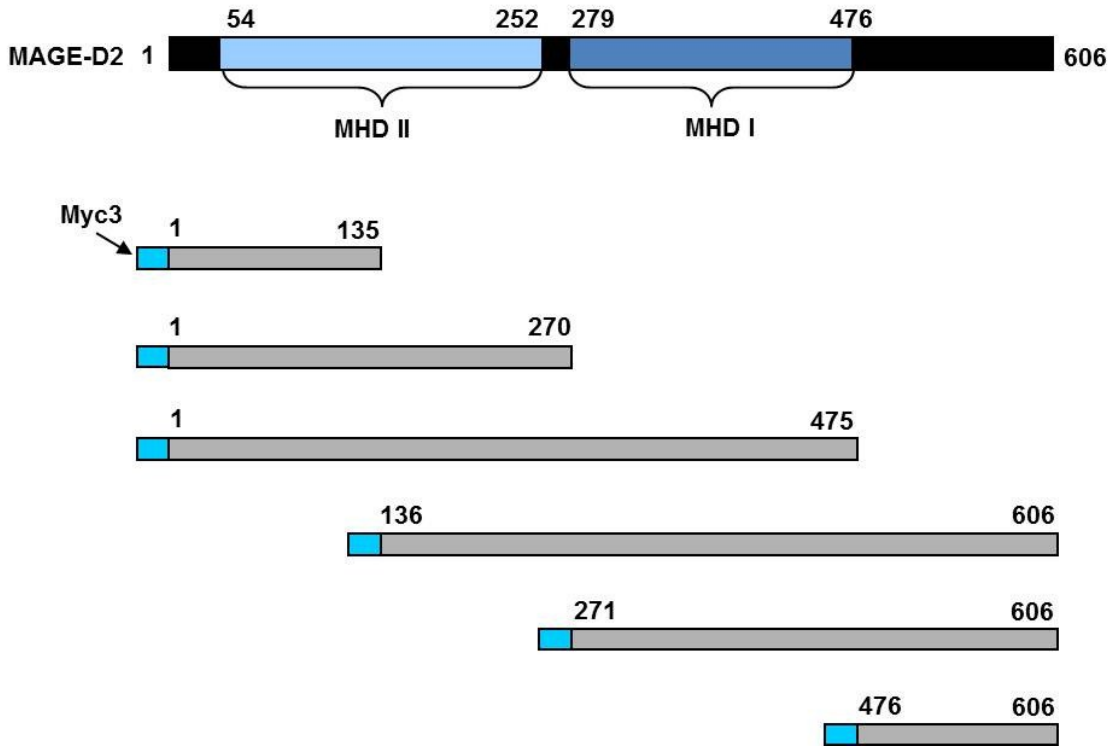

Figure 6-1. MAGE-D2 deletion mutants.
Six Myc-tagged MAGE-D2 deletion mutants have been generated for mapping the interaction between MAGE-D2 and p32 or other proteins.

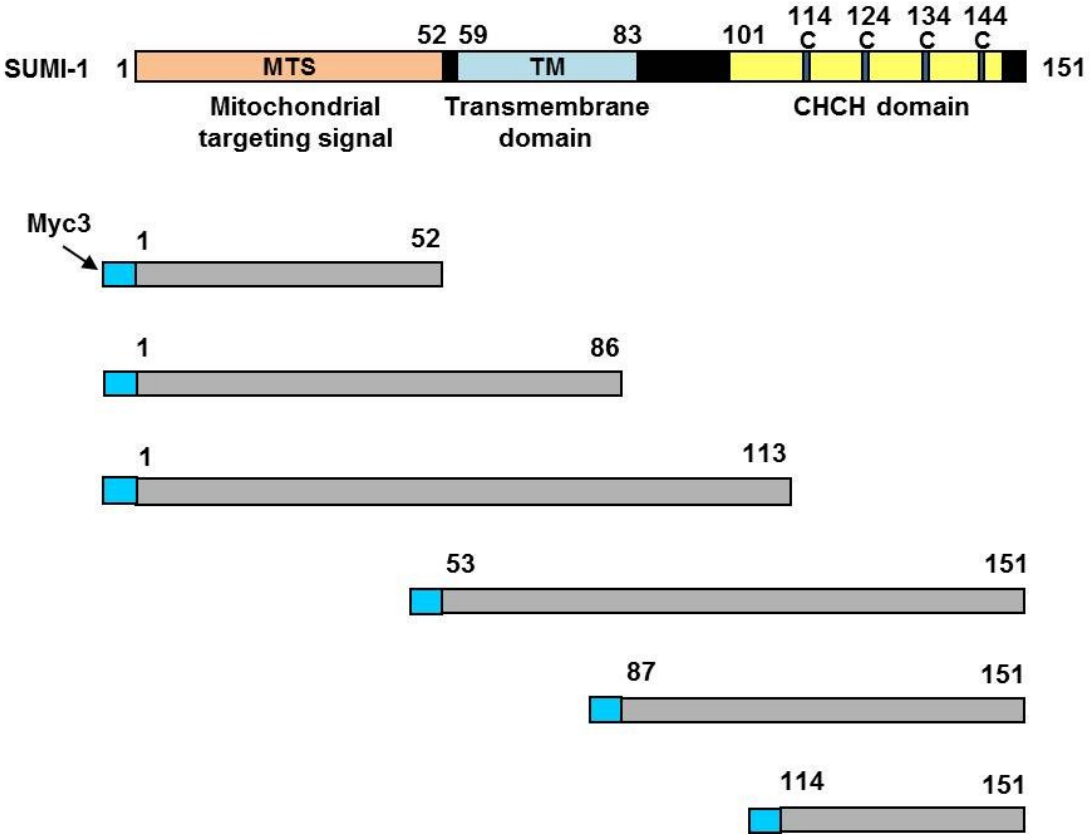

Figure 6-2. SUMI-1 deletion mutants.
Six Myc-tagged SUMI-1 deletion mutants have been generated for mapping the interaction between SUMI-1 and p32 or other proteins.

REFERENCES

Albino, D., Scaruffi, P., Moretti, S., Coco, S., Truini, M., Di Cristofano, C., Cavazzana, A., Stigliani, S., Bonassi, S., and Tonini, G.P. (2008). Identification of low intratumoral gene expression heterogeneity in neuroblastic tumors by genome-wide expression analysis and game theory. Cancer *113*, 1412-1422.

Andersson, A., Ritz, C., Lindgren, D., Eden, P., Lassen, C., Heldrup, J., Olofsson, T., Rade, J., Fontes, M., Porwit-Macdonald, A.*, et al.* (2007). Microarray-based classification of a consecutive series of 121 childhood acute leukemias: prediction of leukemic and genetic subtype as well as of minimal residual disease status. Leukemia *21*, 1198-1203.

Annilo, T., Laan, M., Stahl, J., and Metspalu, A. (1995). The human ribosomal protein S7-encoding gene: isolation, structure and localization in 2p25. Gene *165*, 297-302.

Arnesano, F., Balatri, E., Banci, L., Bertini, I., and Winge, D.R. (2005). Folding studies of Cox17 reveal an important interplay of cysteine oxidation and copper binding. Structure *13*, 713-722.

Arnoult, D. (2008). Apoptosis-associated mitochondrial outer membrane permeabilization assays. Methods *44*, 229-234.

Arslantas, A., Artan, S., Oner, U., Muslumanoglu, H., Durmaz, R., Cosan, E., Atasoy, M.A., Basaran, N., and Tel, E. (2004). The importance of genomic copy number changes in the prognosis of glioblastoma multiforme. Neurosurg Rev *27*, 58-64.

Ashkenazi, A., and Dixit, V.M. (1998). Death receptors: signaling and modulation. Science *281*, 1305-1308.

Bakhshi, A., Jensen, J.P., Goldman, P., Wright, J.J., McBride, O.W., Epstein, A.L., and Korsmeyer, S.J. (1985). Cloning the chromosomal breakpoint of t(14;18) human lymphomas: clustering around JH on chromosome 14 and near a transcriptional unit on 18. Cell *41*, 899-906.

Banci, L., Bertini, I., Ciofi-Baffoni, S., Hadjiloi, T., Martinelli, M., and Palumaa, P. (2008a). Mitochondrial copper(I) transfer from Cox17 to Sco1 is coupled to electron transfer. Proceedings of the National Academy of Sciences of the United States of America *105*, 6803-6808.

Banci, L., Bertini, I., Ciofi-Baffoni, S., Janicka, A., Martinelli, M., Kozlowski, H., and Palumaa, P. (2008b). A structural-dynamical characterization of human Cox17. J Biol Chem *283*, 7912-7920.

Barker, P.A., and Salehi, A. (2002). The MAGE proteins: emerging roles in cell cycle progression, apoptosis, and neurogenetic disease. J Neurosci Res *67*, 705-712.

Barros, M.H., Johnson, A., and Tzagoloff, A. (2004). COX23, a homologue of COX17, is required for cytochrome oxidase assembly. J Biol Chem *279*, 31943-31947.

Baughman, J.M., Nilsson, R., Gohil, V.M., Arlow, D.H., Gauhar, Z., and Mootha, V.K. (2009). A computational screen for regulators of oxidative phosphorylation implicates SLIRP in mitochondrial RNA homeostasis. PLoS Genet *5*, e1000590.

Baumeister, W., Walz, J., Zuhl, F., and Seemuller, E. (1998). The proteasome: paradigm of a self-compartmentalizing protease. Cell *92*, 367-380.

Biswas, S.C., Shi, Y., Vonsattel, J.P., Leung, C.L., Troy, C.M., and Greene, L.A. (2007). Bim is elevated in Alzheimer's disease neurons and is required for beta-amyloid-induced neuronal apoptosis. J Neurosci *27*, 893-900.

Blalock, E.M., Geddes, J.W., Chen, K.C., Porter, N.M., Markesbery, W.R., and Landfield, P.W. (2004). Incipient Alzheimer's disease: microarray correlation analyses reveal major transcriptional and tumor suppressor responses. Proc Natl Acad Sci U S A *101*, 2173-2178.

Boise, L.H., Gonzalez-Garcia, M., Postema, C.E., Ding, L., Lindsten, T., Turka, L.A., Mao, X., Nunez, G., and Thompson, C.B. (1993). bcl-x, a bcl-2-related gene that functions as a dominant regulator of apoptotic cell death. Cell *74*, 597-608.

Bowes, T.J., and Gupta, R.S. (2005). Induction of mitochondrial fusion by cysteine-alkylators ethacrynic acid and N-ethylmaleimide. J Cell Physiol *202*, 796-804.

Brookmeyer, R., Johnson, E., Ziegler-Graham, K., and Arrighi, H.M. (2007). Forecasting the global burden of Alzheimer's disease. Alzheimers Dement *3*, 186-191.

Brooks, C., Cho, S.G., Wang, C.Y., Yang, T., and Dong, Z. (2011). Fragmented mitochondria are sensitized to Bax insertion and activation during apoptosis. Am J Physiol Cell Physiol *300*, C447-455.

Brooks, C., Wei, Q., Feng, L., Dong, G., Tao, Y., Mei, L., Xie, Z.J., and Dong, Z. (2007). Bak regulates mitochondrial morphology and pathology during apoptosis by interacting with mitofusins. Proc Natl Acad Sci U S A *104*, 11649-11654.

Bruhn, L., Munnerlyn, A., and Grosschedl, R. (1997). ALY, a context-dependent coactivator of LEF-1 and AML-1, is required for TCRalpha enhancer function. Genes & development *11*, 640-653.

Cassidy-Stone, A., Chipuk, J.E., Ingerman, E., Song, C., Yoo, C., Kuwana, T., Kurth, M.J., Shaw, J.T., Hinshaw, J.E., Green, D.R*., et al.* (2008). Chemical inhibition of the mitochondrial division dynamin reveals its role in Bax/Bak-dependent mitochondrial outer membrane permeabilization. Dev Cell *14*, 193-204.

Certo, M., Del Gaizo Moore, V., Nishino, M., Wei, G., Korsmeyer, S., Armstrong, S.A., and Letai, A. (2006). Mitochondria primed by death signals determine cellular addiction to antiapoptotic BCL-2 family members. Cancer Cell *9*, 351-365.

Chacinska, A., Pfannschmidt, S., Wiedemann, N., Kozjak, V., Sanjuan Szklarz, L.K., Schulze-Specking, A., Truscott, K.N., Guiard, B., Meisinger, C., and Pfanner, N. (2004). Essential role of Mia40 in import and assembly of mitochondrial intermembrane space proteins. Embo J *23*, 3735-3746.

Chen, G.G., and Lai, P.B.S. (2009). Apoptosis in Carcinogenesis and Chemotherapy: Apoptosis in Cancer (Springer).

Chen, H., Detmer, S.A., Ewald, A.J., Griffin, E.E., Fraser, S.E., and Chan, D.C. (2003). Mitofusins Mfn1 and Mfn2 coordinately regulate mitochondrial fusion and are essential for embryonic development. The Journal of cell biology *160*, 189-200.

Chen, I.T., and Roufa, D.J. (1988). The transcriptionally active human ribosomal protein S17 gene. Gene *70*, 107-116.

Chen, L., Willis, S.N., Wei, A., Smith, B.J., Fletcher, J.I., Hinds, M.G., Colman, P.M., Day, C.L., Adams, J.M., and Huang, D.C. (2005). Differential targeting of prosurvival Bcl-2 proteins by their BH3-only ligands allows complementary apoptotic function. Molecular cell *17*, 393-403.

Chipuk, J.E., Bouchier-Hayes, L., Kuwana, T., Newmeyer, D.D., and Green, D.R. (2005). PUMA couples the nuclear and cytoplasmic proapoptotic function of p53. Science *309*, 1732-1735.

Chipuk, J.E., Fisher, J.C., Dillon, C.P., Kriwacki, R.W., Kuwana, T., and Green, D.R. (2008). Mechanism of apoptosis induction by inhibition of the anti-apoptotic BCL-2 proteins. Proceedings of the National Academy of Sciences of the United States of America *105*, 20327-20332.

Chipuk, J.E., and Green, D.R. (2008). How do BCL-2 proteins induce mitochondrial outer membrane permeabilization? Trends Cell Biol *18*, 157-164.

Chipuk, J.E., Kuwana, T., Bouchier-Hayes, L., Droin, N.M., Newmeyer, D.D., Schuler, M., and Green, D.R. (2004). Direct activation of Bax by p53 mediates mitochondrial membrane permeabilization and apoptosis. Science *303*, 1010-1014.

Chipuk, J.E., Moldoveanu, T., Llambi, F., Parsons, M.J., and Green, D.R. (2010). The BCL-2 family reunion. Mol Cell *37*, 299-310.

Chomez, P., De Backer, O., Bertrand, M., De Plaen, E., Boon, T., and Lucas, S. (2001). An overview of the MAGE gene family with the identification of all human members of the family. Cancer research *61*, 5544-5551.

Chowdhury, A.R., Ghosh, I., and Datta, K. (2008). Excessive reactive oxygen species induces apoptosis in fibroblasts: role of mitochondrially accumulated hyaluronic acid binding protein 1 (HABP1/p32/gC1qR). Exp Cell Res *314*, 651-667.

Claros, M.G., and Vincens, P. (1996). Computational method to predict mitochondrially imported proteins and their targeting sequences. Eur J Biochem *241*, 779-786.

Cleary, M.L., Smith, S.D., and Sklar, J. (1986). Cloning and structural analysis of cDNAs for bcl-2 and a hybrid bcl-2/immunoglobulin transcript resulting from the t(14;18) translocation. Cell *47*, 19-28.

Darshi, M., Mendiola, V.L., Mackey, M.R., Murphy, A.N., Koller, A., Perkins, G.A., Ellisman, M.H., and Taylor, S.S. (2011). ChChd3, an inner mitochondrial membrane protein, is essential for maintaining crista integrity and mitochondrial function. The Journal of biological chemistry *286*, 2918-2932.

Dauer, W., and Przedborski, S. (2003). Parkinson's disease: mechanisms and models. Neuron *39*, 889-909.

Dedio, J., Jahnen-Dechent, W., Bachmann, M., and Muller-Esterl, W. (1998). The multiligand-binding protein gC1qR, putative C1q receptor, is a mitochondrial protein. J Immunol *160*, 3534-3542.

Del Gaizo Moore, V., Brown, J.R., Certo, M., Love, T.M., Novina, C.D., and Letai, A. (2007). Chronic lymphocytic leukemia requires BCL2 to sequester prodeath BIM, explaining sensitivity to BCL2 antagonist ABT-737. J Clin Invest *117*, 112-121.

Deverman, B.E., Cook, B.L., Manson, S.R., Niederhoff, R.A., Langer, E.M., Rosova, I., Kulans, L.A., Fu, X., Weinberg, J.S., Heinecke, J.W*., et al.* (2002). Bcl-xL deamidation is a critical switch in the regulation of the response to DNA damage. Cell *111*, 51-62.

Doyle, J.M., Gao, J., Wang, J., Yang, M., and Potts, P.R. (2010). MAGE-RING protein complexes comprise a family of E3 ubiquitin ligases. Molecular cell *39*, 963-974.

Drexler, H.C. (1997). Activation of the cell death program by inhibition of proteasome function. Proceedings of the National Academy of Sciences of the United States of America *94*, 855-860.

Du, C., Fang, M., Li, Y., Li, L., and Wang, X. (2000). Smac, a mitochondrial protein that promotes cytochrome c-dependent caspase activation by eliminating IAP inhibition. Cell *102*, 33-42.

Duckett, C.S., Nava, V.E., Gedrich, R.W., Clem, R.J., Van Dongen, J.L., Gilfillan, M.C., Shiels, H., Hardwick, J.M., and Thompson, C.B. (1996). A conserved family of cellular genes related to the baculovirus iap gene and encoding apoptosis inhibitors. The EMBO journal *15*, 2685-2694.

Edlich, F., Banerjee, S., Suzuki, M., Cleland, M.M., Arnoult, D., Wang, C., Neutzner, A., Tjandra, N., and Youle, R.J. (2011). Bcl-x(L) Retrotranslocates Bax from the Mitochondria into the Cytosol. Cell *145*, 104-116.

Eilbracht, J., Reichenzeller, M., Hergt, M., Schnolzer, M., Heid, H., Stohr, M., Franke, W.W., and Schmidt-Zachmann, M.S. (2004). NO66, a highly conserved dual location protein in the nucleolus and in a special type of synchronously replicating chromatin. Mol Biol Cell *15*, 1816-1832.

Estus, S., Tucker, H.M., van Rooyen, C., Wright, S., Brigham, E.F., Wogulis, M., and Rydel, R.E. (1997). Aggregated amyloid-beta protein induces cortical neuronal apoptosis and concomitant "apoptotic" pattern of gene induction. J Neurosci *17*, 7736-7745.

Ethell, D.W., and Buhler, L.A. (2003). Fas ligand-mediated apoptosis in degenerative disorders of the brain. J Clin Immunol *23*, 439-446.

Evan, G., and Littlewood, T. (1998). A matter of life and cell death. Science *281*, 1317-1322.

Faccio, L., Fusco, C., Chen, A., Martinotti, S., Bonventre, J.V., and Zervos, A.S. (2000). Characterization of a novel human serine protease that has extensive homology to bacterial heat shock endoprotease HtrA and is regulated by kidney ischemia. The Journal of biological chemistry *275*, 2581-2588.

Fadok, V.A., de Cathelineau, A., Daleke, D.L., Henson, P.M., and Bratton, D.L. (2001). Loss of phospholipid asymmetry and surface exposure of phosphatidylserine is required for phagocytosis of apoptotic cells by macrophages and fibroblasts. The Journal of biological chemistry *276*, 1071-1077.

Ferraro-Peyret, C., Quemeneur, L., Flacher, M., Revillard, J.P., and Genestier, L. (2002). Caspase-independent phosphatidylserine exposure during apoptosis of primary T lymphocytes. J Immunol *169*, 4805-4810.

Ferre, F., and Clote, P. (2005a). DiANNA: a web server for disulfide connectivity prediction. Nucleic Acids Res *33*, W230-232.

Ferre, F., and Clote, P. (2005b). Disulfide connectivity prediction using secondary structure information and diresidue frequencies. Bioinformatics *21*, 2336-2346.

Frank, S., Gaume, B., Bergmann-Leitner, E.S., Leitner, W.W., Robert, E.G., Catez, F., Smith, C.L., and Youle, R.J. (2001). The role of dynamin-related protein 1, a mediator of mitochondrial fission, in apoptosis. Dev Cell *1*, 515-525.

Gavathiotis, E., Reyna, D.E., Davis, M.L., Bird, G.H., and Walensky, L.D. (2010). BH3-triggered structural reorganization drives the activation of proapoptotic BAX. Mol Cell *40*, 481-492.

Ghebrehiwet, B., Lim, B.L., Peerschke, E.I., Willis, A.C., and Reid, K.B. (1994). Isolation, cDNA cloning, and overexpression of a 33-kD cell surface glycoprotein that binds to the globular "heads" of C1q. J Exp Med *179*, 1809-1821.

Gordon, G.J., Rockwell, G.N., Jensen, R.V., Rheinwald, J.G., Glickman, J.N., Aronson, J.P., Pottorf, B.J., Nitz, M.D., Richards, W.G., Sugarbaker, D.J.*, et al.* (2005). Identification of novel candidate oncogenes and tumor suppressors in malignant pleural mesothelioma using large-scale transcriptional profiling. Am J Pathol *166*, 1827-1840.

Greenhalgh, D.G. (1998). The role of apoptosis in wound healing. Int J Biochem Cell Biol *30*, 1019-1030.

Grimm, S., Stanger, B.Z., and Leder, P. (1996). RIP and FADD: two "death domain"-containing proteins can induce apoptosis by convergent, but dissociable, pathways. Proceedings of the National Academy of Sciences of the United States of America *93*, 10923-10927.

Hanahan, D., and Weinberg, R.A. (2000). The hallmarks of cancer. Cell *100*, 57-70.

Hanahan, D., and Weinberg, R.A. (2011). Hallmarks of cancer: the next generation. Cell *144*, 646-674.

Haqq, C., Nosrati, M., Sudilovsky, D., Crothers, J., Khodabakhsh, D., Pulliam, B.L., Federman, S., Miller, J.R., 3rd, Allen, R.E., Singer, M.I.*, et al.* (2005). The gene expression signatures of melanoma progression. Proceedings of the National Academy of Sciences of the United States of America *102*, 6092-6097.

Hartman, R.E., Izumi, Y., Bales, K.R., Paul, S.M., Wozniak, D.F., and Holtzman, D.M. (2005). Treatment with an amyloid-beta antibody ameliorates plaque load, learning deficits, and hippocampal long-term potentiation in a mouse model of Alzheimer's disease. J Neurosci *25*, 6213-6220.

Hayashi, T., and Faustman, D.L. (2003). Role of defective apoptosis in type 1 diabetes and other autoimmune diseases. Recent Prog Horm Res *58*, 131-153.

Hofmann, S., Rothbauer, U., Muhlenbein, N., Baiker, K., Hell, K., and Bauer, M.F. (2005). Functional and mutational characterization of human MIA40 acting during import into the mitochondrial intermembrane space. J Mol Biol *353*, 517-528.

Hsu, H., Xiong, J., and Goeddel, D.V. (1995). The TNF receptor 1-associated protein TRADD signals cell death and NF-kappa B activation. Cell *81*, 495-504.

Huang, H.D., Lee, T.Y., Tzeng, S.W., and Horng, J.T. (2005). KinasePhos: a web tool for identifying protein kinase-specific phosphorylation sites. Nucleic Acids Res *33*, W226-229.

Hudelist, G., Singer, C.F., Pischinger, K.I., Kaserer, K., Manavi, M., Kubista, E., and Czerwenka, K.F. (2006). Proteomic analysis in human breast cancer: identification of a characteristic protein expression profile of malignant breast epithelium. Proteomics *6*, 1989-2002.

Itahana, K., and Zhang, Y. (2008). Mitochondrial p32 is a critical mediator of ARF-induced apoptosis. Cancer Cell *13*, 542-553.

Jin, C., Myers, A.M., and Tzagoloff, A. (1997). Cloning and characterization of MRP10, a yeast gene coding for a mitochondrial ribosomal protein. Curr Genet *31*, 228-234.

Jordan, B.W., Dinev, D., LeMellay, V., Troppmair, J., Gotz, R., Wixler, L., Sendtner, M., Ludwig, S., and Rapp, U.R. (2001). Neurotrophin receptor-interacting mage homologue is an inducible inhibitor of apoptosis protein-interacting protein that augments cell death. The Journal of biological chemistry *276*, 39985-39989.

Jurchott, K., Bergmann, S., Stein, U., Walther, W., Janz, M., Manni, I., Piaggio, G., Fietze, E., Dietel, M., and Royer, H.D. (2003). YB-1 as a cell cycle-regulated transcription factor facilitating cyclin A and cyclin B1 gene expression. The Journal of biological chemistry *278*, 27988-27996.

Kamal, A., and Datta, K. (2006). Upregulation of hyaluronan binding protein 1 (HABP1/p32/gC1qR) is associated with Cisplatin induced apoptosis. Apoptosis *11*, 861-874.

Karbowski, M., Lee, Y.J., Gaume, B., Jeong, S.Y., Frank, S., Nechushtan, A., Santel, A., Fuller, M., Smith, C.L., and Youle, R.J. (2002). Spatial and temporal association of Bax with mitochondrial fission sites, Drp1, and Mfn2 during apoptosis. J Cell Biol *159*, 931-938.

Kendall, S.E., Battelli, C., Irwin, S., Mitchell, J.G., Glackin, C.A., and Verdi, J.M. (2005). NRAGE mediates p38 activation and neural progenitor apoptosis via the bone morphogenetic protein signaling cascade. Molecular and cellular biology *25*, 7711-7724.

Kerr, J.F., Winterford, C.M., and Harmon, B.V. (1994). Apoptosis. Its significance in cancer and cancer therapy. Cancer *73*, 2013-2026.

Kerr, J.F., Wyllie, A.H., and Currie, A.R. (1972). Apoptosis: a basic biological phenomenon with wide-ranging implications in tissue kinetics. Br J Cancer *26*, 239-257.

Kidd, M., Modlin, I.M., Mane, S.M., Camp, R.L., Eick, G., and Latich, I. (2006a). The role of genetic markers--NAP1L1, MAGE-D2, and MTA1--in defining small-intestinal carcinoid neoplasia. Ann Surg Oncol *13*, 253-262.

Kidd, M., Modlin, I.M., Mane, S.M., Camp, R.L., Eick, G.N., Latich, I., and Zikusoka, M.N. (2006b). Utility of molecular genetic signatures in the delineation of gastric neoplasia. Cancer *106*, 1480-1488.

Kim, H., Rafiuddin-Shah, M., Tu, H.C., Jeffers, J.R., Zambetti, G.P., Hsieh, J.J., and Cheng, E.H. (2006). Hierarchical regulation of mitochondrion-dependent apoptosis by BCL-2 subfamilies. Nat Cell Biol *8*, 1348-1358.

Kim, H., Tu, H.C., Ren, D., Takeuchi, O., Jeffers, J.R., Zambetti, G.P., Hsieh, J.J., and Cheng, E.H. (2009). Stepwise activation of BAX and BAK by tBID, BIM, and PUMA initiates mitochondrial apoptosis. Molecular cell *36*, 487-499.

Kischkel, F.C., Hellbardt, S., Behrmann, I., Germer, M., Pawlita, M., Krammer, P.H., and Peter, M.E. (1995). Cytotoxicity-dependent APO-1 (Fas/CD95)-associated proteins form a death-inducing signaling complex (DISC) with the receptor. The EMBO journal *14*, 5579-5588.

Kothakota, S., Azuma, T., Reinhard, C., Klippel, A., Tang, J., Chu, K., McGarry, T.J., Kirschner, M.W., Koths, K., Kwiatkowski, D.J*., et al.* (1997). Caspase-3-generated fragment of gelsolin: effector of morphological change in apoptosis. Science *278*, 294-298.

Kozopas, K.M., Yang, T., Buchan, H.L., Zhou, P., and Craig, R.W. (1993). MCL1, a gene expressed in programmed myeloid cell differentiation, has sequence similarity to BCL2. Proceedings of the National Academy of Sciences of the United States of America *90*, 3516-3520.

Kuwana, T., Bouchier-Hayes, L., Chipuk, J.E., Bonzon, C., Sullivan, B.A., Green, D.R., and Newmeyer, D.D. (2005). BH3 domains of BH3-only proteins differentially regulate Bax-mediated mitochondrial membrane permeabilization both directly and indirectly. Molecular cell *17*, 525-535.

Labrousse, A.M., Zappaterra, M.D., Rube, D.A., and van der Bliek, A.M. (1999). C. elegans dynamin-related protein DRP-1 controls severing of the mitochondrial outer membrane. Molecular cell *4*, 815-826.

LaMarche, A.E., Abate, M.I., Chan, S.H., and Trumpower, B.L. (1992). Isolation and characterization of COX12, the nuclear gene for a previously unrecognized subunit of Saccharomyces cerevisiae cytochrome c oxidase. J Biol Chem *267*, 22473-22480.

Landi, M.T., Dracheva, T., Rotunno, M., Figueroa, J.D., Liu, H., Dasgupta, A., Mann, F.E., Fukuoka, J., Hames, M., Bergen, A.W*., et al.* (2008). Gene expression signature of cigarette smoking and its role in lung adenocarcinoma development and survival. PLoS One *3*, e1651.

Langnaese, K., Kloos, D.U., Wehnert, M., Seidel, B., and Wieacker, P. (2001). Expression pattern and further characterization of human MAGED2 and identification of rodent orthologues. Cytogenet Cell Genet *94*, 233-240.

Lee, Y.J., Jeong, S.Y., Karbowski, M., Smith, C.L., and Youle, R.J. (2004). Roles of the mammalian mitochondrial fission and fusion mediators Fis1, Drp1, and Opa1 in apoptosis. Mol Biol Cell *15*, 5001-5011.

Letai, A., Bassik, M.C., Walensky, L.D., Sorcinelli, M.D., Weiler, S., and Korsmeyer, S.J. (2002). Distinct BH3 domains either sensitize or activate mitochondrial apoptosis, serving as prototype cancer therapeutics. Cancer Cell *2*, 183-192.

Leu, J.I., Dumont, P., Hafey, M., Murphy, M.E., and George, D.L. (2004). Mitochondrial p53 activates Bak and causes disruption of a Bak-Mcl1 complex. Nat Cell Biol *6*, 443-450.

Levine, A.J. (1997). p53, the cellular gatekeeper for growth and division. Cell *88*, 323-331.

Levy, O.A., Malagelada, C., and Greene, L.A. (2009). Cell death pathways in Parkinson's disease: proximal triggers, distal effectors, and final steps. Apoptosis : an international journal on programmed cell death *14*, 478-500.

Li, M., Lin, Y.M., Hasegawa, S., Shimokawa, T., Murata, K., Kameyama, M., Ishikawa, O., Katagiri, T., Tsunoda, T., Nakamura, Y.*, et al.* (2004). Genes associated with liver metastasis of colon cancer, identified by genome-wide cDNA microarray. International journal of oncology *24*, 305-312.

Liu, H., and Pope, R.M. (2003). The role of apoptosis in rheumatoid arthritis. Curr Opin Pharmacol *3*, 317-322.

Locksley, R.M., Killeen, N., and Lenardo, M.J. (2001). The TNF and TNF receptor superfamilies: integrating mammalian biology. Cell *104*, 487-501.

Lovell, J.F., Billen, L.P., Bindner, S., Shamas-Din, A., Fradin, C., Leber, B., and Andrews, D.W. (2008). Membrane binding by tBid initiates an ordered series of events culminating in membrane permeabilization by Bax. Cell *135*, 1074-1084.

Lucken-Ardjomande, S., Montessuit, S., and Martinou, J.C. (2008). Bax activation and stress-induced apoptosis delayed by the accumulation of cholesterol in mitochondrial membranes. Cell death and differentiation *15*, 484-493.

Luo, M.L., Zhou, Z., Magni, K., Christoforides, C., Rappsilber, J., Mann, M., and Reed, R. (2001). Pre-mRNA splicing and mRNA export linked by direct interactions between UAP56 and Aly. Nature *413*, 644-647.

Marcar, L., Maclaine, N.J., Hupp, T.R., and Meek, D.W. (2010). Mage-A cancer/testis antigens inhibit p53 function by blocking its interaction with chromatin. Cancer research *70*, 10362-10370.

Marchenko, N.D., Zaika, A., and Moll, U.M. (2000). Death signal-induced localization of p53 protein to mitochondria. A potential role in apoptotic signaling. J Biol Chem *275*, 16202-16212.

Martinou, J.C., and Youle, R.J. (2011). Mitochondria in apoptosis: bcl-2 family members and mitochondrial dynamics. Dev Cell *21*, 92-101.

Masters, C.L., Multhaup, G., Simms, G., Pottgiesser, J., Martins, R.N., and Beyreuther, K. (1985). Neuronal origin of a cerebral amyloid: neurofibrillary tangles of Alzheimer's disease contain the same protein as the amyloid of plaque cores and blood vessels. The EMBO journal *4*, 2757-2763.

Masuda, Y., Sasaki, A., Shibuya, H., Ueno, N., Ikeda, K., and Watanabe, K. (2001). Dlxin-1, a novel protein that binds Dlx5 and regulates its transcriptional function. The Journal of biological chemistry *276*, 5331-5338.

Matsuoka, S., Ballif, B.A., Smogorzewska, A., McDonald, E.R., 3rd, Hurov, K.E., Luo, J., Bakalarski, C.E., Zhao, Z., Solimini, N., Lerenthal, Y.*, et al.* (2007). ATM and ATR substrate analysis reveals extensive protein networks responsive to DNA damage. Science *316*, 1160-1166.

Matsuoka, S., Rotman, G., Ogawa, A., Shiloh, Y., Tamai, K., and Elledge, S.J. (2000). Ataxia telangiectasia-mutated phosphorylates Chk2 in vivo and in vitro. Proceedings of the National Academy of Sciences of the United States of America *97*, 10389-10394.

Maya, R., Balass, M., Kim, S.T., Shkedy, D., Leal, J.F., Shifman, O., Moas, M., Buschmann, T., Ronai, Z., Shiloh, Y.*, et al.* (2001). ATM-dependent phosphorylation of Mdm2 on serine 395: role in p53 activation by DNA damage. Genes Dev *15*, 1067-1077.

Merino, D., Giam, M., Hughes, P.D., Siggs, O.M., Heger, K., O'Reilly, L.A., Adams, J.M., Strasser, A., Lee, E.F., Fairlie, W.D.*, et al.* (2009). The role of BH3-only protein Bim extends beyond inhibiting Bcl-2-like prosurvival proteins. The Journal of cell biology *186*, 355-362.

Mihara, M., Erster, S., Zaika, A., Petrenko, O., Chittenden, T., Pancoska, P., and Moll, U.M. (2003). p53 has a direct apoptogenic role at the mitochondria. Molecular cell *11*, 577-590.

Modlin, I.M., Kidd, M., Latich, I., Zikusoka, M.N., Eick, G.N., Mane, S.M., and Camp, R.L. (2006). Genetic differentiation of appendiceal tumor malignancy: a guide for the perplexed. Ann Surg *244*, 52-60.

Monte, M., Simonatto, M., Peche, L.Y., Bublik, D.R., Gobessi, S., Pierotti, M.A., Rodolfo, M., and Schneider, C. (2006). MAGE-A tumor antigens target p53 transactivation function through histone deacetylase recruitment and confer resistance to chemotherapeutic agents. Proceedings of the National Academy of Sciences of the United States of America *103*, 11160-11165.

Montessuit, S., Somasekharan, S.P., Terrones, O., Lucken-Ardjomande, S., Herzig, S., Schwarzenbacher, R., Manstein, D.J., Bossy-Wetzel, E., Basanez, G., Meda, P.*, et al.* (2010). Membrane remodeling induced by the dynamin-related protein Drp1 stimulates Bax oligomerization. Cell *142*, 889-901.

Muta, T., Kang, D., Kitajima, S., Fujiwara, T., and Hamasaki, N. (1997). p32 protein, a splicing factor 2-associated protein, is localized in mitochondrial matrix and is functionally important in maintaining oxidative phosphorylation. J Biol Chem *272*, 24363-24370.

Nijhawan, D., Honarpour, N., and Wang, X. (2000). Apoptosis in neural development and disease. Annu Rev Neurosci *23*, 73-87.

Nobrega, M.P., Bandeira, S.C., Beers, J., and Tzagoloff, A. (2002). Characterization of COX19, a widely distributed gene required for expression of mitochondrial cytochrome oxidase. J Biol Chem *277*, 40206-40211.

Norbury, C.J., and Zhivotovsky, B. (2004). DNA damage-induced apoptosis. Oncogene *23*, 2797-2808.

O'Connor, L., Strasser, A., O'Reilly, L.A., Hausmann, G., Adams, J.M., Cory, S., and Huang, D.C. (1998). Bim: a novel member of the Bcl-2 family that promotes apoptosis. The EMBO journal *17*, 384-395.

Olsen, J.V., Blagoev, B., Gnad, F., Macek, B., Kumar, C., Mortensen, P., and Mann, M. (2006). Global, in vivo, and site-specific phosphorylation dynamics in signaling networks. Cell *127*, 635-648.

Oltvai, Z.N., Milliman, C.L., and Korsmeyer, S.J. (1993). Bcl-2 heterodimerizes in vivo with a conserved homolog, Bax, that accelerates programmed cell death. Cell *74*, 609-619.

Opferman, J.T., and Korsmeyer, S.J. (2003). Apoptosis in the development and maintenance of the immune system. Nat Immunol *4*, 410-415.

Otsuga, D., Keegan, B.R., Brisch, E., Thatcher, J.W., Hermann, G.J., Bleazard, W., and Shaw, J.M. (1998). The dynamin-related GTPase, Dnm1p, controls mitochondrial morphology in yeast. The Journal of cell biology *143*, 333-349.

Papageorgio, C., Brachmann, R., Zeng, J., Culverhouse, R., Zhang, W., and McLeod, H. (2007). MAGED2: a novel p53-dissociator. International journal of oncology *31*, 1205-1211.

Pederson, T., and Tsai, R.Y. (2009). In search of nonribosomal nucleolar protein function and regulation. The Journal of cell biology *184*, 771-776.

Pei, H., Li, L., Fridley, B.L., Jenkins, G.D., Kalari, K.R., Lingle, W., Petersen, G., Lou, Z., and Wang, L. (2009). FKBP51 affects cancer cell response to chemotherapy by negatively regulating Akt. Cancer Cell *16*, 259-266.

Petersen-Mahrt, S.K., Estmer, C., Ohrmalm, C., Matthews, D.A., Russell, W.C., and Akusjarvi, G. (1999). The splicing factor-associated protein, p32, regulates RNA splicing by inhibiting ASF/SF2 RNA binding and phosphorylation. Embo J *18*, 1014-1024.

Pike, C.J., Walencewicz, A.J., Glabe, C.G., and Cotman, C.W. (1991). Aggregation-related toxicity of synthetic beta-amyloid protein in hippocampal cultures. Eur J Pharmacol *207*, 367-368.

Pyeon, D., Newton, M.A., Lambert, P.F., den Boon, J.A., Sengupta, S., Marsit, C.J., Woodworth, C.D., Connor, J.P., Haugen, T.H., Smith, E.M.*, et al.* (2007). Fundamental differences in cell cycle deregulation in human papillomavirus-positive and human papillomavirus-negative head/neck and cervical cancers. Cancer research *67*, 4605-4619.

Rajpal, A., Cho, Y.A., Yelent, B., Koza-Taylor, P.H., Li, D., Chen, E., Whang, M., Kang, C., Turi, T.G., and Winoto, A. (2003). Transcriptional activation of known and novel apoptotic pathways by Nur77 orphan steroid receptor. EMBO J *22*, 6526-6536.

Ren, D., Tu, H.C., Kim, H., Wang, G.X., Bean, G.R., Takeuchi, O., Jeffers, J.R., Zambetti, G.P., Hsieh, J.J., and Cheng, E.H. (2010). BID, BIM, and PUMA are essential for activation of the BAX- and BAK-dependent cell death program. Science *330*, 1390-1393.

Reynolds, E.S. (1963). The use of lead citrate at high pH as an electron-opaque stain in electron microscopy. The Journal of cell biology *17*, 208-212.

Roulston, A., Marcellus, R.C., and Branton, P.E. (1999). Viruses and apoptosis. Annu Rev Microbiol *53*, 577-628.

Sakahira, H., Enari, M., and Nagata, S. (1998). Cleavage of CAD inhibitor in CAD activation and DNA degradation during apoptosis. Nature *391*, 96-99.

Salehi, A.H., Roux, P.P., Kubu, C.J., Zeindler, C., Bhakar, A., Tannis, L.L., Verdi, J.M., and Barker, P.A. (2000). NRAGE, a novel MAGE protein, interacts with the p75 neurotrophin receptor and facilitates nerve growth factor-dependent apoptosis. Neuron *27*, 279-288.

Salehi, A.H., Xanthoudakis, S., and Barker, P.A. (2002). NRAGE, a p75 neurotrophin receptor-interacting protein, induces caspase activation and cell death through a JNK-dependent mitochondrial pathway. The Journal of biological chemistry *277*, 48043-48050.

Santel, A., and Fuller, M.T. (2001). Control of mitochondrial morphology by a human mitofusin. J Cell Sci *114*, 867-874.

Schauble, S., King, C.C., Darshi, M., Koller, A., Shah, K., and Taylor, S.S. (2007). Identification of ChChd3 as a novel substrate of the cAMP-dependent protein kinase (PKA) using an analog-sensitive catalytic subunit. The Journal of biological chemistry *282*, 14952-14959.

Schultz, J., Milpetz, F., Bork, P., and Ponting, C.P. (1998). SMART, a simple modular architecture research tool: identification of signaling domains. Proceedings of the National Academy of Sciences of the United States of America *95*, 5857-5864.

Selkoe, D.J. (2001). Alzheimer's disease results from the cerebral accumulation and cytotoxicity of amyloid beta-protein. J Alzheimers Dis *3*, 75-80.

Seo, M., Lee, W.H., and Suk, K. (2010). Identification of novel cell migration-promoting genes by a functional genetic screen. The FASEB journal : official publication of the Federation of American Societies for Experimental Biology *24*, 464-478.

Shieh, S.-Y., Ahn, J., Tamai, K., Taya, Y., and Prives, C. (2000). The human homologs of checkpoint kinases Chk1 and Cds1 (Chk2) phosphorylate p53 at multiple DNA damage-inducible sites Genes & Dev *14*, 289-300.

Shmueli, O., Horn-Saban, S., Chalifa-Caspi, V., Shmoish, M., Ophir, R., Benjamin-Rodrig, H., Safran, M., Domany, E., and Lancet, D. (2003). GeneNote: whole genome expression profiles in normal human tissues. C R Biol *326*, 1067-1072.

Sideris, D.P., Petrakis, N., Katrakili, N., Mikropoulou, D., Gallo, A., Ciofi-Baffoni, S., Banci, L., Bertini, I., and Tokatlidis, K. (2009). A novel intermembrane space-targeting signal docks cysteines onto Mia40 during mitochondrial oxidative folding. The Journal of cell biology *187*, 1007-1022.

Simbulan-Rosenthal, C.M., Rosenthal, D.S., Iyer, S., Boulares, A.H., and Smulson, M.E. (1998). Transient poly(ADP-ribosyl)ation of nuclear proteins and role of poly(ADP-ribose) polymerase in the early stages of apoptosis. J Biol Chem *273*, 13703-13712.

Slee, E.A., Adrain, C., and Martin, S.J. (2001). Executioner caspase-3, -6, and -7 perform distinct, non-redundant roles during the demolition phase of apoptosis. J Biol Chem *276*, 7320-7326.

Smirnova, E., Griparic, L., Shurland, D.L., and van der Bliek, A.M. (2001). Dynamin-related protein Drp1 is required for mitochondrial division in mammalian cells. Mol Biol Cell *12*, 2245-2256.

Sorlie, T., Tibshirani, R., Parker, J., Hastie, T., Marron, J.S., Nobel, A., Deng, S., Johnsen, H., Pesich, R., Geisler, S*., et al.* (2003). Repeated observation of breast tumor subtypes in independent gene expression data sets. Proceedings of the National Academy of Sciences of the United States of America *100*, 8418-8423.

Storz, M.N., van de Rijn, M., Kim, Y.H., Mraz-Gernhard, S., Hoppe, R.T., and Kohler, S. (2003). Gene expression profiles of cutaneous B cell lymphoma. J Invest Dermatol *120*, 865-870.

Stuart, L., and Hughes, J. (2002). Apoptosis and autoimmunity. Nephrol Dial Transplant *17*, 697-700.

Sugioka, R., Shimizu, S., and Tsujimoto, Y. (2004). Fzo1, a protein involved in mitochondrial fusion, inhibits apoptosis. The Journal of biological chemistry *279*, 52726-52734.

Tait, S.W., and Green, D.R. (2010). Mitochondria and cell death: outer membrane permeabilization and beyond. Nat Rev Mol Cell Biol *11*, 621-632.

Tatton, W.G., Chalmers-Redman, R., Brown, D., and Tatton, N. (2003). Apoptosis in Parkinson's disease: signals for neuronal degradation. Ann Neurol *53 Suppl 3*, S61-70; discussion S70-62.

Thompson, J., and Winoto, A. (2008). During negative selection, Nur77 family proteins translocate to mitochondria where they associate with Bcl-2 and expose its proapoptotic BH3 domain. J Exp Med *205*, 1029-1036.

Tomlins, S.A., Mehra, R., Rhodes, D.R., Cao, X., Wang, L., Dhanasekaran, S.M., Kalyana-Sundaram, S., Wei, J.T., Rubin, M.A., Pienta, K.J*., et al.* (2007). Integrative molecular concept modeling of prostate cancer progression. Nat Genet *39*, 41-51.

Tsubuki, S., Saito, Y., Tomioka, M., Ito, H., and Kawashima, S. (1996). Differential inhibition of calpain and proteasome activities by peptidyl aldehydes of di-leucine and tri-leucine. J Biochem *119*, 572-576.

Tsujimoto, Y., Cossman, J., Jaffe, E., and Croce, C.M. (1985). Involvement of the bcl-2 gene in human follicular lymphoma. Science *228*, 1440-1443.

Unoki, M., Okutsu, J., and Nakamura, Y. (2003). Identification of a novel human gene, ZFP91, involved in acute myelogenous leukemia. International journal of oncology *22*, 1217-1223.

Vaux, D.L., Cory, S., and Adams, J.M. (1988). Bcl-2 gene promotes haemopoietic cell survival and cooperates with c-myc to immortalize pre-B cells. Nature *335*, 440-442.

Verhagen, A.M., Ekert, P.G., Pakusch, M., Silke, J., Connolly, L.M., Reid, G.E., Moritz, R.L., Simpson, R.J., and Vaux, D.L. (2000). Identification of DIABLO, a mammalian protein that promotes apoptosis by binding to and antagonizing IAP proteins. Cell *102*, 43-53.

Vogt, C. (1842). Untersuchungen uber die Entwicklungsgeschichte der Geburtshelferkroete (Alytes obstetricians) ((Jent & Gassman, Solothurn, Switzerland)).

Wei, M.C., Lindsten, T., Mootha, V.K., Weiler, S., Gross, A., Ashiya, M., Thompson, C.B., and Korsmeyer, S.J. (2000). tBID, a membrane-targeted death ligand, oligomerizes BAK to release cytochrome c. Genes & development *14*, 2060-2071.

Wei, M.C., Zong, W.X., Cheng, E.H., Lindsten, T., Panoutsakopoulou, V., Ross, A.J., Roth, K.A., MacGregor, G.R., Thompson, C.B., and Korsmeyer, S.J. (2001). Proapoptotic BAX and BAK: a requisite gateway to mitochondrial dysfunction and death. Science *292*, 727-730.

Wen, C.J., Xue, B., Qin, W.X., Yu, M., Zhang, M.Y., Zhao, D.H., Gao, X., Gu, J.R., and Li, C.J. (2004). hNRAGE, a human neurotrophin receptor interacting MAGE homologue, regulates p53 transcriptional activity and inhibits cell proliferation. FEBS Lett *564*, 171-176.

Westerman, B.A., Poutsma, A., Steegers, E.A., and Oudejans, C.B. (2004). C2360, a nuclear protein expressed in human proliferative cytotrophoblasts, is a representative member of a novel protein family with a conserved coiled coil-helix-coiled coil-helix domain. Genomics *83*, 1094-1104.

Wheatley, S.P., Henzing, A.J., Dodson, H., Khaled, W., and Earnshaw, W.C. (2004). Aurora-B phosphorylation in vitro identifies a residue of survivin that is essential for its localization and binding to inner centromere protein (INCENP) in vivo. The Journal of biological chemistry *279*, 5655-5660.

Wolter, K.G., Hsu, Y.T., Smith, C.L., Nechushtan, A., Xi, X.G., and Youle, R.J. (1997). Movement of Bax from the cytosol to mitochondria during apoptosis. J Cell Biol *139*, 1281-1292.

Yang, B., O'Herrin, S.M., Wu, J., Reagan-Shaw, S., Ma, Y., Bhat, K.M., Gravekamp, C., Setaluri, V., Peters, N., Hoffmann, F.M*., et al.* (2007). MAGE-A, mMage-b, and MAGE-C proteins form complexes with KAP1 and suppress p53-dependent apoptosis in MAGE-positive cell lines. Cancer research *67*, 9954-9962.

Yankner, B.A. (1996). Mechanisms of neuronal degeneration in Alzheimer's disease. Neuron *16*, 921-932.

Yi, H., Leunissen, J., Shi, G., Gutekunst, C., and Hersch, S. (2001). A novel procedure for pre-embedding double immunogold-silver labeling at the ultrastructural level. J Histochem Cytochem *49*, 279-284.

Youle, R.J., and Strasser, A. (2008). The BCL-2 protein family: opposing activities that mediate cell death. Nat Rev Mol Cell Biol *9*, 47-59.

Yusenko, M.V., Kuiper, R.P., Boethe, T., Ljungberg, B., van Kessel, A.G., and Kovacs, G. (2009). High-resolution DNA copy number and gene expression analyses distinguish chromophobe renal cell carcinomas and renal oncocytomas. BMC Cancer *9*, 152.

Zhan, F., Barlogie, B., Arzoumanian, V., Huang, Y., Williams, D.R., Hollmig, K., Pineda-Roman, M., Tricot, G., van Rhee, F., Zangari, M.*, et al.* (2007). Gene-expression signature of benign monoclonal gammopathy evident in multiple myeloma is linked to good prognosis. Blood *109*, 1692-1700.

Zhang, L., Zambon, A.C., Vranizan, K., Pothula, K., Conklin, B.R., and Insel, P.A. (2008). Gene expression signatures of cAMP/protein kinase A (PKA)-promoted, mitochondrial-dependent apoptosis. Comparative analysis of wild-type and cAMP-deathless S49 lymphoma cells. The Journal of biological chemistry *283*, 4304-4313.